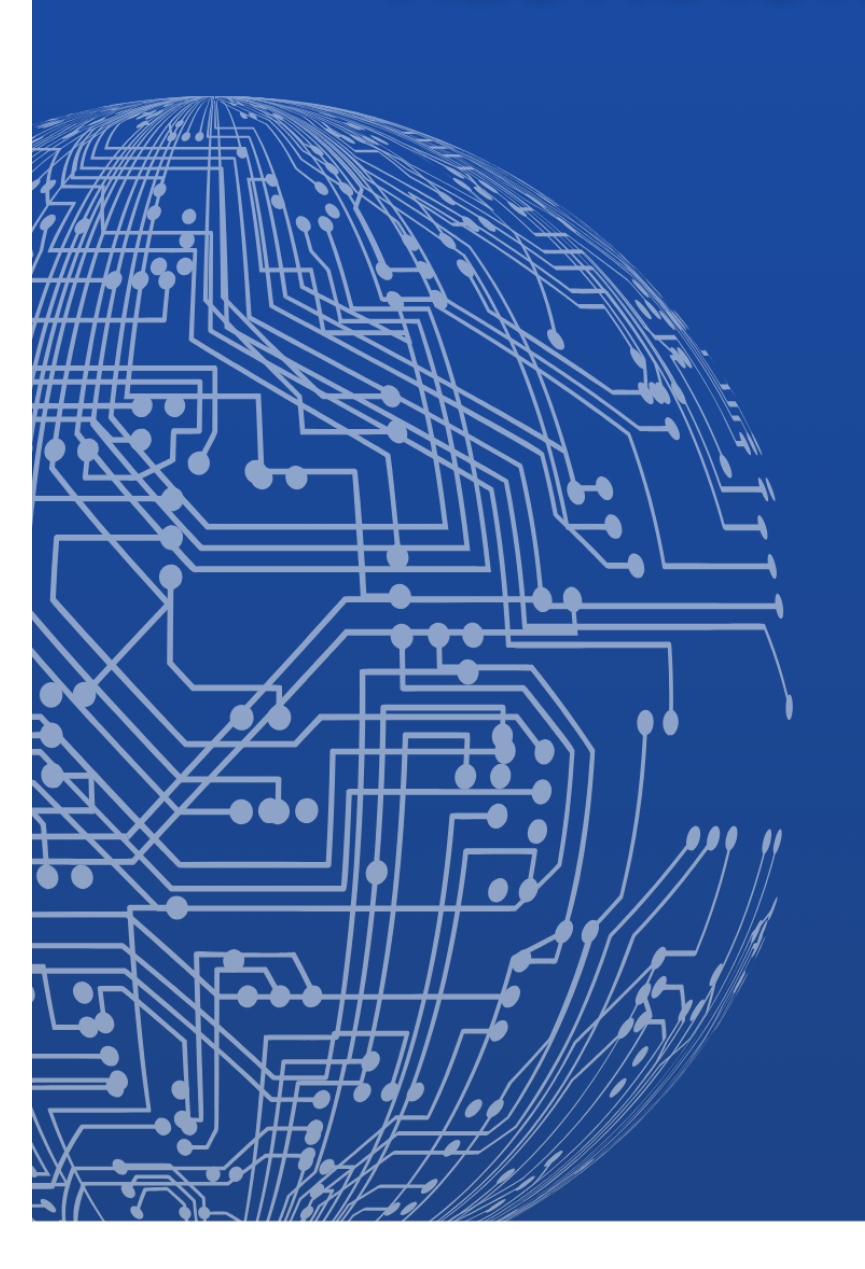
# 14th ISAJ ANNUAL SYMPOSIUM

ON INTEGRATED SCIENCE FOR A SUSTAINABLE SOCIETY

5F CONFERENCE HALL, CRIS BUILDING, NORTH CAMPUS HOKKAIDO UNIVERSITY, KITA 20 NISHI 10, SAPPORO, HOKKAIDO, JAPAN

November 10, 2023 (Friday)

# **ABSTRACTS BOOK**



Conveners

Dr. P. K. Hashim

Dr. Abhijit Shrotri

Dr. B. G. Siddabasave Gowda



ORGANIZED BY: INDIAN SCIENTISTS ASSOCIATION IN JAPAN (ISAJ) SUPPORTED BY: HOKKAIDO UNIVERSITY, THE EMBASSY OF INDIA



### Indian Scientists Association in Japan

## 特定非営利活動法人

(NPO Reg. No. 0503-05-001817)

http://www.isaj.org

ISAJ is registered as a Japanese non-profit organization (NPO) under Japan's NPO law. Tsukuba has been decided to be ISAJ's headquarter. The Executive Body is ISAJ's governing body and is responsible for directing the affairs and determining the future of the society. The Executive Body will appoint some of the Executive Body members to take responsibilities such as the Chapter Presidents of six different regions in Japan (Hokkaido, Tohoku, Tokyo, Tsukuba, Fukuoka, and Osaka).

## **Honorary Patron:**

H. E Mr. Sibi George The Ambassador of India to Japan

## **Honorary Advisors:**

Counsellor (Science & Technology), Embassy of India, Japan

Mr. Ryuko Hira Sai Hira India Foundation (SHIF), Japan

### Advisors (komon):

Mr. Ikuo Kawauchi, Economist

## **Executive Body:**

Dr. Sunil Kaul, AIST, Tsukuba (Chairman)

Dr. Alok Singh, NIMS, Tsukuba (Vice Chairman)

Dr. Kedar Mahapatra, Tokai University, Shizuoka (General Secretary)

Dr. Swadhin Behera, JAMSTEC, Yokohama (Chief Editor)

Dr. Samik Ghosh, Systems Biology Institute, Tokyo (Treasurer)

Prof. D. Sakhti Kumar, Toyo University, Saitama (Executive Body Member)

Dr. Manish Biyani, JAIST, Ishikawa (Executive Body Member)

Prof. Ruby Pawankar, Nippon Medical School, Tokyo (Executive Body Member)

# 14th ISAJ Annual Symposium

## **Honorary Patron**

H. E Mr. Sibi George The Ambassador of India, Japan

## **Honorary Advisor**

Counsellor (S&T) Embassy of India, Japan

Mr. Ryuko Hira Sai Hira India Foundation (SHIF), Japan

#### Advisor

Mr. Ikuo Kawauchi, Economist

Dr. Vasudevan Pillai Biju, Professor, RIES, Hokkaido University

#### Conveners

Dr. P. K Hashim

Dr. Abhijit Shrotri

Dr. B. G. Siddabasave Gowda

Dr. Ram Avtar Dr. Alok Singh Dr. Amrutha A. S Dr. Sunil Kaul Dr. Mahadeva Swamy Dr. Kedar Mahapatra Dr. Pinku Dr. Renu Wadhwa Dr. Prashant Ghediya Dr. Archana K. Singh Dr. Yogananadan Govindaraj Dr. Santosh Gothwal Dr. Sugata Sahu Dr. Samik Ghosh Dr. Nazmul Shaikh Dr. Swadhin Behera

Prof. D. Sakthi Kumar

Dr. Shivakumar K. I.

# भारत के राजदूत AMBASSADOR OF INDIA



# भारत का राजदूतावास Embassy of India

2-2-11 Kudan Minami, Chiyoda-ku Tokyo 102 0074



# **MESSAGE**

I am delighted to know that Indian Scientists Association in Japan (ISAJ) is organizing its 14th Annual Symposium titled 'Integrated Science for a Sustainable Society' to be held at Hokkaido University, Sapporo.

- 2. India-Japan Science and Technology Cooperation is formally anchored in the 1985 Inter-Governmental Agreement, which has laid the foundation for multifaceted cooperation across various domains. ISAJ has been making important contributions in fostering scientific research and cooperation between Indian and Japanese scientists and researchers. The Annual Symposium organized by them, provides an important opportunity for young and inspiring minds to further contribute towards enriching India-Japan scientific relationship.
- The title of the symposium points to the importance of integrated 3. science towards achieving a sustainable society. As we delve upon our efforts to tackle issues towards the future of human race, India has consciously chosen to deploy Science, Technology and Innovation (STI) in its policy interventions. A classic example is 'India Stack', which rests on digital identity, data and digital payments, thereby making our development pie bigger and more inclusive. 'India Stack' delivers tangible progress on SDG8 and is a harbinger towards a 'Global Stack' for sustainable societies. Similarly our Lunar, Mars and Solar Missions derived from India's scientific rigour nurtured in Indian Universities and research institutions with significant participation of our women universities, is a proof of our commitment towards human-centric growth. Our efforts towards harnessing technology to foster inclusive development and facilitate last mile delivery have given a strong fillip to India's skilled workforce. India's educational and research ecosystems are playing a major role in the transformation of STI framework.

- 4. Japan is a leader in technology-enabled manufacturing, while India possesses a large manufacturing base. Both the countries have traditions of research in the field of manufacturing science and systems. The existing cooperation in the field of Life Sciences and Healthcare, Ayurveda, Digital Partnership, Agriculture, Environment, Nuclear Science and Technology, Earth and Marine Sciences beckons cooperation in new age technologies which have the power of enhancing knowledge and attitudinal changes, thereby creating a lifestyle to promote future societies.
- 5. I once again commend the efforts of the Organizing Committee of the ISAJ and extend my best wishes for the 14th Annual Symposium.

(Sibi George)

Tokyo October 30, 2023

## **Message from the Executive Vice-President**

Prof. TAKAHASHI, Aya Executive Vice-President, Hokkaido University, Japan



On behalf of Hokkaido University, I would like to extend my sincere congratulations to the Indian Scientists Association in Japan for organizing the 14<sup>th</sup> Annual Symposium on "Integrated Science for a Sustainable Society".

Japan and India have a long history of friendship, spanning more than 70 years since the establishment of diplomatic relations in 1952 and are mutually recognized as strategic partners in diplomacy. I sincerely hope that India, with its high potential in the fields of AI, ICT, space, and nuclear energy, and Japan, a world leader in basic science, materials, life science, and environment, will continue to cooperate with each other in various fields.

Hokkaido University has 13 academic exchange agreements with Indian institutions, and in 2017, we launched a collaborative education program, "International Research Skills Program for Developing Sustainable Transportation System and Infrastructure" with IIT Bombay, IIT Hyderabad and IIT Madras. Under the program, Hokkaido University and the three institutions have together provided courses to their students and exchanged students with each other to supervise them in research. This program has motivated engineering professors in the University to accept more students from India. I hope that it will also further foster joint research between researchers at the University and Indian researchers.

I would like to express my gratitude to the Indian Scientists Association in Japan for their efforts in organizing the annual symposium and providing a valuable opportunity for the participants from various universities and research institutions in Japan and India to exchange their ideas and information. I hope you will have a successful symposium.



On behalf of the Indian Scientists Association in Japan (ISAJ), we extend our warmest greetings to all the distinguished delegates and guests attending the 14th Annual Symposium. This year's symposium, themed "Integrated Science for a Sustainable Society," promises to be an intellectually enriching and thought-provoking experience.

ISAJ, a Non-profit Organization (NPO), had its inception in 2008 as a vibrant community platform, uniting Indian scientists working in Japan. It was formally inaugurated by Dr. R. Chidambaram, the then Principal Scientific Adviser to the Government of India, in the esteemed presence of His Excellency Hemant Krishan Singh, the former Ambassador of India, in January 2009. Since those early days, ISAJ has made remarkable strides.

In 2010, ISAJ obtained official registration as an NPO in Japan, solidifying its commitment to fostering academic growth and scientific collaboration. Over the years, ISAJ has diligently worked to promote seminars, facilitate community discussions, and foster networking opportunities across all levels, from bright undergraduate students to accomplished academic and industrial professionals. This pivotal role has united countless scientists and researchers, paving the way for young Indian students to gain invaluable professional training and experience in Japan.

ISAJ's efforts have significantly contributed to the successful advancement of India-Japan Science and Technology cooperation, making it a vital catalyst for mutual progress and scientific exchange.

The Annual Symposium has consistently stood out as a flagship event in ISAJ's calendar for the past 13 years. Today, we take immense pride in commemorating its 14th anniversary. As customary, this symposium remains dedicated to showcasing the remarkable research endeavors undertaken by Indian researchers and their counterparts in Japan. Each year has witnessed robust and diverse participation from various multidisciplinary fields. The first seven symposia were held in the main auditorium of the Embassy of India in Tokyo. Subsequently, the eighth was held on the Tokyo University campus, the ninth at the AIST Tsukuba campus, and the tenth ventured to the Kansai region, settling at the Osaka University campus. The eleventh symposium was conducted online due to the challenges posed by the COVID-19 pandemic, defying physical limitations. The 12th Annual Symposium embraced a hybrid format, with both on-site and online components, hosted by Tokai University in Shimizu, Shizuoka City. The 13th symposium took place at the Embassy Auditorium. This year's event is being organized at Hokkaido University.

Our commitment to maintaining the interdisciplinary format of the symposium endures, fostering a platform for the exchange of ideas and experiences among participants. The wealth of scientific presentations over the years vividly showcases the diverse and ever-expanding scientific and technological domains in which Indian researchers are actively engaged in Japan. Additionally, it's heartening to observe a growing trend where more and more Indian researchers are ascending the ranks, assuming roles as young researchers and faculty members in Japan, as well as securing positions in esteemed universities in India.

We extend a warm welcome to our esteemed guests and eagerly anticipate engaging in profound interactions. It is noteworthy that the presentations by young researchers have consistently shone as the highlights of our previous symposia, and we have every reason to believe that this year will be no exception. We also eagerly look forward to insights from our senior scientists, who will share their extensive experiences of working in Japan and their valuable contributions to furthering India-Japan science and technology cooperation.

We hold a sincere conviction that this occasion stands as a unique opportunity for all of us to transcend our daily routines and the confines of our specialized research roles. We have full confidence that coming together on this platform will yield numerous benefits for young Indian students and researchers in various significant ways.

Our heartfelt gratitude goes out to His Excellency Mr. Sibi George, the Ambassador of India to Japan, and all other distinguished dignitaries who have graciously chosen to be part of the 14th Annual Symposium. We extend our sincerest thanks to all our guests for accepting our invitation and making the journey to contribute to this event. Our earnest hope is that all participants will thoroughly relish the symposium and capitalize on this outstanding opportunity to foster connections, forging new friendships and collaborations that strengthen the bonds of India-Japan science and technology cooperation.

With best regards,



Simil Caul.

(Sunil Kaul) Chairman



Ju

(Alok Singh) Vice-Chairman



Kedarnth Mahapatra

(Kedarnath Mahapatra) General Secretary

# **Message from the Conveners**

We extend our warmest welcome to the guests and participants of the 14<sup>th</sup> ISAJ annual symposium on "**Integrated Science for a Sustainable Society**," to take place on November 10, 2023, at the 5F, CRIS building conference hall, Hokkaido University, Sapporo, Japan. It is an honor to host this gathering of brilliant scientists and passionate students across interdisciplinary sciences. We are very privileged to have the esteemed presence of His Excellency Mr Sibi George, Ambassador of India to Japan, Prof. Aya Takahashi, Vice President of Hokkaido University, and Prof. Kuniharu Ijiro, Director of RIES, Hokkaido University, who have made significant contributions to the fields of diplomacy, education, and research.

This symposium offers a platform for scientific exchanges between very diverse research topics, to gain a wider understanding in scientific fields. By promoting interactions between researchers from various backgrounds, we hope to generate more collaboration between Indian and other researchers working in Japan.

The one-day program comprises an opening session, 4 oral technical sessions, and a poster session. The program features 3 plenary, 4 invited, and 9 young invited talks, together with regular 9 oral and 43 poster presentations. We hope that this will provide wide opportunities for exchange of knowledge. A luncheon seminar on "*The chances and pitfalls of aiming at an academic career in Japan*" is aimed at young researchers to help plan their careers in Japan and abroad.

We encourage you to participate actively and make the most of this exceptional gathering. Your ideas, research, and insights are crucial to advancing the cause of sustainability and integrated science. We are confident that the 14<sup>th</sup> ISAJ Symposium will be an enriching and inspiring experience for all.

It is very encouraging to have participants from universities and research institutes across Japan. We hope that this will be a rewarding experience for everyone.

Instituted by ISAJ two years ago to honor extraordinary contributions to our community, "ISAJ Distinguished Mentor Award," will be presented in the symposium's opening session.

Your presence and contributions are essential to the success of the 14<sup>th</sup> ISAJ Symposium. Let us come together to explore new horizons in sustainable science and work towards a brighter future.

Thank you for your dedication and support. We look forward to meeting you at Hokkaido University on November 10th, 2023.

With our best regards, Conveners, 14<sup>th</sup> ISAJ Symposium

P. K Hashim

Abhijit Shrotri

B. Siddabasave Gowda

# **Abstracts**

PL: Plenary Lecture
IL: Invited Lecture
YL: Young Leader
OL: Oral presentation

P: Poster presentation

#### **Abstracts Session 1** Page A thermoelectric oxide, Ba<sub>1/3</sub>CoO<sub>2</sub> PL1 1 Hiromichi Ohta, RIES, Hokkaido University Experimental evidence of the nutraceutical and pharmaceutical potential of ... IL1 2 Renu Wadhwa, AIST Tsukuba Direction dependent contraction forces on cell boundaries drive unidirectional ... YL1 3 Katsuhiko Sato, Hokkaido University Towards adjoint tomography of Nankai-Kyushu subduction zones; Can this ... OL1 4 Samriddhi Prakash Mishra, Kyoto University Session 2 Application of nanomaterials as theranostic materials PL2 5 D. Sakthi Kumar, Toyo University Development of near-infrared light-controlled phototherapeutic compounds YL2 6 Yuta Takano, Hokkaido University Exploring the influence of chain length on conformation, metal-ion binding, ... OL<sub>2</sub> 7 Shivakumar Kilingaru Ishwara, Hokkaido University Catalytic pathways for biobased C4 chemicals OL<sub>3</sub> 8 Yayati Naresh Palai, Hokkaido University Effects of ecotourism on land use land cover dynamics: Evidence... OL4 9 Ankita Gupta, Hokkaido University Application of remote sensing in civil engineering IL2 10 Kedar Mahapatra, Shizuoka Institute of Science and Technology Luncheon The chances and pitfalls of aiming at an academic career in Japan 11 Seminar Olaf Karthaus, Chitose Institue of Science and Technology

### **Session 3**

IL3	Next-generation mRNA vaccines against infectious diseases and cancer Satoshi Uchida, Tokyo Medical and Dental University		
	Active control of plasmonic nanoparticles using polymer gels		
YL3	Hideyuki Mitomo, Hokkaido University	13	
377. 4	Construction of functionalized red-light photoswitches by selective	- 4 4	
YL4	Dennis Chung-Yang Huang, Hokkaido University	14	
VI 5	Objective discrimination of drug resistant cells in chronic myeloid leukemia by	15	
YL5	Hemanth Noothalapati, Shimane University	15	
YL6	Predicting Highly Enantioselective Catalysts Using Machine Learning	16	
110	Pavel Sidorov, Hokkaido University	10	
OL5	User evaluation of a 360-degree video of home-ventilator care for	17	
OLS	Noriyo Colley, Hokkaido University	1/	
OL6	State of data assurance in corporate environmental disclosures in India	18	
OL0	Ahmad Mohd Khalid, United Nations University, Tokyo	10	
Session 4			
DI 2	Plant transcription factor engineering for our sustainable future	10	
PL3	Nobutaka Mitsuda, AIST Hokkaido	19	
II 4	Innovative environmental technologies for "garbage"	20	
IL4	Toshikazu Kawaguchi, Hokkaido University	20	
IL5	Investigation of cathodic polarization characteristics of steel bars in	21	
11.3	Takahiro Nishida, Shizuoka Institute of Science and Technology	21	
YL7	Harnessing nanostructured materials: Pushing the limits of ultra-sensitive	22	
11./	G Akhilesh Babu, NIMS Tsukuba	22	
YL8	"Pathological role of macrophage in cartilage degeneration: Insights	23	
110	Alaa Terkawi, Hokkaido University	25	
YL9	Selective and transient stealth coating of liver scavenger wall enables	24	
12,	Dirisala Anjaneyulu, iCONM, Kawasaki		
OL7	Design and synthesis of piezochromic materials exploring intermolecular	25	
<u></u>	Sanhita Patil, Savitribai Phule Pune University		
OL8	Fabrication and thermoelectric properties of freestanding Ba <sub>1/3</sub> CoO <sub>2</sub>	26	
	Kungwan Kang, Hokkaido University		
Posters			
P1	Chitosan and PVA foam material	27	
11	Taiyo Nagai, Chitose Institute of Science Technology	41	
P2	Exploring the feasibility to estimate DBH from trunk point cloud data	28	
1 2	Yoshito Shimizu, Hokkaido University	20	
Р3	Heterojunction formation strategy to realize Z-scheme g-C3N4/SnS2	29	
10	Yohei Mori, Shizuoka University	4	
P4	Utilizing Artificial Intelligence and Expert Knowledge to Optimize	30	
	Vickey Nandal, National Institute for Materials Science (NIMS), Tsukuba	20	
P5	Energy-saving preparation of chitin/chitosan composite materials	31	
	Tomohisa Suzuki, Chitose Institute of Science and Technology		
P6	Universal Design Features and their Accessible Continuity in Shopping Malls	32	

	Sudeshna Chakraborty, Hokkaido University	
P7	"All-aqueous" tandem Boc-deprotection and alkylation of benzimidazole	33
	Suchismita Rath, Shiv Nadar University, India	
P8	Shallow landslide occurrence relative to forest management including  Sowmya Nagaraj, Shizuoka University	34
D0	Export and energy efficiency: Evidence from manufacturing firms in transition	
P9	Shohruh Khasanov, Hokkaido University	35
D10	A low-cost downflow hanging sponge (DHS) reactor for nitrogen removal	36
P10	Shehani Sharadha Maheepala, Nagaoka University of Technology	30
P11	Photoresponsive-Auxin Induced Degron (PAID) technology for spatiotemporal	37
	Saugata Sahu, Hokkaido University	37
P12	Development of alternative materials to plastics using Fomes fomentarius	38
	Ryuya Abe, Chitose Institute of Science and Technology	
P13	Photoinduced electron transfer from perovskites nanocrystals to a C60	39
	Rumana Akter, Hokkaido University	
P14	Near Future projection of rainfall distribution pattern assessment under	40
	Reza Kusuma Nurrohman, Hokkaido University  Non Tangatad I.C. MS analysis of lipid composition in Adauki and	
P15	Non-Targeted LC-MS analysis of lipid composition in Adzuki and  Rachana M. Gangadhara, Hokkaido University	41
	"Caging bioactive Imidazoles: A photopharmacological approach to achieve	
P16	Jiajun Qi, Hokkaido University	42
	Development of LC/MS based screening assay for sphingomyelin synthase	
P17	Punith M. Sundaraswamy, Hokkaido University	43
7.10	Defluorinative Cross Couplings of Trifluoromethyl Arenes by Copper	
P18	Priya Saha, Hokkaido University	44
D10	Photocatalytic Conversion of Glucose into Formate with Comparison of	45
P19	Pratiksha Babgonda Patil, Hokkaido University	45
P20	Development of visible-light active "heteroaryl azo" photoswitches for	46
120	Nusaiba Madappuram Cheruthu, Hokkaido University	70
P21	Oxygen deficient Co doped ZrO2 for selective CO2 reduction to CO	47
	Nazmul Shaikh, Hokkaido University	
P22	Interfacial defect passivation of amphiphilic ligand-capped halide perovskite	48
	Most Farida Khatun, Hokkaido University	
P23	Evaluation of biodegradability of chitin and chitosan plastics in various	49
	Akihiro Mizuyama, Chitose Institute of Science and Technology	
P24	Dissecting sorghum cultivars lipidome by untargeted analysis	50
	Lipsa Rani Nath, Hokkaido University  Synthesis of Shortwave-Infrared (SWIR) Organic Fluorescent Probes for	
P25	Aravind K. Swamy, Hokkaido University	51
	Investigating the impact of ethanol on colon content lipidome in mice models	
P26	Jayashankar Jayaprakash, Hokkaido University	52
	Low-dimensional fluorescent hybrid metal halide crystals	
P27	Rahul Ghosh Dastidar, Hokkaido University	53
D20	Phenylazothiazoles pH indicators	
P28	Shifa Ahmad, Hokkaido University	54
D20	Tunable chiroptical activities of discrete chiral gold nanorods by pH and	
P29	Han Lin, Hokkaido University	55
P30	Investigation of Ni-doped Metal-Organic Framework (MOF-5) for	56
1 30	<b>Baskar Malathi</b> Shizuoka University	30

P31	Selective Mono-Hydrodefluorination of Trifluoromethyl Arenes with NHC	57	
	Amit K Jaiswal, Hokkaido University		
P32	Development of quantitative analysis method for oxylipins by LC/MS	58	
	Yonghan Li, Hokkaido University		
P33	Effectiveness of using visual deterrents in lotus root cultivation to control duck	59	
P34	Uchini Bandaranayake, Nagaoka University of Technology		
	Development of a DNA aptamer inhibiting vitamin-D inactivation enzyme	60	
P35	V. Sharma, Toyama Prefectural University	00	
	Synthesis of 'Dressed' ZnO Nanowires by Overtime Hydrothermal Growth with	61	
	Yuta Kazama, Hokkaido University	01	
	Enhancement of mitochondrial function with kaempferol, contained as	62	
P36	Akiko Sakurai, Hokkaido University	02	
D25	Development of sensitive LC/MS method for trans fatty acid analysis		
P37	Rinako Ueda, Hokkaido University	63	
D20	Analysis of lipid nutrients in edible rose samples by LC/MS		
P38	Malek Md Abdul, Hokkaido University	64	
D20	Confocal laser microscopy examination of surface coating of an algal cell with		
P39	Yingqi Mu, Hokkaido University	65	
D 40	What Determines Milk Consumption in Indian Households? - Insights from		
P40	Sakshi Pandey, The University of Tokyo	66	
D 44	Prevention of Byproduct Synthesis in Ionic Layer Epitaxy of Monolayered Zinc		
P41	Ryunosuke Matsumura, Hokkaido University	67	
	RNA-seq analysis to reveal biosynthetic pathways of bioactive triterpenoids		
P42	Hayato Suzuki, National Institute of Advanced Industrial Sci. and Tech. (AIST)	68	
	Phenylazothiazoles as Visible-Light Photoswitches		
P43	Pnenviazotniazoies as visible-Light Pnotoswitches	69	

## A Thermoelectric Oxide, Ba<sub>1/3</sub>CoO<sub>2</sub>

## Hiromichi Ohta

Research Institute for Electronic Science, Hokkaido University

Thermoelectric energy conversion technology has attracted attention as an energy harvesting technology that converts waste heat into electricity by means of the Seebeck effect. Oxide-based thermoelectric materials that show a high figure of merit (ZT) are promising because of their good chemical and thermal stability as well as their harmless nature compared to chalcogenide-based state-of-the-art thermoelectric materials. Here, we show a reliable high-ZT thermoelectric oxide, Ba<sub>1/3</sub>CoO<sub>2</sub>. We fabricated Ba<sub>1/3</sub>CoO<sub>2</sub> epitaxial films by the reactive solid-phase epitaxy method (Na<sub>3/4</sub>CoO<sub>2</sub>) followed by ion exchange (Na<sup>+</sup>  $\rightarrow$  Ba<sup>2+</sup>) [1] treatment and performed thermal annealing of the film at high temperatures and structural and electrical measurements. The crystal structure and electrical resistivity of the Ba<sub>1/3</sub>CoO<sub>2</sub> epitaxial films were found to be maintained up to 600 °C. The power factor gradually increased to ~1.2 mW m<sup>-1</sup> K<sup>-2</sup> and the thermal conductivity gradually decreased to ~1.9 W m<sup>-1</sup> K<sup>-1</sup> with increasing temperature up to 600 °C. Consequently, the ZT reached ~0.55 at 600 °C in air [2]. In addition, we recently realized to fabricate freestanding Ba<sub>1/3</sub>CoO<sub>2</sub> single crystalline films [3].

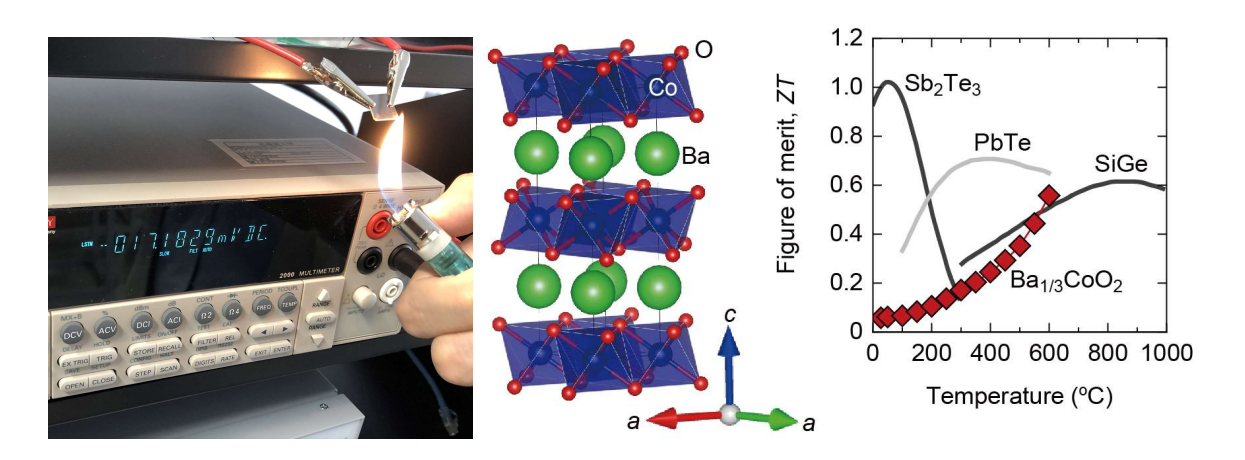


**Figure.** (Left) Photograph that shows the Seebeck effect of a  $Ba_{1/3}CoO_2$  epitaxial film. Thermo-electromotive force is generated by heating one end of the film. (Center) Schematic crystal structure of  $Ba_{1/3}CoO_2$  that is composed of alternative stacking of  $CoO_2$  and Ba layers along the *c*-axis. (Right) Temperature dependence of the *ZT* for  $Ba_{1/3}CoO_2$  epitaxial films in air. The *ZT* reaches ~0.55, which is comparable to that of chalcogenide-based thermoelectric materials.

- 1. Y. Takashima, Y. Zhang, J. Wei, B. Feng, Y. Ikuhara, H.J. Cho, H. Ohta, J. Mater. Chem. A 2021, 9, 274.
- 2. X. Zhang, Y. Zhang, L. Wu, A. Tsuruta, M. Mikami, H.J. Cho, H. Ohta, *ACS Appl. Mater. Interfaces* **2022**, 14, 33355.
- 3. K. Kang, F. Kato, A. Nakano, I. Terasaki, T. Endo, Y. Matsuo, H. Jeen, H. Ohta, *ACS Appl. Electron. Mater.* in revision.

## IL1

# **Experimental Evidence of the Nutraceutical and Pharmaceutical Potential of Honeybee Propolis**

Renu Wadhwa<sup>1</sup>, Ashish Kaul<sup>1</sup>, Yoshiyuki Ishida<sup>2</sup>, Keiji Terao<sup>2</sup>, Sunil C. Kaul<sup>1</sup>
<sup>1</sup>AIST-INDIA DAILAB, National Institute of Advanced Industrial Science & Technology (AIST),

Central 5-41, Tsukuba 305-8565, Japan

<sup>2</sup>CycloChem Bio Co., Ltd., 7-4-5 Minatojima-minamimachi, Kobe 650-0047, Japan

Honeybees generate propolis, a resinous compound used for building hives, by combining their saliva with the plant elements they consume. The compound caffeic acid phenethyl ester (CAPE), which is a component of honeybee glue, has a complicated chemical makeup and a variety of bioactivities (anticancer, anti-stress, and anti-inflammatory). We investigated the molecular mechanism of such activities using human cultured cells. Biochemical and imaging analyses of expression at the transcript and protein levels revealed that CAPE modulates oxidative stress, hypoxia, protein aggregation, and cancer signaling. Analyses of control and CAPEtreated cells showed growth arrest/apoptosis as supported by molecular markers. Low non-toxic doses of CAPE caused activation of pro-hypoxia and neurodifferentiation activities, which are expected to be beneficial for the treatment of neurodegenerative diseases. Indeed, the Drosophila model of Alzheimer's disease and the mouse model of amnesia/memory loss supported the improvement of disease symptoms and the activation of physiological functions in CAPE-treated groups. In the recent pandemic, we extended the analyses to investigate the anti-COVID-19 potential of CAPE by computational and experimental approaches. We found that CAPE has the ability to interact with the highly conserved substrate binding pocket of M<sup>pro</sup>, a viral protein critically involved in its replication. Furthermore, CAPE-treated cells showed downregulation of TMPRSS2, a host cell surface receptor involved in viral infection. Taken together, CAPE is proposed to possess nutraceutical and pharmaceutical potential that could be enrolled in the management of stress, cancer, neurodegenerative diseases, and COVID-19.

Keywords: Propolis, caffeic acid phenethyl ester, growth inhibition, COVID-19, management

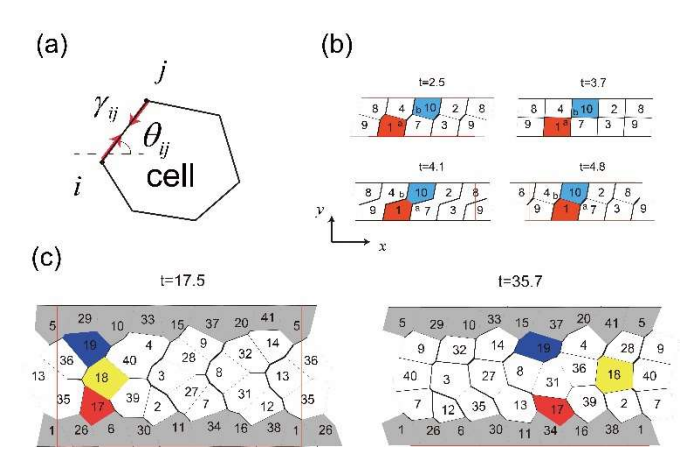
# **Direction Dependent Contraction Forces on Cell Boundaries Drive Unidirectional Movement of Epithelial Cells Within Their Sheet**

Katsuhiko Sato<sup>1</sup>, Tetsuya Hiraiwa<sup>2</sup>, Tatsuo Shibata<sup>3</sup>, and Erina Kuranaga<sup>4</sup>

<sup>1</sup>Research Institute for Electronic Science, Hokkaido University; <sup>2</sup>Institute of Physics, Academia Sinica, Taiwan; <sup>3</sup>RIKEN Center for Biosystems Dynamics Research; <sup>4</sup>Graduate School of Life Sciences, Tohoku University

Introduction. During early development and wound healing, epithelial cells (cohesive cells) that form a monolayer sheet sometimes move collectively in a definite direction in the sheet; that is, the cohesive cells move unidirectionally while maintaining the attachments with adjacent cells. This phenomenon is called collective migration of epithelial cells [1] and is considered to be an essential factor for morphological changes of multicellular organisms [2]. While the molecular mechanisms underlying this phenomenon are becoming understood, much of the mechanical mechanisms remain still unclear. In the present talk, I will provide one possible mechanism for collective migration from a theoretical point of view [3]: If the cell boundaries contract depending on their orientation (generalized planar polarity), and spatial inhomogeneity about the cell properties, such as strength of cell adhesion, exists, then the cohesive cells collectively move in the direction perpendicular to that of spatial inhomogeneity, by repeating rearrangement of neighbor relationships. I will demonstrate this scenario by using the vertex model, and reproduce the behaviors of typical collective cell migration such as that seen in zebrafish lateral line primordium. I also provide experimental evidence for this type of movement by investigating a phenomenon in development of fly, where monolayer epithelial sheets move 360 degrees clockwise around the genital disc [4].

**Results and Discussion.** In this model, epithelial cells are represented by polygons (Fig. 1 (a)). This model can assign the contraction force on each cell boundary, denoted by  $\gamma_{ij}$ . If  $\gamma_{ij}$  is the largest when the cell boundary is oriented at 45 degrees to the x axis, continuous shear motion of epithelial cells occurs (Fig. 1 (b)). By combining this shear motion and the inhomogeneity of friction coefficient along the y axis, the cells can continuously migrate in the x direction while keeping the sheet structure (Fig. 1 (c)).



It may be surprising that contraction forces on cell boundaries, which satisfy the action-reaction principle, generates unidirectional motion of epithelial sheet.

- 1. P. Friedl and D. Gilmour, (2009) Nat. Rev. Mol. Cell Biol. 10, 445-457.
- 2. J. Davies, Mechanisms of Morphogenesis (Academic Press, Second Edition, 2013).
- 3. K. Sato, T. Hiraiwa, and T. Shibata, Phys. Rev. Lett. 115, 188102 (2015).
- 4. K. Sato, T. Hiraiwa, E. Maekawa, A. Isomura, T. Shibata, and E. Kuranaga, Nat. Commun. 6, 10074 (2015).

## OL<sub>1</sub>

# Towards Adjoint Tomography of Nankai-Kyushu Subduction Zones; Can This Tool be Applied to Himalayan Tectonics to Image Crustal Heterogeneities?

Samriddhi Prakash Mishra<sup>1</sup>, Yoshihiro Kaneko<sup>1</sup>, Bryant Chow<sup>2</sup>, Yusuke Yamashita<sup>3</sup>, Masanao Shinohara<sup>4</sup>, AP Singh<sup>5</sup>

<sup>1</sup>Graduate School of Science, Kyoto University; <sup>2</sup>Geophysical Institute, University of Alaska Fairbanks, Fairbanks, Alaska, USA; <sup>3</sup>Disaster Prevention Research Institute, Kyoto University; <sup>4</sup>Earthquake Research Institute, University of Tokyo; <sup>5</sup>National Centre for Seismology (NCS), Ministry of Earth Sciences (MoES), New Delhi, India

**Introduction**: The Nankai-Kyushu subduction system is a complex seismo-tectonic region marked by an abrupt transition in the inter-plate coupling, with a fully coupled megathrust to the northeast region. In this study we utilize an earthquake-based, full waveform inversion technique, termed adjoint tomography, to develop an accurate and high-resolution shear wave velocity model of the megathrust region. Our aim is to reveal the subsurface crustal structure responsible for the origin of the interpolate coupling transition. Adjoint tomography been previously applied to regional, continental, and global scales, with a proven track record of high probing applicability in subduction regions elsewhere in the world (e.g., Chow et al., 2022).

Results and Discussion: Our target region includes ~100 moderate sized earthquake events (4.5<M<sub>w</sub><6) with ~150 permanent stations as well as ~20 temporary Ocean Bottom Seismometer (OBS) stationed in the Hyuganada region. We first conduct a series of 2-D synthetic inversion tests for an SH-wave problem (e.g., Tape et al., 2007) using a recently developed automated tool (Chow et al., 2020; Modrak et al., 2018) to address the resolvability of small-scale heterogeneities given the source-station coverage within the target region. We demonstrate that adjoint tomography which utilizes adjoint-state methods, in conjunction with our existing dataset, has the potential to visualize and resolve a realistic crustal structure in fine detail, and construct an accurate shear-wave velocity model in our study region.

Hereby, we present our ongoing efforts towards improving images of the subsurface complexities of Nankai-Kyushu subduction system. Additionally, the prospects and viability of this technique could be tested in the complex land-locked collision zones of Himalayan region extended to the Indian Ocean to interpret the lateral heterogeneities in terms of velocity anomalies with an accurate shear wave model and further understand the seismo-genesis in different tectonic settings.

- 1. C. Tape, Q. Liu, J. Tromp, Geophysical Journal International, 2007, 168(3), 1105-1129.
- 2. J. Tromp, C. Tape, Q. Liu, Geophysical Journal International, 2005, 160(1), 195-216.
- 3. C. Tape, Q. Liu, A. Maggi, J. Tromp, Geophysical Journal International, 2010, 180(1), 433-462.

## PL2

# **Application of Nanomaterials as Theranostic Materials**

## D. Sakthi Kumar

Graduate School of Interdisciplinary New Science Toyo University, Kawagoe, Saitama, Japan 350-8585

The field of nanotechnology has seen many applications in various research areas. However, it is widely recognized that the bio field has benefited the most from the application of nanotechnology. In the bio field, nanodrug delivery has greatly advanced the fight against cancer by allowing for precise drug delivery to cancer cells without causing damage to healthy tissues. This has addressed a major challenge faced by many effective drugs. Nanotechnology has also allowed for surface modification of drugs and packaging hydrophobic drugs in biocompatible polymers, resulting in significant advancements. Additionally, imaging moieties have recently been incorporated into nano assemblies, providing diagnostic capabilities. This technology, known as theranostics (Therapy + Diagnosis), allows for simultaneous diagnosis and therapy.

The talk will focus on the application of nanoparticles for nanodrug delivery and their development as theranostic materials.

# Development of Near-Infrared Light-Controlled Phototherapeutic Compounds

Yuta Takano<sup>1,2</sup>

<sup>1</sup>Research Institute for Electronic Science, Hokkaido University.; <sup>2</sup>Graduate School of Environmental Science, Hokkaido University.

**Introduction.** Photodynamic therapy (PDT) is a promising treatment modality that uses light energy to selectively treat patients in a spatiotemporal manner. PDT on cancers can selectively destroy tumor cells, vasculature, and tissues with  $^{1}O_{2}$ . This makes PDT more advantageous than conventional treatments such as surgery, chemotherapy, and radiotherapy [1]. Recently, near-infrared (NIR) light, particularly in the 700-1300 nm range called the biological window, is considered to be essential to achieve efficient PDT. NIR light is more penetrative to cells and tissues than ultraviolet (UV) and visible light, which are absorbed and scattered by the surface of biological tissue. In this context, several research groups, including ours, have recently developed photofunctional molecules that absorb NIR light [1].

Results and Discussion. We recently developed a NIR-sensitizer molecule consisting of a  $\pi$ -extended porphyrin-type (**rTPA**), which shows remarkable optical absorption around 700 nm light and singlet oxygen ( $^{1}O_{2}$ ) ability under the illumination [2]. The combination of **rTPA** and a mitochondrial-targeting career, **MITO-Porter**, demonstrated more than one-order effective photoactivated cancer-killing ability than approved PDT drugs. The pi-extended porphyrin can also be used for efficient NIR light harvesting for utilizing photoinduced charge separation. With such molecule, we succeeded in inducing modulation of plasma membrane potential by introducing molecules having both positive and negative charges (i.e., charge-separating molecules) into the plasma membrane upon photoirradiation [3]. Moreover, **rTPA**-embedded carbon nanohorns (CNHs) demonstrated the bactericidal effect for a promising approach to cure peri-implantitis for dental medicine [4]. We believe that methods using NIR light will be further developed. This is based on the higher performance and resolution achieved by efficiently utilizing the photo-excited states of molecules.

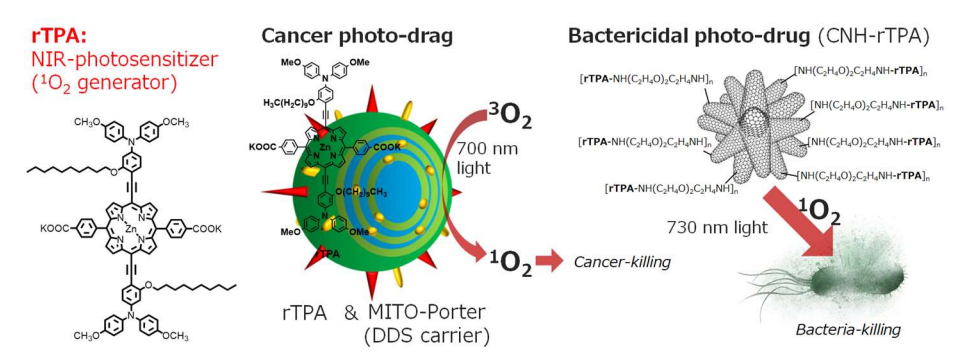


Figure. Near-infrared light-controlled phototherapeutic compounds based on a  $\pi$ -extended porphyrin-type, rTPA.

- 1. J. Zhao, W. Wu, J. Sun, S. Guo, Triplet photosensitizers: from molecular design to applications, *Chem. Soc. Rev.* 2013, **42**, 5323.
- 2. (a) Satrialdi, R. Munechika, V. Biju, Y. Takano, H. Harashima and Y. Yamada, *Chem. Commun.*, 2020, **56**, 1145. (b) Satrialdi, Y. Takano, E. Hirata, N. Ushijima, H. Harashima and Y. Yamada, *Nanoscale Adv.*, 2021, **3**, 5919.
- 3. Y. Takano, K. Miyake, J. Sobhanan, V. Biju, N. V. Tkachenko, H. Imahori, *Chem. Commun.* 2020, **56**, 12562.
- 4. E. Hirata, Y. Takano, D. Konishi, Y. Maeda, N. Ushijima, M. Yudasaka, A. Yokoyama, *Chem. Commun.* 2023, **59**, 11000.

# **Exploring the Influence of Chain Length on Conformation, Metal-ion Binding, and Self-assembly of Discrete Polyketones**

Kilingaru I. Shivakumar, 1,† Yasuhide Inokuma<sup>1,2</sup>

<sup>1</sup>Institute for Chemical Reaction Design and Discovery (WPI-ICReDD), Hokkaido University; <sup>2</sup>Division of Applied Chemistry, Faculty of Engineering, Hokkaido University;

†Present affiliation: Faculty of Environmental Earth Science, Hokkaido University

**Introduction.** Molecular precision in organic synthesis is critical, particularly in the study of oligomers and polymers. Even a slight change in molecular weights can result in entirely different properties and functions. We synthesized a new series of flexible, yet shapable, aliphatic polyketones consisting of alternating 1,3- and 1,4-diketones through oligomerization of an acetylacetone derivate, 3,3-dimethylpentane-2,4-dione. These polyketones chains exist as stable all-*keto* forms, avoiding synthetic complications such as keto-enol tautomerism and spontaneous intramolecular cyclization. In this presentation, we describe our recent works on the influence of chain length on conformation, alkali metal-ion binding and self-assembling behaviors of polyketones.

**Results and Discussion.** Polyketone analogs were synthesized in a stepwise manner by elongating their chain lengths through the alternate repetition of silylation and oxidative coupling reactions (**Fig. 1a**). Single crystal and powder X-ray diffraction studies revealed that the shorter analogs adopted unique conformations, while the

longer oligomers above tetramers exhibited helical structures (Fig. 1b). Cyclized polyketones were obtained through cyclization of linear polyketones or ring-opening reactions of corresponding calix[n] furans. Depending on their ring size, these macrocyclic oligoketones exhibited alkali-metal ion binding behavior like crown ethers (Fig. 1c). This binding behavior was utilized to catalyze a halogen-exchange reaction.2 The terminal functionalization with carboxylic acids followed by 3aminopyridines led to the synthesis of discrete polyketones with varying chain lengths, each bearing Hbonding groups at both ends (Fig. 1d). Chain-lengthdependent self-assembly behavior was observed for carboxyland 3-acylaminopyridine terminated polyketones in solid-state. The gelation of chloroform by P2 was attributed to the double-helix-like self-assembly supported by NH···N interactions in both solid- and solution-states. These results illustrate that precise control of polyketone chain lengths can significantly influence their conformation, metal-ion binding, and self-assembly behaviors, even when they share same repeating units.

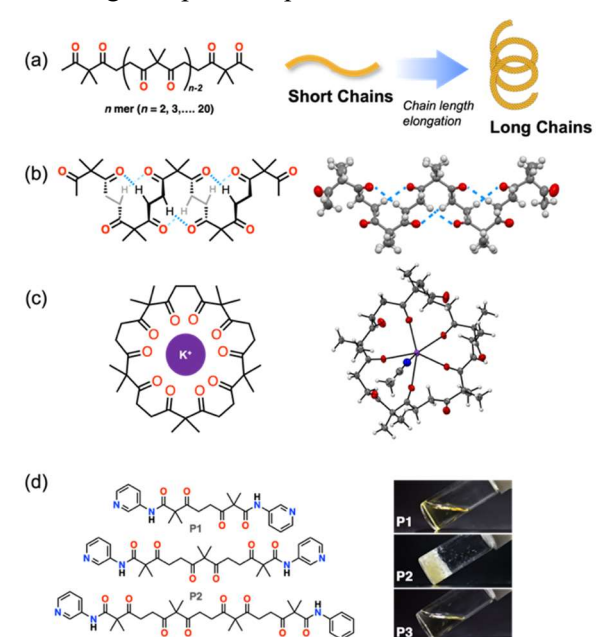


Figure 1 (a) Chemical structures of discrete aliphatic polyketones and a schematic representation of their synthesis. Molecular structures and their corresponding crystal structures: (b) linear pentamer, and (c) potassium ion encapsulated cyclic pentamer. (d) Pictures of 100 mM chloroform solution at 25 °C of P1-P3 showing gelation only in P2.

- 1. Y. Ide, Y. Manabe, Y. Inaba, Y. Kinoshita, J. Pirillo, Y. Hijikata, T. Yoneda, K. I. Shivakumar, S. Tanaka, H. Asakawa, Y. Inokuma, *Chem. Sci.* **2022**, *13*, 9848.
- 2. N. Ozawa, K. I. Shivakumar, M. Murugavel, Y. Inaba, T. Yoneda, Y. Ide, J. Pirillo, Y. Hijikata, Y. Inokuma, *Chem. Commun.*, **2022**, *58*, 2971.
- 3. K. I. Shivakumar, Y. Manabe, T. Yoneda, Y. Ide, Y. Inokuma, Precis. Chem., 2023, 1, 34.

## **Catalytic Pathways for Biobased C4 Chemicals**

Yayati Naresh Palai, Abhijit Shrotri, Atsushi Fukuoka Institute for Catalysis, Hokkaido University.

### Introduction.

Industrial chemicals with a four-carbon structure, including maleic acid, 1,4-butanediol,  $\gamma$ -butyrolactone, and pyrrolidones, are presently derived from petroleum. Scarcity of C4 sugars in biomass and the absence of a suitable C4 platform pose challenges for their direct synthesis from biomass, emphasizing the need for development of a new C4 platform chemical. This study delves into catalytic mechanism guided discovery of new C4 platform chemicals and their transformation into value added chemicals.

### Results and Discussion.

We tested several zeolite catalysts for oxidation of furfural with H<sub>2</sub>O<sub>2</sub>. Sn-Beta, a pure Lewis acid catalyst, produced succinic acid with 53% yield (Figure 1a). 2(3H)-Furanone was detected as a crucial intermediate for formation of succinic acid. Detailed characterization showed that Sn-Beta activates furfural by coordinating to the carbonyl group and it does not activate H<sub>2</sub>O<sub>2</sub> leading to Baeyer-Villiger oxidation (Figure 1b). TS-1, another Lewis acid zeolite, produced maleic acid as the main product. TS-1 was able to activate H<sub>2</sub>O<sub>2</sub> as a hydroperoxy species as shown in Fig 2b leading to epoxidation of furfural to 5-hydroxy-2(5H)-furanone (5H5F). Therefore, the oxidation of furfural in the first step was highly dependent on the ability of Lewis acid site to activate furfural and H<sub>2</sub>O<sub>2</sub>. TS-1 catalyzed epoxidation of furfural oxidation at room temperature with H<sub>2</sub>O<sub>2</sub> led to formation of 5H5F with 92 % yield and further reaction to maleic acid did not happen.<sup>2</sup> 5H5H is a stable molecule with four carbon atoms that can serve as a versatile platform chemical. While its oxidation produced maleic acid in high yield, hydrogenation of 5H5F produced, γ-butyrolactone, 5-hydroxy-γ-butyrolactone, 1,4-butanediol, tetrahydrofuran based on catalyst choice (Fig 1c). The 5H5F pathway to form these C4 chemicals is energetically efficient compared to current industrial routes because of its milder reaction conditions. Due to the highly electrophilic nature of the fourth carbon in 5H5F, it can be attacked by different nucleophiles. Therefore, its reductive aminolysis directly produced 2-pyrrolidone and n-methyl-2- pyrrolidone (Fig 1c). The easy preparation of 5H5F from furfural and one step transformation into various chemicals makes it a suitable platform chemical for C4 chemicals.

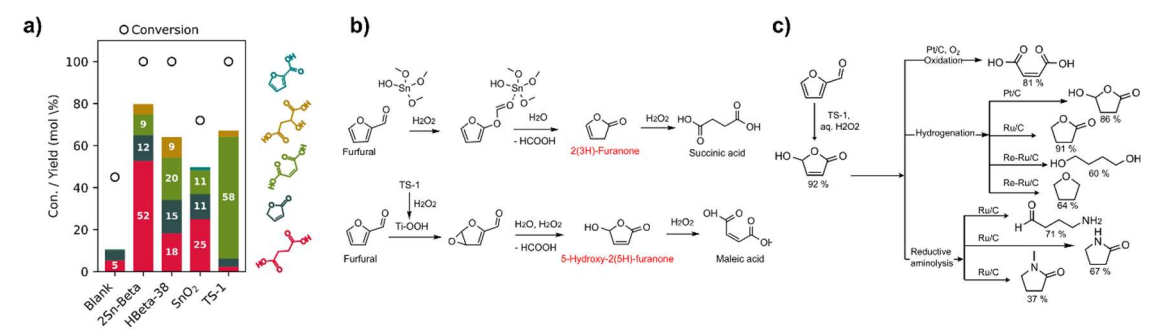


Figure 2. a) Furfural oxidation over different catalysts. Reaction conditions – 1 mmol furfural (96 mg), catalyst 50 mg, 15 % H<sub>2</sub>O<sub>2</sub> solution 10 mL, 50 °C, 6 h, b) Baeyer-Villiger oxidation reaction of furfural in presence of Sn-Beta catalyst and Epoxidation reaction of furfural in presence of TS-1 catalyst, c) Production of 5H5F from furfural oxidation and its transformation of a range of C4 chemicals.

- 1. Palai, Y. N.; Shrotri, A.; Fukuoka, A. Selective Oxidation of Furfural to Succinic Acid over Lewis Acidic Sn-Beta. *ACS Catalysis* **2022**, *12*, 3534–3542.
- 2. Palai, Y. N.; Fukuoka, A.; Shrotri, A. 5-Hydroxy-2(5H)-Furanone: A New Platform Chemical for Bio-Based Four Carbon Chemicals. ChemRxiv August 25, 2023. https://doi.org/10.26434/chemrxiv-2023-n5pl8.

## OL4

# Effects of Ecotourism on Land Use Land Cover Dynamics: Evidence from Sagarmatha National Park and Khaptad National Park, Nepal

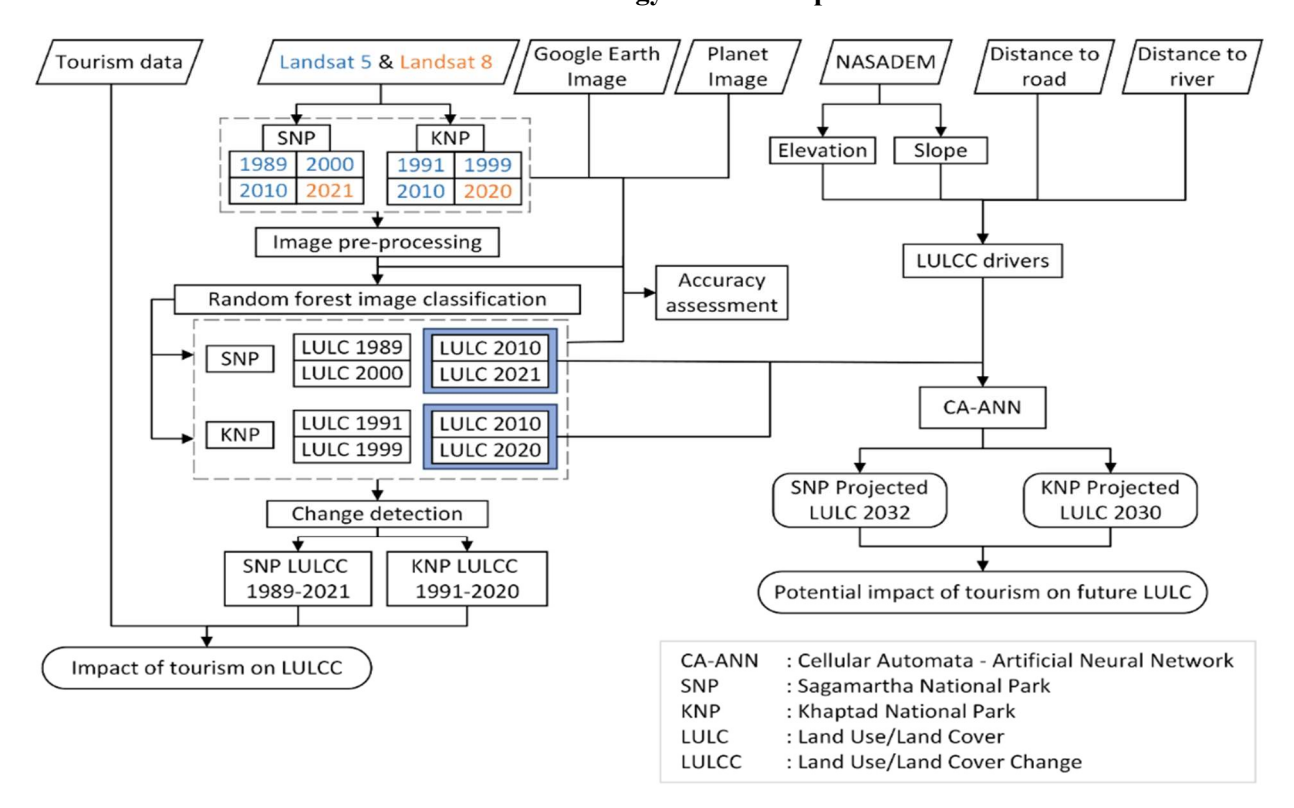
Ankita Gupta, Teiji Watanabe

<sup>1</sup>Graduate School of Earth and Environmental Science, Hokkaido University.

**Introduction.** In Nepal, ecotourism revolves around encouraging the involvement of people in the planning and management of tourism, promoting community development and nature conservation through tourism linkages. This study aims to investigate the contribution of ecotourism activities within SNP and KNP on LULC change based on a remote sensing approach.

Results and Discussion. Ecotourism can have a negative impact on the environment if it is not properly planned and managed. This study investigated the impact of ecotourism on land use and land cover (LULC) in Sagarmatha National Park (SNP) and Khaptad National Park (KNP) in Nepal. This loss of forest cover has been accompanied by an increase in built-up, agricultural, grassland, and bare land. The increase in built-up area is a direct result of increased tourist activity. This increased activity has the potential to lead to environmental problems such as landslides, floods, and changes. The study also found that the loss of snow and glaciers in the core zone of SNP is a cause for concern. The study recommends that better planning and management of ecotourism is needed to ensure the sustainability of these national parks.

#### The chart describes the detailed methodology used for impact of tourism LULC:



- 1. Baral, N., Kaul, S., Heinen, J. T., & Ale, S. B. Journal of Sustainable Tourism, 25(12), 1776–1791.
- 2. Bashyal, A. et.al. (2022). Journal of Threatened Taxa, 14(11), 22156–22.

<sup>&</sup>lt;sup>2</sup>Graduate School of Earth and Environmental Science, Hokkaido University.

## IL<sub>2</sub>

# **Application of Remote Sensing in Civil Engineering**

## Kedarnath Mahapatra

Department of Civil Engineering, Faculty of Science and Engineering, Shizuoka Institute of Science and Technology

With technological advances in satellite remote sensing over the last 40 years, there is tremendous potential in leveraging the vast pool of high-resolution multi-sensor data collected by space agencies of different countries for Civil Engineering applications. This study presents a framework to utilize remote sensing data in civil engineering projects focusing on sustainable land utilization, construction planning, and monitoring the impact of climate change phenomena and natural disasters on existing constructions. Finally, this study offers a perspective of how Civil Engineering could make greater use of the geospatial data in conjunction with conventional methods/techniques and contribute to achieving sustainability goals.

# **Luncheon Seminar**

# The Chances and Pitfalls of Aiming at an Academic Career in Japan

## Olaf Karthaus

Chitose Institute of Science and Technology

I will start this presentation with a short self-introduction of how, when and why I came to Japan.

Then I will give a short assessment and a personal view of the labor market and the labor policies of Japanese academia.

I will conclude my talk with my strategies to cope with cultural differences.

There will be ample time for a discussion and questions.

## IL3

# Next-Generation mRNA Vaccines Against Infectious Diseases and Cancer

## Satoshi Uchida<sup>1,2</sup>

<sup>1</sup>Medical Research Institute, Tokyo Medical and Dental University (TMDU); <sup>2</sup>Innovation Center of NanoMedicine (iCONM), Kawasaki Institute of Industrial Promotion

**Introduction.** mRNA vaccines have demonstrated their potential in COVID-19 vaccines. The success has prompted vigorous research and development in this field. However, mRNA vaccines still have several issues, including relatively severe adverse effects in infectious disease vaccines and low effectiveness in cancer vaccines. We are developing next-generation mRNA vaccines to address these issues.

Results and Discussion. In mRNA vaccines against infectious diseases, immunostimulatory lipids in lipid nanoparticles (LNPs) are a cause of adverse effects. Therefore, vigorous efforts have been devoted to refining LNP design to reduce the adverse effects. Alternatively, we attempted to develop naked mRNA-based vaccines, avoiding using LNPs. To obtain efficient vaccination even with naked mRNA, we injected mRNA into the dermal tissue, rich in antigen-presenting cells, and used a jet injector to enhance mRNA delivery efficiency. Naked mRNA jet injection exhibited vaccination effects comparable with a commonly used LNP in mice. Notably, in applying to the COVID-19 vaccine using mRNA encoding SARS-CoV-2 spike protein, this strategy protects mice from the SARS-CoV-2 challenge. Furthermore, jet injection effectively induced antibody production in non-human primates. This study demonstrated the utility of naked mRNA jet injection for safe and effective vaccination against infectious diseases.

Cancer vaccines need improvement in effectiveness to overcome immune-suppressive tumor microenvironment and relatively low antigenicity of tumor antigens. We tackled this effectiveness issue by focusing on adjuvanticity. Herein, vaccine adjuvanticity was enhanced by hybridizing mRNA with immunostimulatory double-stranded RNA strands (Figure 1). The comb-structured mRNA thus prepared expresses antigen proteins, and the immunostimulatory teeth function as an adjuvant. As a result, the comb-structured mRNA improved the vaccination effects of several LNPs, including lipoplex, used in cancer vaccine clinical trials. Our strategy has successfully demonstrated its feasibility in mouse cancer models by targeting model and tumor-associated antigens. Collectively, these two studies provide new insights into mRNA vaccine developments targeting infectious diseases and cancers.

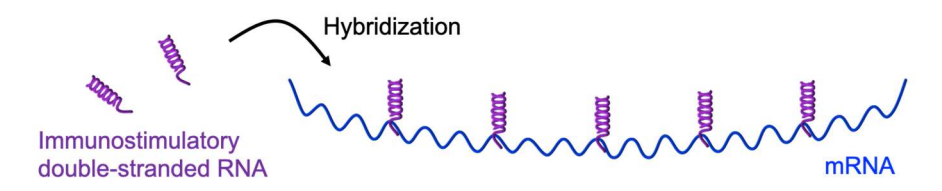


Figure 1. Comb-structured mRNA

- 1. S. Abbasi, M. Matsui-Masai, A. Hayashi, T. Tockary, S. Akinaga, K. Kataoka, S. Uchida, *bioRxiv* **2023**, 10.1101/2023.02.27.530188.
- 2. T. A. Tockary, S. Abbasi, M. Matsui-Masai, A. Hayashi, N. Yoshinaga, E. Boonstra, Z. Wang, S. Fukushima, K. Kataoka, S. Uchida, *Proceedings of the National Academy of Sciences* **2023**, *120* (29), e2214320120.

# **Active Control of Plasmonic Nanoparticles Using Polymer Gels**

### Hideyuki Mitomo

<sup>1</sup>Research Institute for Electronic Science, Hokkaido University.

Gold nanoparticles (AuNPs) show unique optical phenomena called localized surface plasmon resonance (LSPR), which is a collective oscillation of electrons in AuNPs induced by light irradiation. These properties are governed by size and shape of AuNPs as well as three-dimensional arrangement in their assemblies such as distance among them. To enhance plasmonic properties for practical applications, structure control of self-assembled AuNP arrays is important. In particular, dynamic control of their structures is one of the new topics [1]. Polymer substrates as soft matters could support active tuning of AuNP assemblies [2].

In this talk, I will introduce one approach on this topic [3]. That is "active control of the self-assembled AuNP film on the hydrogel" (Fig. 1A). We prepared self-assembled AuNP thin films on the solid substrate and transferred them onto the polymer hydrogel. Plasmonic properties were tuned depending on the volume changes of the gel, as the gap distance of AuNPs in the film changed. This active control of the gap distance can be applied to the substrate for molecular detection by surface-enhanced Raman scattering (SERS), that is Raman signals can be greatly enhanced at the enhanced electric field around metal nanostructures. As narrow gap structures can provide good hotspots for the SERS detection, self-assembled nanoparticle arrays are good substrates for this. However, there is an significant issue on this application. One of the important target

molecules is bio-molecules, such as proteins and DNAs. As they have large volumes, it is difficult to be inserted into the narrow gaps due to steric hindrance (Fig. 1B-ii). Here, actively gap tunable AuNP array could provide wider gaps for the target insertion between particles, which release steric effects, and also narrow gaps for SERS detection, which allow great enhancing effect (Fig. 1B-i). We first detected Crystal violet as a typical example of small target molecules. Active gap approach provided two times stronger signals compared to the closed gap array. For the protein detection, in which we cytochrome c, as a biopolymer, we obtained 10 times stronger signals (Fig. 1B-iii). This result indicates that actively gap tunable AuNP arrays can be a good SERS substrate for biomolecular detection.

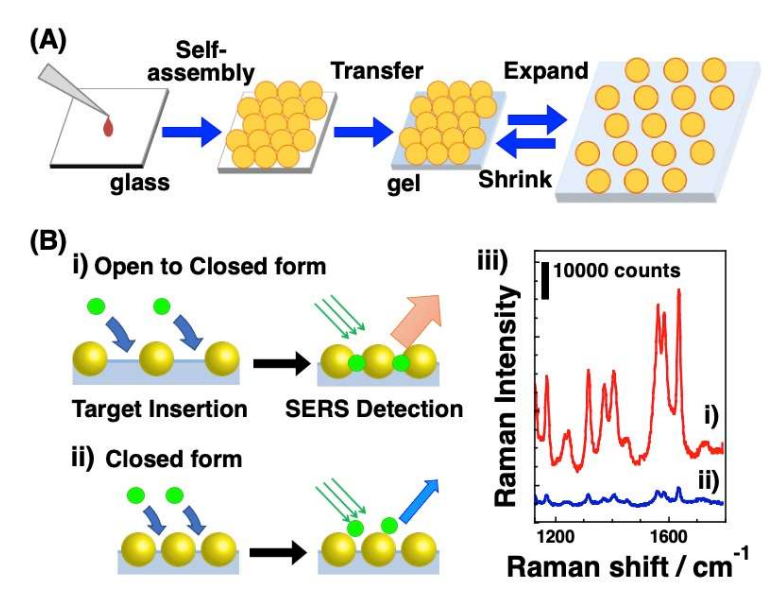


**Figure 1.** (A) Schematic illustration of the preparation of gap tunable AuNP arrays on the hydrogel and (B) SERS detection using active gap tunable AuNP arrays; i) scheme of active gap approach, in which gap is open for the target insertion and then closed for SERS detection, ii) scheme of conventional approach, in which gap is closed for target insertion and SERS detection, and iii) SERS spectra of cytochrome c measured by these approaches.

- 1. H. Mitomo, K. Ijiro, *BCSJ* **2021**, *94*, 1300. (Review, Open Access)
- 2. S. Nakamura, H. Mitomo, K. Ijiro, *Chem. Lett.*, **2021**, *50*, 361 (Review, Open Access)
- 3. H. Mitomo, K. Horie, Y. Matsuo, K. Niikura, T. Tani, M. Naya, and K. Ijiro, *Adv. Opt. Mater.*, **2016**, *4*, 259.

# Construction of Functionalized Red-Light Photoswitches by Selective Copper-Catalyzed Indigo N-Arylation

<u>Dennis Chung-Yang Huang</u><sup>1\*</sup>, Amit K. Jaiswal, Priya Saha, Julong Jiang, Kimichi Suzuki, Anna Jasny, Bernd M. Schmidt, Satoshi Maeda, Stefan Hecht<sup>2\*</sup>

<sup>1</sup>Institute for Chemical Reaction Design and Discovery (WPI-ICReDD), Hokkaido University, N21W10, Kita-Ward, Sapporo 001-0021, Japan

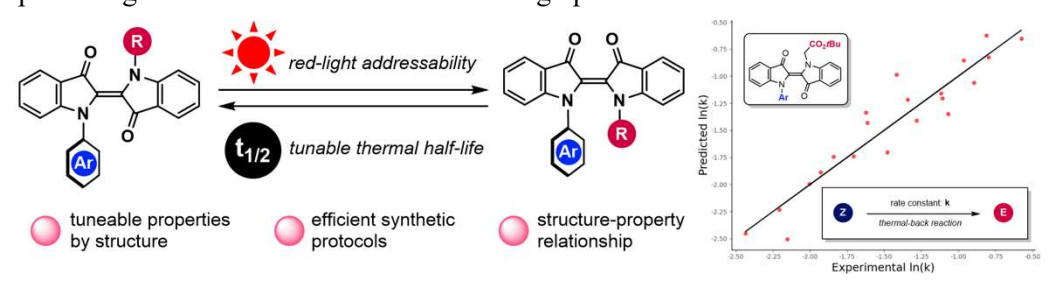
<sup>2</sup>Department of Chemistry & IRIS Adlershof, Humboldt-Universität zu Berlin, Brook-Taylor-Strasse 2, Berlin 12489, Germany

<sup>3</sup>Institute for Organic Chemistry and Macromolecular Chemistry, Heinrich Heine University Düsseldorf, Universitätsstr. 1, 40225 Düsseldorf, Germany

**Introduction.** In this work, we developed a new Cu-catalyzed *N*-arylation methodology to directly build redlight photoswitches from the indigo dye. This method operates at mild conditions and can tolerate various synthetically useful functional groups. DFT parameterization and multivariate linear regression modelling provides correlation between the molecular structures and their thermal half-lives.

**Results and Discussion.** Introducing photocontrol to molecular systems is an attractive strategy due to the ability of light to achieve high spatial, temporal, and spectral resolution. In particular, red- and infrared light has emerged as ideal sources of irradiation because of their low probability of causing photo-damage as well as higher penetration depth into biological tissues. Indigo, one of the most abundant dyes utilized in human history, has thus become a promising candidate for developing photo-responsive molecular tools thanks to its push-pull molecular structure that allows for natural red-light absorbance. It was found that when both nitrogens are substituted, these compounds undergo efficient E-Z photoisomerization under red-light irradiation, where the dramatic steric and electronic changes during this process can be exploited for system design.

However, the lack of robust and divergent synthetic methods to prepare indigo derivatives from the inexpensive parent dye has been a great hurdle preventing their broad application. We previously reported preliminary synthetic protocols leading to N,N'-disubstituted indigos and found that especially the N-aryl groups can be used to rationally tune the thermal half-lives. Herein, we present an efficient Cu-catalyzed mono-N-arylation of indigo dye. Under the optimal conditions, we could achieve selective installation of aryl moieties carrying a wide variety of functional groups, including ones that can be further derivatized for applications. With an additional N-alkylation step, N,N'-disubstituted indigo photoswitches could be easily generated. All compounds switch efficiently under the influence of red light, where the thermal half-lives are dependent on the N-substituents. We then applied multivariate analysis to correlate the molecular structures with the rate of thermal-back reactions. This data science workflow first utilized simple DFT calculation to obtain molecular descriptors, which serve as inputs for constructing suitable linear regression models. This approach thus provides a general method for predicting the thermal half-lives of new indigo photoswitches.



- 1. Huang, C.-Y.; Bonasera, A.; Hristov, L.; Garmshausen, Y.; Schmidt, B. M.; Jacquemin, D.; Hecht, S. *J. Am. Chem. Soc.* **2017**, *139*, 15205.
- 2. Huang, C.-Y.; Hecht, S. *Chem. Eur. J.* **2023**, *29*, e202300981.
- 3. Jaiswal, A. K.; Saha, P.; Jiang, J.; Suzuki, K.; Jasny, A.; Schmidt, B. M.; Maeda, S.; Hecht, S.; Huang, C.-Y. manuscript in preparation.

# Objective Discrimination of Drug Resistant Cells in Chronic Myeloid Leukemia by Multivariate Analysis Assisted Raman Spectroscopy

<u>Hemanth Noothalapati</u><sup>1</sup>, Rahul Mojidra<sup>2,3</sup>, Arti Hole<sup>2</sup>, Keita Iwasaki<sup>4</sup>, Tatsuyuki Yamamoto<sup>1</sup>, Murali Krishna C<sup>2,3</sup> and Rukmini Govekar<sup>2,3</sup>

**Introduction.** Chronic myeloid leukemia (CML) is a type of cancer that starts in myeloid cells which make red blood cells, platelets and most white blood cells. CML is caused due to genetic abnormality, especially due to translocation of parts of two chromosomes leading to continuous production of fused gene product with tyrosine kinase activity. Targeted therapy of CML with imatinib, a tyrosine kinase inhibitor (TKI), is the most successful oncotherapy so far. However, success of this therapy is limited to the initial chronic phase (CP), wherein 90% of patients reach hematological remission. In the remaining patients, treatment failure occurs initially (primary resistance) or the initial responders may develop resistance during the course of treatment (secondary resistance). If the resistant patients are unresponsive to other TKIs, they will progress to the terminal phase of blast crisis where the survival is only 7–11 months. Current protocols to predict resistance include qRT-PCR to detect residual disease and assessment of mechanisms of resistance by chromosome banding analysis for additional chromosomal aberrations, fluorescence in situ hybridization for BCR-ABL1 gene amplification and mutation analysis to detect kinase domain mutations. These tests require specialized technologies, trained manpower and consumables with high recurrent cost. Therefore, development of alternative technologies for reliable and rapid prediction of resistance before or during treatment is necessary to improve treatment outcomes.

**Results and Discussion.** We propose Raman spectroscopy (RS) to be a suitable alternative. RS is a vibrational spectroscopic technique which is sensitive to composition through molecular fingerprint and has found many

applications in biology and medicine. Therefore, we developed Imatinib resistant cells (K562R from drug sensitive cell line (K562S) and investigated genetic changes. Especially copy number variation specific to imatinib-resistant cells were detected by array comparative genomic hybridization (aCGH). Since aCGH is technologically demanding, expensive and not suitable to serve as a single economic test, we explored the potential of RS for diagnosis and screening (Fig.1). We successfully demonstrate that multivariate curve resolution assisted Raman microspectroscopy as a single method to objectively discriminate imatinib-resistant and -sensitive cells by capturing global genomic alterations and the results will be discussed in detail.

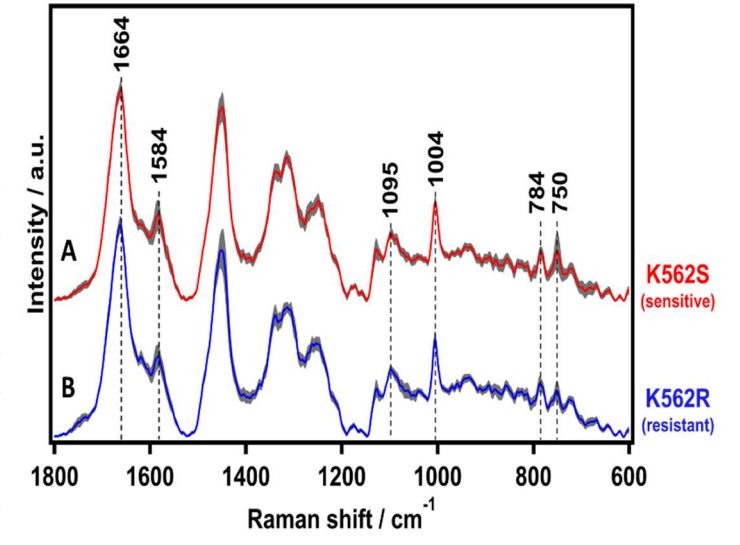


Figure 1. Comparison of average Raman spectra. (A) imatinib- sensitive K562S (red) and (B) imatinib-resistant K562R (blue) cell pellets along with their standard deviation (grey shade)

#### References

1. Rahul Mojidra et al., Cells, 10, 2506 (2021)

<sup>&</sup>lt;sup>1</sup> Faculty of Life and Environmental Sciences, Shimane University, <sup>2</sup>Advanced Centre for Treatment, Research and Education in Cancer, Tata Memorial Centre, India, <sup>3</sup> Homi Bhabha National Institute, BARC Training School Complex, India, <sup>4</sup> The United Graduate School of Agricultural Sciences, Tottori University

# **Predicting Highly Enantioselective Catalysts Using Machine Learning**

<u>Pavel Sidorov</u><sup>1</sup>, Nobuya Tsuji<sup>1</sup>, Chendan Zhu<sup>2</sup>, Yuuya Nagata<sup>1</sup>, Timur Gimadiev<sup>1</sup>, Alexandre Varnek<sup>1,3</sup>, Benjamin List<sup>1,2</sup>

<sup>1</sup> Institute for Chemical Reaction Design and Discovery (WPI-ICReDD), Hokkaido University

<sup>2</sup> Max-Planck-Institut für Kohlenforschung

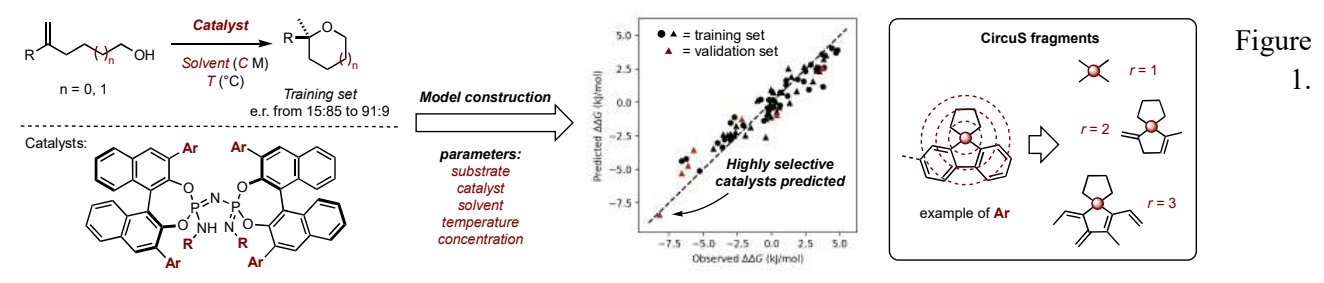
<sup>3</sup> Laboratory of Chemoinformatics, University of Strasbourg

**Introduction.** Asymmetric catalysis is one of the most important techniques in the modern organic synthesis, allowing to guide the chemical reaction to a desired product with high efficiency. While machine learning models using molecular properties enable quantitative data evaluation, costly calculations are often required. In contrast, using models based on 2D molecular descriptors such as binary molecular fingerprints is time- and cost-efficient, but their predictive performance remains insufficient.

**Results and Discussion.** In this work, we design new selective imidodiphosphorimidate (IDPI) catalysts for hydroalkoxylation reactions [1]. In chemistry, machine learning models are built using molecular descriptors – numerical parameters derived from chemical structures. In catalysis, physical parameters or calculated 3D structures are often used, however, for IDPI catalysts it is extremely difficult to calculate such descriptors due to their complex structure. Instead, we employ a machine learning model based on molecular fragments, which are fine-tuned for asymmetric catalysis and represent cyclic or polyaromatic hydrocarbons, enabling robust and efficient virtual screening of these catalysts. We demonstrate that the circular molecular fragments perform better than other 2D descriptors in this task.

The resulting model can process catalyst structures, reaction substrates and products, as well as reaction condition simultaneously, thus providing a general approach to modeling catalyzed reaction outcome. We demonstrate in statistical tests that the circular molecular fragments perform better than other 2D descriptors in this task. Moreover, while the model was trained using data with only moderate selectivities, we have successfully performed the virtual screening of previously experimentally untested catalysts and selected and validated experimentally new hits showing higher selectivities in a previously unaddressed transformation.

We also introduce a way to interpret the models by calculating the contributions of atoms to the modeled property, using the approach called ColorAtom [2]. This allows to guide the design of the catalysts with unknown structures towards desired selectivity.



Hydroalkoxylation reaction and IDPI catalysts are the target of this study. Using machine learning based on Circular Substructure (CircuS) fragment descriptors, we built a model able to predict a new highly selective catalyst.

- 1. N. Tsuji, P. Sidorov, C. Zhu, Y. Nagata, T. Gimadiev, A. Varnek, B. List, B., *Angew. Chem. Int. Ed.* **2023**, 62, e202218659.
- 2. G. Marcou, D. Horvath, V. Solov'ev, A. Arrault, P. Vayer, A. Varnek. Mol. Inf. 2012, 31(9), 639-642.

## OL<sub>5</sub>

# User Evaluation of a 360-Degree Video of Home-Ventilator Care for Curriculum Development

Noriyo Colley<sup>1</sup>, Mari Igarashi<sup>2</sup>, Misuzu Nakamura<sup>3</sup>, Teki Imai<sup>1</sup>, Shinji Ninomiya<sup>4</sup>, Sozo Inoue<sup>5</sup>, Yo Kurashima<sup>1</sup>, Kenji Hirata<sup>1</sup>, Kazutoshi Cho<sup>1</sup>, Yusuke Watanabe<sup>1</sup>, Shunsuke Komizunai<sup>6</sup>, Atsushi Konno<sup>1</sup>, Satoshi Kanai<sup>1</sup>, Minoru Ishida<sup>1</sup>, Makoto Takahashi<sup>1</sup>

<sup>1</sup>Hokkaido University.; <sup>2</sup>International University of Health and Welfare, <sup>3</sup>The JIKEI University, <sup>4</sup>Hiroshima International University, <sup>5</sup>Kyusyu Institute of Technology, <sup>6</sup>Kagawa University

**Introduction.** The number of children with Home-Ventilators (HVs) has been doubled in this decade in Japan<sup>1</sup>. Due to the rapid increase of healthcare service demand, lack of community nurses and special-school nurses with competent to HV care at home or school settings becomes severer. However, there is a limited opportunity for nursing students to learn from real situation of HV care during the COVID-19 pandemic. The aim of this research is, therefore, to evaluate a 360-degree panorama video<sup>2</sup> of HV care at a special need school for curriculum development of undergraduate nursing course.

Results and Discussion. Fifty-five third year bachelor course nursing students (hereafter **B3**), 42 master course nursing students (hereafter **M**) from three universities, and 7 Registered Nurses from a special need school (hereafter **RN**) participated. A 360-degree video at a special need school was developed after the permission from the students, their family, teachers, and the president of the school, then Adobe Premiere Pro was used to blur the face to make the individual unidentifiable. Insta 360 ONE was used to record and PICO G2 4K was used to view the video. Original questionnaire was created by Google Forms using 4 Likert scale to ask if the video was handy, real, motive, enough time, good balance of time and contents, adequate for third graders, and adequate for fourth graders. Data was analyzed by Microsoft Excel for Microsoft 365 MSO. Approval from Ethical Committee in Hokkaido University Hospital was obtained before commencement of this study (022-0093).



Handy Real Motive Enough time Time content balance. 3rd grader 4th grader

#Totally Agree #Agree #Disagree #Estremely Disagree

Figure 1 Our developed 360-degree panorama video

Figure 2 User Evaluation of the 360-degree video

As the number of special-need school RNs is small, Steel-Dwass' Multiple comparison test was used. There are significant differences in "motive" between B3 and M (p<0.05), and in "adequate for third graders" between B3 and RN (p<0.05), which indicates the 360-degree video increased B3 group's motivation more than Master course students. Interestingly, B3 group was stimulated to learn HV care by the video, however, RNs felt it is early for B3 to study about HV care. Overall evaluation was positive to use a 360 video to learn HV care: there are no significant differences among three groups in the rest of questions. In conclusion, the result indicated that B3 is appropriate to start learning at lecture with a 360-degree video, and 4<sup>th</sup> grade would be the best to learn HV care at practicum.

- 1. Japan Visiting Nurses Foundation (JVNF), Nursing Manual of Medical Care at School (for Nurses), 2020, https://www.jvnf.or.jp/home/wp-content/uploads/2020/07/caremanual1-1.pdf
- 2. Tsui-Yun Yang, Chun-Hsia Huang, Chi An, Li-Chueh Weng, Construction and evaluation of a 360 degrees panoramic video on the physical examination of nursing students, Nurse Education in Practice, Volume 63, 2022, 103372, <a href="https://doi.org/10.1016/j.nepr.2022.103372">https://doi.org/10.1016/j.nepr.2022.103372</a>.
- 3. Hanna Lee, & Jeong-Won Han, Development and Evaluation of a Virtual Reality Mechanical Ventilation Education Program for Nursing Students, BMC Medical Education, (2022)22:775.

## OL<sub>6</sub>

# State of Data Assurance in Corporate Environmental Disclosures in India

Ahmad Mohd Khalid<sup>1,2</sup>

<sup>1</sup>Institute for the Advanced Study of Sustainability, United Nations University <sup>2</sup>Faculty of Environment and Information Studies, Keio University

#### Introduction.

Corporate firms undertake assurance/third party evaluation of their sustainability disclosures to increase credibility among investors and fulfill data disclosure requirements as per international and national reporting frameworks such as GRI, TCFD among others. This study explores the state of corporate environmental disclosure (CED) assurance among the Bombay Stock exchange (BSE) 50 firms in India.

#### Results and Discussion.

The analysis of BSE 50 firms in India as per their Business Responsibility and Sustainability Report (BRSR) for the financial year 2022-23 shows that environmental data assurance is at reasonable level and the awareness levels are rising. Climate related disclosures help firms achieve profitability and sustainability simultaneously (Maji and Kalita, 2022). The data set includes 49 firms as BRSR was not available for one firm.

Table 1 CED Assurance Level among BSE 50 Firms in India

Assurance Level	No. of Firms	Percentage
Full Assurance	25	50
Partial Assurance	11	22
No Assurance/yet to do	8	16
No information on assurance	5	10
Total	49	

It was also found that assurance on CED data was higher among the non-financial firms compared to financial/services firms. For example, 18 of the 32 non-financial firms undertook full assurance with respect to seven of 17 financial or services firms. This may also be attributed to the fact that more energy intensive and polluting firms disclose more environmental data and undergo data assurance to show their legitimacy and stakeholder responsibility (Luo et al., 2023). Many firms either undertook partial assurance or plan to do it in future because according to Securities Exchange Board of India (SEBI)'s requirement assurance exercise was voluntary for the financial year 2022-23 but would become mandatory starting FY 2023-24 with reasonable level of assurance. It is expected that Indian firms will ramp up their disclosures and assurance levels in coming years to meet stakeholder expectations, mandates, and requirements to fulfill their environmental responsibilities.

- 1. S.G. Maji, N. Kalita, H. Climate change financial disclosure and firm performance: empirical evidence from Indian energy sector based on TCFD recommendations. *Soc. Bus. Rev.* **2022**, *17*, 594-612.
- 2. L. Luo, Q. Tang, H. Fan, J. Ayers, Corporate carbon assurance and the quality of carbon disclosure. *Acc. Finance.* **2023**, *62*, 657-690.

## PL3

# Plant Transcription Factor Engineering for Our Sustainable Future

### Nobutaka Mitsuda

Bioproduction Research Institute / Global Zero Emission Research Center, National Institute of Advanced Industrial Science and Technology (AIST)

Introduction. Climate change brought by our long-term excess GHG emission becomes undoubtedly serious threat for our sustainable future. According to the latest IPCC report, we have to achieve net "zero emission" around 2050 and enter the era of "negative emission" to suppress the temperature rise less than 1.5 °C from that before industrial revolution. To this end, we must adopt all possible measures to reduce/absorb GHG. One of the expected methods is the utilization of green plants, which can absorb CO<sub>2</sub> for photosynthesis.

**Results and Discussion.** When we consider the utilization of plants, photosynthesis and wood formation are two major issues to be tackled. Wood is the biggest terrestrial biomass and is synthesized in almost all higher plants including herbaceous species like grasses. In terms of plant biology, wood is the accumulated plant secondary cell walls, which are produced in plant tissues where rigidity is required while the thinner primary cell wall is synthesized in all plant cells. More than 50% of plant dry biomass (> 90% in some species like trees) is cell walls. Annual production of woody substances reaches more than 50 billion tons and a part of them is utilized for human being for the construction, paper production, and many other purposes. Therefore the development of fast-growing plants, which accumulate cell walls faster is the important research topics in the plant biotechnology field. More than decade ago, we discovered NST genes, the master transcription factor genes of wood formation and found that loss of this gene makes plants lose their wood formation almost completely (nst mutant, Fig. 1). We then conversely found that the reinforcement of this gene makes plants produce more wood<sup>2</sup> (Fig. 2), which not only absorbs more CO<sub>2</sub> but also supplies stronger wood. By using the nst mutant as a base of systematic screening to find a new regulator of plant cell wall, we further identified the regulators of primary cell walls; GroupIIId/e ERF transcription factors<sup>3</sup>. Forced expression of this gene in woody tissues increased primary cell wall accumulation with concomitant reduction of lignin, one of major components of secondary cell wall<sup>4</sup>. Because lignin is a major obstacle of cellulose extraction from wood, this technology may help the development of new wood which is more feasible for the production of cellulose nano fiber, bioethanol, and other cellulose derivatives. Cell wall engineering by the manipulation of transcription factor genes can dynamically change the nature of cell walls and their productivity. We believe that our findings would contribute to the construction of sustainable society by absorbing more CO<sub>2</sub> and/or reducing petroleum consumption.



**Fig.1** Arabidopsis and poplar plants with loss of *NST* genes (Right)

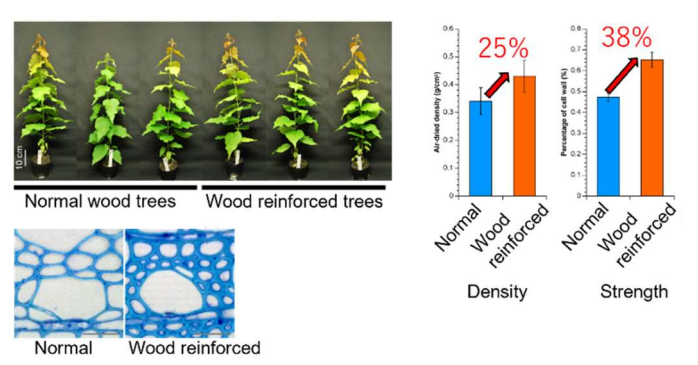


Fig. 2 Poplar trees with reinforced wood accumulation. Left bottom panel shows microscopic images of cross section of wood tissue.

- 1. Mitsuda et al., Plant Cell, 2007, 19, 270.
- 2. Sakamoto et al., Sci Rep., 2016, 6, 19925.
- 3. Sakamoto et al., Nat Plants, 2018, 4, 777.
- 4. Nakata et al., Front. Plant Sci., 2021, 12, 698.

## IL4

# Innovative Environmental Technologies for "Garbage"

Toshikazu Kawaguchi\*, \*\*

\*Graduate School of Global Food Resources, \*\*Faculty of Environmental Earth Sciences Hokkaido University

Our research group is interested in material cycle. Terminal of all the materials is "garbage incinerator". Garbage incinerator is well-organized by industry. However, the chemical system of garbage incinerator is not clarified yet. As you know, garbage generally contains many kinds of molecules and atoms. Therefore, the chemical system is very complicated. Researchers of combustion engineering believe that it is very difficult to understand the system. But technology advances day by day. Especially, the digital camera technology is drastically innovated in the last decade. People instantly take high-speed video by "GoPro camera" and upload to the website of "YouTube". At the beginning of this presentation, I will introduce that the visualization technology of the mass transfer and the chemical reaction in garbage incinerator by this digital camera. Hokkaido is very famous place for seafood. In particular, shrimp and crab are very popular. In market, there is a huge amount of shell of those crustaceans in garbage. Therefore, the application of abandoned shell is introduced here. Shell is made of chitin which is N-Acetyl-D-glucosamine. After deacetylation, useful material, chitosan, is produced. Since chitosan has amine-group, it shows very high affinity with biological material. At the next, I will introduce here the effect of chitosan onto the plants. In Hokkaido, new farmer starts from the cultivation of "tomato" at first. And then, some farmer attempts onion farming, and other farmer tries fruits. Our research group will exhibit the demonstration of cultivation using chitosan for tomato, onion, and grape in farms of Hokkaido University. Beef products and milk products in Hokkaido are very important industry. Livestock needs energy. In recent, livestock farmer installs the biogas plant in paddock to produce electricity. However, the remained wastewater still shows very high value of COD (Chemical Oxidation Demand) which means the index of pollution. Now, farmer requests the method for treatment of COD in wastewater from paddock. Public wastewater facility uses biological treatment. Organic matters are oxidized by bacteria in anaerobic condition. Since this oxidation process involves electron transfer, it is proposed to take electricity from the biological treatment. In other words, the pollution in wastewater is treated and generate electricity simultaneously. This system is so-called microbial fuel cell (MFC). I will introduce the recent aspect of our MFC. Three research regarding the garbage treatment will be introduced in this talk. I believe that those environmental techniques will conduct to the sustainable society directly.

## **IL5**

# Investigation of Cathodic Polarization Characteristics of Steel Bars in Mortar Mixed with Green Tea Leaves

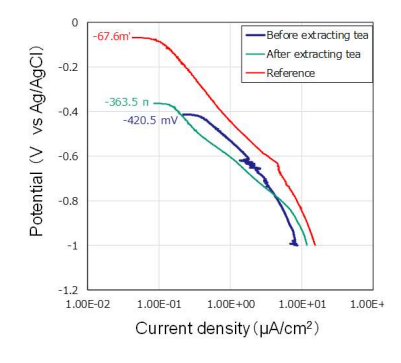
<u>Takahiro Nishida<sup>1</sup></u>, Keiyu Kawaai<sup>2</sup>

<sup>1</sup>Department of Civil Engineering, Shizuoka Institute of Science and Technology.; <sup>2</sup>Department of Civil Engineering, Graduate School of Science and Engineering for Production and Environment, Ehime University

**Introduction.** Reinforced concrete is one of the most common materials used in social infrastructure due to its economic efficiency, construction-friendliness, and structural stability. However, in coastal areas and areas where de-icing agents are applied, Chloride Attack is a major problem as it causes deterioration of the structures. Recently, we found that antioxidants in foodstuffs are effective in inhibiting steel corrosion inside concrete.

**Results and Discussion.** The experiment overview is as follows. The mortar used in the specimen had a water-cement ratio of 0.6. The specimen was 50×40×90 mm, and a D6 steel bar with a length of 50 mm was embedded inside. Lead wires were connected by soldering to the steel bar in order to perform polarization tests. 5.0 kg/m<sup>3</sup> of Cl was mixed in the mortar to cause corrosion reaction of the steel bar. Commercial tea was used (from Kakegawa) and the specimens were dried at 20°C and 20% relative humidity for one month before and after being brewed with 60°C hot water. The specimens were then passed through a sieve of 150μm.

Fig. 1 shows the cathodic polarization curve of mortar-embedded steel mixed with tea leaves. Half-cell potentials that were measured for each are also indicated in the figure. Regarding the half-cell potentials, it shifted to the negative side due to the addition of tea leaves. Generally, it is considered that corrosion will be possible with the decrease of half-cell potentials, but it is speculated that this decrease in half-cell potentials in this case is due to the suppression of cathodic reaction as shown in Fig.2. That is, it is found that half-cell potentials decrease with the lower dissolved oxygen content (C) compared to the higher dissolved oxygen content (D) in the anodic polarization curve (B), hence it can be speculated that the half-cell potentials of mortar-embedded steel mixed with tea leaves have decreased. Moreover, the cathodic polarization curve as a whole shifted to the lower left side due to the mixing of tea leaves, which it is considered as a condition in which it is difficult for cathodic reactions to occur.



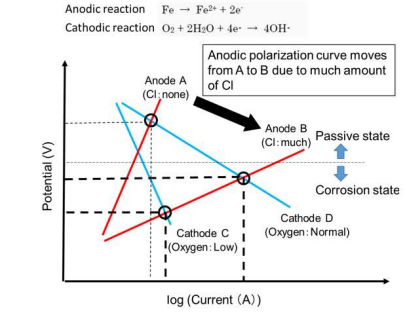


Fig.1 Cathodic polarization curve.

Fig.2 Outline of polarization curves of steel in concrete.

# Harnessing Nanostructured Materials: Pushing the Limits of Ultra-Sensitive Virus Detection

## Akhilesh Babu Ganganboina<sup>1</sup> and Enoch Y Park<sup>2</sup>

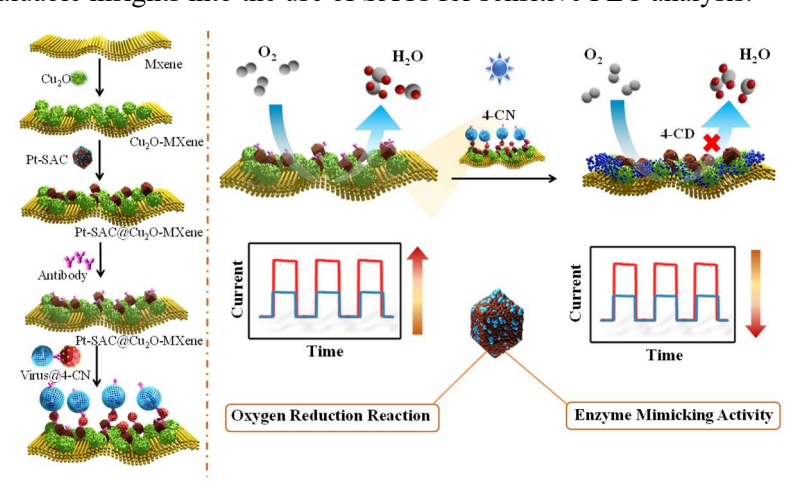
<sup>1</sup>1 International Center for Young Scientists ICYS-NAMIKI, National Institute for Materials Science, 1-1 Namiki, Tsukuba, Ibaraki 305-0044, Japan.; <sup>2</sup> Research Institute of Green Science and Technology, Shizuoka University, 836 Ohya Suruga-ku, Shizuoka 422-8529, Japan

#### Introduction

Re-emerging outbreak of new variant of coronavirus stimulates the requisite of the immunoassay development as a feasible and practical front-line control of the pandemic. Currently, genetic testing by RT-PCR and antigen tests by immunochromatography are performed for virus and pathogen diagnosis. However, the former is highly sensitive but lacks rapidity, and the latter has a problem of low detection sensitivity. The development of a diagnostic method that can detect pathogenic viruses that cause infectious diseases on-site (outbreak site) with higher sensitivity and speed than immunochromatography is desired. To achieve such kind of biosensor, engineering biosensing technologies as well as new strategy of sensing has become one of the most important issues in recent science. Underlying the drawback of the existing bioassay, the more precise and sensitivity in targeting the virus is required to overcome the false-negative regard on biosensor-based approaches. It requires the development of a biosensor that would ideally produce a quantitative signal for individual viral or pathogen particles. To obtain the desired sensitivity, we propose a new class of voltage pulse induced electrochemical sensor, nanozyme-based immunoassay and self-powered photoelectrochemical (PEC) based methods for the ultrasensitive virus and pathogen detection which recently attracted a lot of attention in healthcare systems.

### **Results and Discussion**

The photo-driven electrochemical response is an essential part of the PEC analysis, making it indispensable to amplify the corresponding PEC signals for sensitive detection. Efficient photoelectrochemical (PEC) detection requires a deep understanding of the processes involved in generating, separating, and reacting photoinduced carriers at interfaces. However, slow interfacial reactions and the need for appropriate photoactive layers pose significant challenges to constructing advanced PEC platforms. In this study, platinum single-atom catalysts (Pt SACs) were integrated onto CuO and two dimensional Mxene as a proof of concept, amplifying PEC signals by boosting oxygen reduction reactions. As a newly emerging class of 2D materials, Ti C T MXene was used as fantastic support to uniformly anchor Cu O nanoparticles due to its electronegative surface. Pt SACs were also shown to exhibit efficient peroxidase-like activity, depressing PEC signals through Pt SACs-mediated enzymatic precipitation reactions. By utilizing the oxygen reduction and peroxidase-like activity of Pt SACs, a robust PEC sensing platform was successfully constructed for the sensitive detection of SARSCoV-2. This research provides valuable insights into the use of SACs for sensitive PEC analysis.



**Scheme. 1.** Schematic illustration depicting the Synthesis process of Pt SACs@Cu<sub>2</sub>O-MXene and and principle of the PEC analytical platform with the expected change in photocurrent profile due to the bifunctional Pt SACs.

# Pathological Role of Macrophage in Cartilage Degeneration: Insights into the Pathogenesis of Osteoarthritis and Therapeutic Aspects

Alaa Terukawi & Norimasa Iwasaki
Department of Orthopedic Surgery, Faculty of Medicine, and Graduate School of Medicine, Hokkaido
University, Sapporo, Japan.

#### Introduction

Osteoarthritis (OA) is a musculoskeletal disease characterized by cartilage degeneration and stiffness, with chronic pain in the affected joint. The severity of OA and cartilage degeneration is highly correlated with the development of synovitis, which is mediated by the activity of inflammatory macrophages. Given that unravelling of the mechanisms underlying the immune pathophysiology, namely the impact of inflammatory macrophages on cartilage degeneration, should provide a clue for the discovery therapeutic targets for the treatment of OA, our study was directed to explore the precise function of macrophages in pathogenesis of OA.

#### Results & discussion

Different types of macrophages and primary chondrocytes were used for in vitro studies. Stimulated primary chondrocytes were further subjected to RNA-seq analysis and other functional assays. Two experimental murine OA models were used to evaluate the effect of intraarticular injection of the selected drug. Our results showed that macrophage secretome can initiate noncanonical pyroptosis in chondrocytes, thus leading to cartilage catabolism and the development of osteoarthritis (OA). Histological examination of cartilage revealed that intra-articular injection of wedelolactone significantly reduced OARSI cartilage score and alleviated cartilage damage in the OA mouse models. These collective results demonstrate that non-canonical pyroptosis in chondrocytes represents an attractive therapeutic target for future treatment of OA. Our current findings provide new insight into the pathologic mechanisms of OA and suggest that noncanonical pyroptosis in chondrocytes represents an attractive therapeutic target for treatment.

### YL9

### Selective and Transient Stealth Coating of Liver Scavenger Wall Enables Retargeting of Nanomedicines

Anjaneyulu Dirisala<sup>1</sup>, Satoshi Uchida<sup>1,2</sup> and Kazunori Kataoka<sup>1</sup> Innovation Center of NanoMedicine (iCONM), Kawasaki Institute of Industrial Promotion, 3-25-14

Tonomachi, Kawasaki 210-0821, Japan; <sup>2</sup>Department of Advanced Nanomedical Engineering, Medical Research Institute, Tokyo Medical and Dental University (TMDU), Tokyo 113-8510, Japan.

**Introduction.** Cell-specific targeting of nanomedicines potentiates the delivery efficiency of pharmacological agents for improving the diagnosis and treatment. However, the reticuloendothelial cells, particularly the liver scavenger wall cells (resident macrophagic Kupffer cells and liver sinusoidal endothelial cells), capture most of the administered dose, causing a substantial decrease in the delivery efficiency of nanomedicines into the targeted organs and often raising toxicity concerns<sup>1</sup>. We addressed this issue by selective *in situ* stealth coating of liver scavenger wall cells using one-armed or two-armed poly(ethylene glycol) (PEG)—conjugated oligo(L-peptide)<sup>2</sup>.

Results and Discussion. The PEG coating must be transient and selective to the liver scavenger wall cells to avoid toxicity and immunogenicity concerns. We achieve this by employing oligo(L-lysine) (OligoLys) conjugated two-armed PEG for anchoring PEG to scavenger walls (Figure 1)<sup>2</sup>. The PEGylation of OligoLys aided in avoiding nonspecific binding to extra-liver endothelial walls, presumably via the steric repulsion of PEG, with the preserved attachment to liver scavenger wall cells, which shows high binding affinity to oligocations due to abundant availability of heparan sulfates and scavenger receptors. The coating duration of PEGylated OligoLys was successfully controlled by optimizing the PEG configuration. Two-arm-PEG-OligoLys presented transient PEG coating to the liver sinusoidal walls, followed by gradual biliary excretion, whereas one-arm-PEG-OligoLys persistently attached to liver scavenger walls. Ultimately, transient and selective PEG coating of liver sinusoidal wall scavenger cells by two-arm-PEG-OligoLys effectively prevented the capture of nonviral and viral gene vectors, representatives of synthetic and nature-derived nanomedicines, respectively, thereby boosting their targeting efficiency via their relocation from the liver sinusoids to target organs<sup>2</sup>.

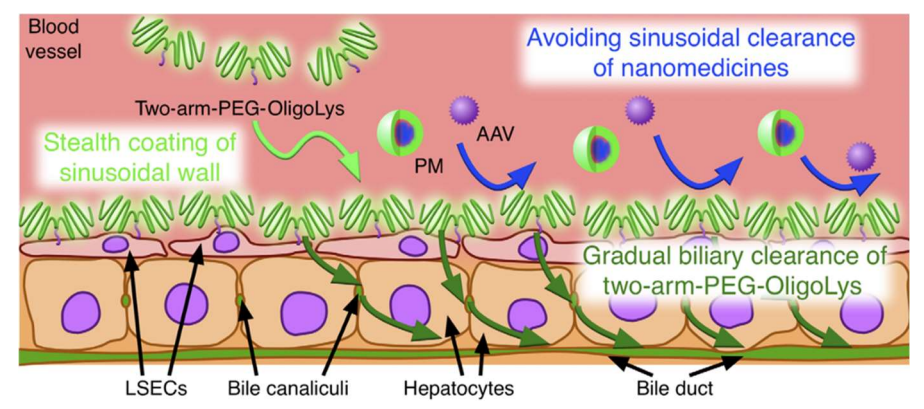


Figure 1. In situ stealth coating of the liver scavenger wall cells using PEG-OligoLys. Two-arm-PEG-OligoLys selectively attaches to the sinusoidal scavenger wall cells to prevent the capture of nanomedicines, such as polyplex micelle (PM) and adeno-associated virus (AAV), to the wall via the stealth property of PEG. Two-arm-PEG-OligoLys is gradually removed from the sinusoidal walls and excreted to bile, thereby avoiding prolonged disturbance of normal physiological functions of the liver.

- 1. P. Wen, W. Ke, A. Dirisala, K. Toh, M. Tanaka, and J. Li, Adv Drug Deliv Rev. 2023, 198,114895.
- 2. A. Dirisala, S. Uchida, K. Toh, J. Li, S. Osawa, T. A. Tockary, X. Liu, S. Abbasi, K. Hayashi, Y. Mochida, S. Fukushima, H. Kinoh, K. Osada, K. Kataoka. 2020, *Science Advances* 6, eabb8133.

### OL7

# Design and Synthesis of Piezochromic Materials Exploring Intermolecular Charge Transfer: Chalconoids Bound to *p*-sulfonatocalix[6] arene Macrocycle

Sanhita Patil, Shridhar Gejji and Dipalee Malkhede

Department of Chemistry, Savitribai Phule Pune University, Ganeshkhind, Pune, Maharashtra, India

**Introduction.** Solid-state systems comprised of chalconoid encapsulated within p-sulfonatocalix[6] arene (SCX6) scaffolds that exhibit mechanochromism and thermochromism have been developed. The introduction of supramolecular host promises a variety of applications in diverse areas which makes them fascinating. Large hydrogen bonding/ $\pi \cdots \pi$  interactions are responsible for the host-guest complexation.

**Results and Discussion.** The structure of the complex reveals one of the phenyl rings of chalcone (guest) is held inside the SCX6 cavity whilst other phenyl rings that exclude the cavity are hydrogen-bonded to sulfonate portals of the host. The hydrogen bonding triggers proton transfer engendering mechanochromic switch. The complexes are further characterized through cyclic voltammetry (CV), steady-state fluorescence, vibrational spectroscopy, and proton or 2D NMR (NOESY) experiments. Detailed structural analyses points to the deshielding of the Ha-e (guest) protons whereas, the hydroxyl protons from the host experience shielding as evidenced from the <sup>1</sup>H NMR spectra Electrochemical investigations suggested an irreversible one-electron transfer in the host-guest binding. Underlying noncovalent interactions emanate the characteristic 'frequency shift' for the intense carbonyl vibration in the infrared spectra which is correlated to the kinetic energy density parameter, G(r) in the quantum theory of atoms in molecules (QTAIM).

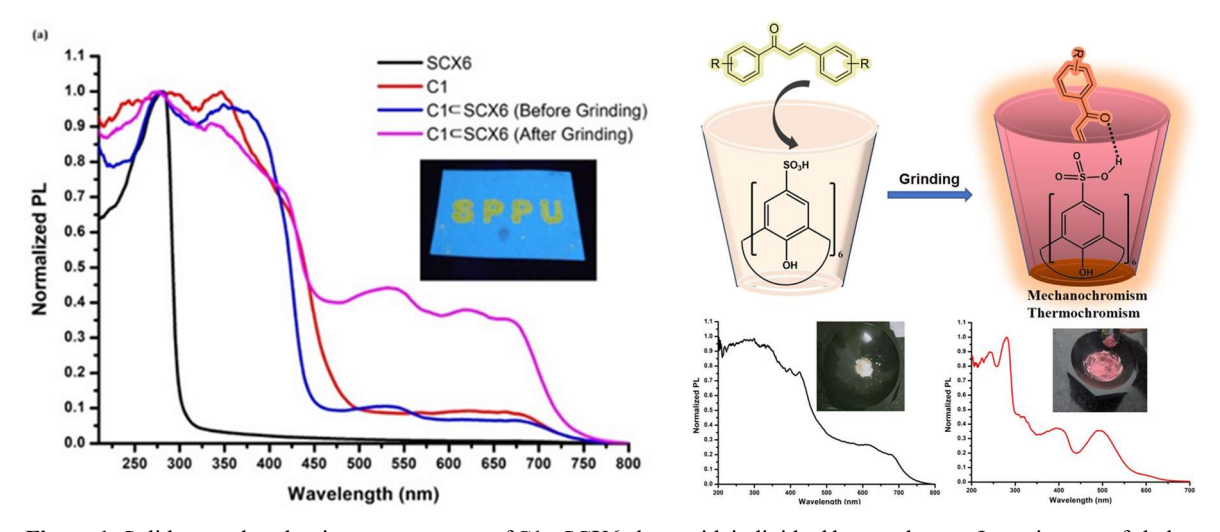


Figure 1: Solid-state photoluminescence spectra of C1 $\subset$ SCX6 along with individual host and guest. Inset: images of chalcone complexes under UV light ( $\lambda = 365$ nm).

- 1. K. Ohno, S. Yamaguchi, A. Nagasawa and T. Fujihara, Dalton Transactions, 2016, 45, 5492-5503.
- 2. T. Yuan, M. Vazquez, A. N. Goldner, Y. Xu, R. Contrucci, M. A. Firestone, M. A. Olson and L. Fang, J Advanced Functional Materials, **2016**, 26, 8604-8612.
- 3. A. Li, S. Xu, C. Bi, Y. Geng, H. Cui and W. Xu, Materials Chemistry Frontiers, 2021, 5, 2588-2606.
- 4. Y. Wang, M. Li, Y. Zhang, J. Yang, S. Zhu, L. Sheng, X. Wang, B. Yang and S. X.-A. Zhang, Chemical Communications, 2013, 49, 6587-6589.
- 5. G. Zhang, J. Sun, P. Xue, Z. Zhang, P. Gong, J. Peng and R. Lu, Journal of Materials Chemistry C, 2015, 3, 2925-2932.
- 6. B. Wang, Z. Wu, B. Fang and M. Yin, Dyes and Pigments, 2020, 182, 108618.
- 7. T. Han, X. Feng, D. Chen and Y. Dong, Journal of Materials Chemistry C, 2015, 3, 7446-7454.

### OL8

## Fabrication and Thermoelectric Properties of Freestanding Ba<sub>1/3</sub>CoO<sub>2</sub> Single Crystalline Films

Kungwan Kang<sup>1</sup>, Fumiaki Kato<sup>2</sup>, Akitoshi Nakano<sup>2</sup>, Ichiro Terasaki<sup>2</sup>, Takashi Endo<sup>3</sup>, Yasutaka Matsuo<sup>3</sup>, Hyoungjeen Jeen<sup>4</sup>, and Hiromichi Ohta<sup>3</sup>

<sup>1</sup>Graduate School of Information Science and Technology, Hokkaido University,

<sup>2</sup>Department of Physics, Nagoya University,

<sup>3</sup>Research Institute for Electronic Science, Hokkaido University,

<sup>4</sup>Department of Physics, Pusan National University

Thermoelectric energy conversion technology garnered significant attention as a means of harnessing energy from waste heat, utilizing Seebeck effect to convert it into electricity. Among the array of thermoelectric materials, based on conducting oxides exhibiting a high of merit have emerged as particularly promising. These materials offer notable advantages, including excellent chemical and thermal stability, along with a non-hazardous distinguishing them from chalcogenide-based thermoelectric materials commonly considered state-of-the-art. Within the realm oxide thermoelectric materials, one standout candidate is Ba<sub>1/3</sub>CoO<sub>2</sub>, characterized by its layered crystal structure<sup>[1]</sup>. This material showcases an impressive thermoelectric figure merit (ZT) value of 0.55 at 600 °C when measured in the in-plane direction under standard conditions. Notably, this ZT value not represents the highest among reliable measurements but also places it in the same as other renowned p-type thermoelectric materials like PbTe and SiGe when evaluated

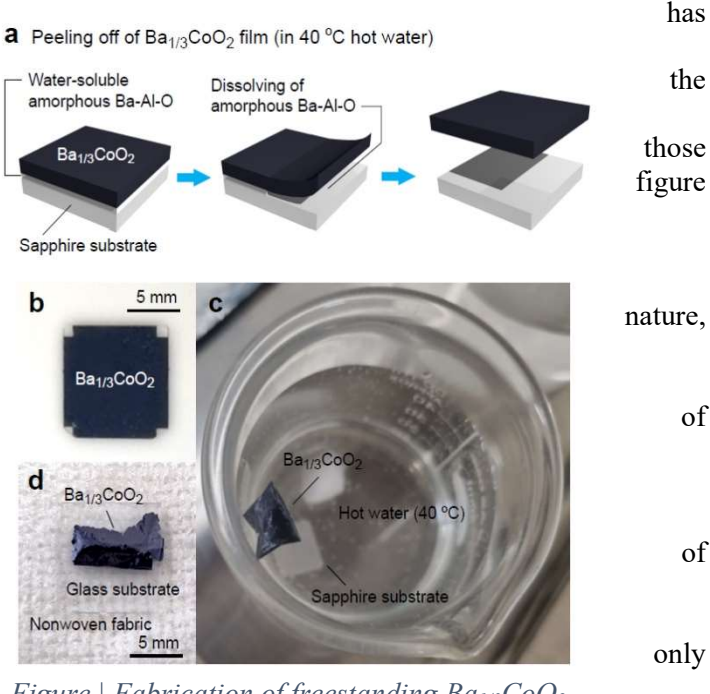


Figure | Fabrication of freestanding  $Ba_{1/3}CoO_2$  single crystalline films. Peeling-off procedure of  $Ba_{1/3}CoO_2$  epitaxial films.

materials like PbTe and SiGe when evaluated at 600 °C <sup>[2]</sup>. In practical applications, the utilization of Ba<sub>1/3</sub>CoO<sub>2</sub> necessitates the fabrication of bulk ceramics or single crystalline forms. Here, we present a novel approach for the production of freestanding Ba<sub>1/3</sub>CoO<sub>2</sub> single crystalline films, accomplished by delicately detaching the Ba<sub>1/3</sub>CoO<sub>2</sub> epitaxial films from their substrate (see Figure) <sup>[3]</sup>. The process entails creating Ba<sub>1/3</sub>CoO<sub>2</sub> epitaxial films and immersing them in 40 °C hot water for several minutes. Subsequently, the Ba<sub>1/3</sub>CoO<sub>2</sub> epitaxial film naturally separates from the substrate and floats atop the water's surface, akin to seaweed. We conducted an exhaustive analysis of the crystal structure, chemical composition, and thermoelectric properties both before and after this peeling process, revealing negligible differences. These findings represent a valuable advancement, offering a practical methodology for producing freestanding oxide single crystalline films specifically tailored for thermoelectric applications.

- 1. Y. Takashima, Y. Zhang, J. Wei, B. Feng, Y. Ikuhara, H.J. Cho, H. Ohta, J. Mater. Chem. A 2021, 9, 274.
- 2. X. Zhang, Y. Zhang, L. Wu, A. Tsuruta, M. Mikami, H.J. Cho, H. Ohta, ACS Appl. Mater. Interfaces 2022, 14, 33355.
- 3. K. Kang, F. Kato, A. Nakano, I. Terasaki, T. Endo, Y. Matsuo, H. Jeen, H. Ohta, *ACS Appl. Electron. Mater.* in revision.

### Chitosan and PVA foam material

<u>Taiyo Nagai</u>, Fuka Sato, Akihiro Mizuyama, Olaf Karthaus <sup>1</sup>Chitose Institute of Science Technology

**Introduction.** There is a garbage problem in which Styrofoam used in the cultivation of shiitake mushroom logs is left uncollected. It has also been found that foamed materials made only of chitosan decompose faster than shiitake mushrooms can grow.

We aim to create a foam material using chitosan and PVA that is biodegradable and has excellent dimensional stability.

**Results and Discussion.** A 5% chitosan aqueous solution is prepared by adding 1.5 times as much citric acid as chitosan to distilled water. An equal amount of PVA as chitosan was added to the chitosan aqueous solution.

A foam is prepared by adding a crosslinking agent sodium phosphinate and sodium bicarbonate as blowing agents to the final aqueous chitosan solution.

The foam is sandwiched between an iron plate lined with parchment paper with cuts in it. Then it is baked in an oven heated to 220°C for 40 minutes.

After baking, it is neutralized with acetic acid aqueous solution.

We are investigating the biodegradation of the foam materials by collecting soil from two locations near the university and filling them with three types: PVA thin film, chitosan + PVA foam material, and chitosan foam material. These are photos before burying it in the soil and two months after burying it in the soil.



The pictures shows partial decomposition, as indicated by a color change and weight loss after two months. The left picture is the original foam, the right one after 2 months in soil.

## Exploring the Feasibility to Estimate DBH from Trunk Point Cloud Data Captured by UAV-LiDAR System

Yoshito Shimizu<sup>1</sup>, Ram Avtar<sup>1</sup>

<sup>1</sup>Graduate School of Environmental Science, Hokkaido University

### Introduction.

The distribution of Diamer at Brest Height (DBH) in forests has traditionally been used as an indicator of the economic and ecological value of forests, however, often requires labor-intensive field surveys. In this study, we tested the feasibility to estimate DBH from 3D point clouds of tree trunks using relatively inexpensive UAV and LiDAR sensor in deciduous coniferous forests in winter season.

### Results and Discussion.

Data acquisition was carried out in a *Larix gmelinii* var. *japonica* plantation forest during the defoliation season in 2023 using a DJI Matrice 300 and L1 sensor. Two different speed (s / f) and altitude (25m / 35m) combinations were used, and Stripe path (North-South, 0d) and Orthogonal path (North - South & East - West, mix) were applied for each combination. As a result, 8 different data were acquired. In all data, the trunks were visible. The data processing flow is shown in figure 1. Table 1 shows the results of the estimation of DBH in the 8 combinations. 89 trees with field data were used for the validation, and the average DBH of the trees was 22.5 (cm).

The detection rate, i.e., the probability of having point cloud data for the trunks, was above 90% in most cases, indicating a high probability of obtaining trunk data in this study.

When focusing on the average estimated DBH in each combination, the results were significantly overestimated (19-31%). The quality of the point cloud data and the estimation method may have influenced this result.

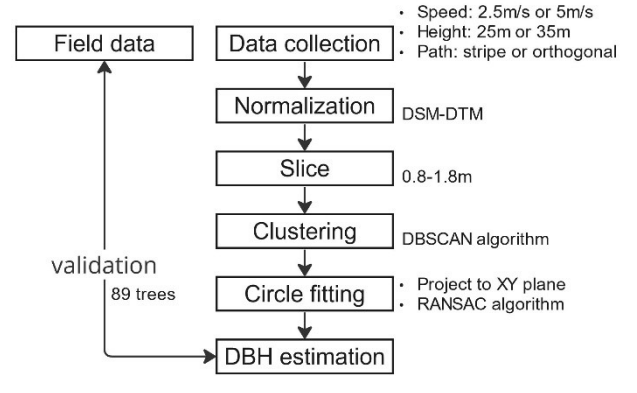


Figure 1. Data processing flow

Table 1 summary of the result

	detection	number of points in a	average DBH	RMSE	
	rate (%)	stem	(cm)	(cm)	R^2
S_25_0d	97.8	136	27.6	10.1	0.12
S_25_mix	98.9	298	28.8	9.3	0.34
S_35_0d	87.6	55	29.5	11.2	0.16
S_35_mix	98.9	106	28.6	8.1	0.47
F_25_0d	93.3	54	26.8	9.1	0.16
F_25_mix	100	130	28.8	7.5	0.49
F_35_0d	82	38	28.0	8.8	0.3
F_35_mix	97.8	107	28.7	7.9	0.41

The shape of the stems in the data captured with Stripe path sometimes is not clear like a cylinder. This is probably because the Stripe path obtained the data only from 2 directions, not from 4 directions. RMSE value showed 7.5 - 11.2 cm. This is 33 - 50 % of the actual average DBH. The highest R-squared value was 0.49, which does not seem to indicate a good relationship. The R-squared value and the detection rate of trunks improved when data was acquired orthogonally. This could be due to data acquisition from multiple directions and an increase in the number of point clouds in Orthogonal path.

Compared to previous studies that directly measured DBH using UAV-LiDAR data, a similar trend of overestimation was shown in this study. However, the calculated mean DBH error and RMSE values were relatively larger. This could be due to the characteristics of the sensors, our methodology of using 1m slice length, and relatively dense canopy cover of the forest.

- 1. Kuželka, K., Slavík, M., & Surový, P. Remote Sensing 2020, 12, 1236, 12(8), 1236.
- 2. Wieser, M., Mandlburger, G., Hollaus, M., Otepka, J., Glira, P. Remote Sensing 2017, 9, 1154, 9(11), 1154.

## Heterojunction Formation Strategy to Realize Z-Scheme g-C<sub>3</sub>N<sub>4</sub>/SnS<sub>2</sub> Photocatalyst

<u>Yohei Mori<sup>1</sup></u>, Basker Malathi<sup>1</sup>, Harish Santhanakrishnan<sup>2</sup>, Navaneethan Mani<sup>2</sup>, Atsushi Nakamura<sup>1</sup> Graduate School of Shizuoka University, <sup>2</sup>SRM University

#### Introduction.

To realize artificial photosynthesis, it is important to design photocatalysts with visible light absorption, high redox potential, and high charge separation [1]. In this study, we formed a Z-scheme heterojunction of  $g-C_3N_4$  and  $SnS_2$  to satisfy these conditions using a wet chemical method. Simultaneously, we increase the junction area and improve the catalytic activity by selecting a precursor of  $g-C_3N_4$ .

### Results and Discussion.

Four types g- $C_3N_4$  were prepared by using melamine, melamine & thiourea, urea & thiourea, and urea precursor. SEM images and surface area values of the four types of g- $C_3N_4$  are shown in Figure 1. From Figure 1, the bulk structure was observed for the melamine and melamine & thiourea precursor, while the urea & thiourea precursor had an aggregated particle structure, and the urea precursor had a thin sheet structure with a thin thickness. The urea g- $C_3N_4$  had a larger specific surface area than the other g- $C_3N_4$ . Therefore, we selected urea g- $C_3N_4$  because it has a large junction area with SnS<sub>2</sub>.

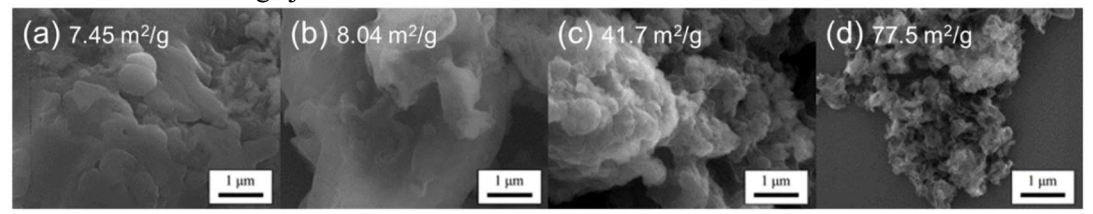


Fig.1 SEM images of four types of g-C<sub>3</sub>N<sub>4</sub> made by (a)melamine,(b) melamine & thiourea,(c) urea & thiourea,(d) urea

The g- $C_3N_4$  was protonated by stirring in a nitric acid solution, and the heterojunction was formed by sonication of the protonated g- $C_3N_4$  and  $SnS_2$  in solution for 1h and stirring for 3h. From Figures 2(a), (b), and (c), we can see that countless  $SnS_2$  particles are attached to the protonated g- $C_3N_4$ .

The catalytic activity of the photocatalyst was evaluated by degrading methylene blue dye under LED irradiation. From Figures 2(d) and (e), the heterojunction photocatalyst degrades the MB solution more efficiently than the single material. The apparent rate constant of the heterojunction photocatalyst is the highest, which explains the effect of enhanced charge separation by forming a heterojunction [2].

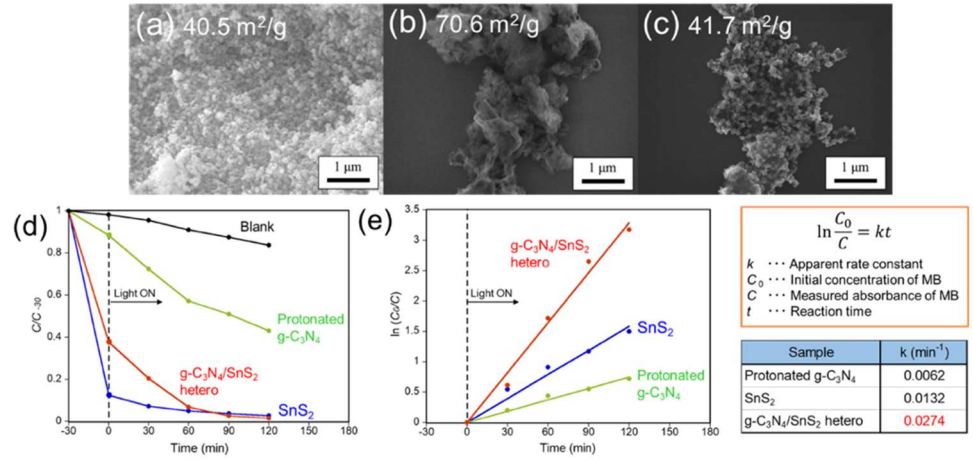


Fig.2 (a) SEM images of  $SnS_2$ ,(b) SEM images of protonated g-C<sub>3</sub>N<sub>4</sub>,(c) SEM images of g-C<sub>3</sub>N<sub>4</sub>/ $SnS_2$  hetero, (d) photocatalytic degradation of MB,(e) linear transform  $ln(C_0/C)$  of the kinetic curves of MB degradation

- [1] Wenhao Zhang et al., Angew. Chem. Int. Int. Ed. Vol 51, pp.22894-22915(2020)
- [2] Kai Dai et al, Appl. Catal. B, Vol 156-157, pp.331-340, (2014)

# Utilizing Artificial Intelligence and Expert Knowledge to Optimize Non-Isothermal Aging Heat Treatment for Enhancing 0.2% Proof Stress in $\gamma - \gamma'$ Binary Ni-Al Alloys

<u>Vickey Nandal</u><sup>1</sup>, Sae Dieb<sup>1</sup>, Dmitry S. Bulgarevich<sup>1</sup>, Toshio Osada<sup>1</sup>, Toshiyuki Koyama<sup>2</sup>, Satoshi Minamoto<sup>1</sup>, Masahiko Demura<sup>1</sup>

<sup>1</sup>National Institute for Materials Science (NIMS), Tsukuba, Japan <sup>2</sup>Graduate School of Engineering, Nagoya University, Nagoya, Japan

**Introduction.** The high-temperature strength of Ni-based alloys is significantly influenced by the aging heat treatment process. Consequently, it is essential to design the heat treatment schedule carefully. Traditionally, these designs have been limited to isothermal aging. However, broadening the possibilities to include more flexible non-isothermal aging (NIA) presents the opportunity to attain an optimized two-phase microstructure, thereby enhancing the high-temperature strength in Ni-based alloys.

Computational Methodologies. We have integrated a computational workflow into our original material design system, Materials Integration by Network Technology (MInt) [1,2], which allows us to model microstructure changes and assess the high-temperature strength of Ni/Ni<sub>3</sub>Al two-phase alloys with  $\gamma - \gamma'$  microstructure [3]. In a previous investigation [4], we showcased the potential of an artificial intelligence (AI) algorithm to suggest aging patterns that outperformed the conventional isothermal aging standard. In this current study, we have extended our thorough examination of AI techniques employing 22 independent MCTS trees [5].

**Results and Discussion.** We devised a novel heat treatment approach to enhance the high-temperature mechanical properties of binary Ni-Al alloys, employing advanced AI algorithms. Our investigation entailed the exploration of NIA patterns that outperform the conventional isothermal aging method within an extensive search space of complex heat treatment patterns, including thermal ramping up and down (approximately 3.5 billion possible ways), while maintaining the isothermal aging method as a benchmark, as depicted in Figure 1. Intriguingly, within the pool of 2823 NIA schedules examined, we identified 173 schedules that exhibited superior performance relative to the isothermal aging benchmark. The findings from these observations may serve as evidence for the potential of AI-driven approaches in achieving enhanced strength in Ni-Al alloys.

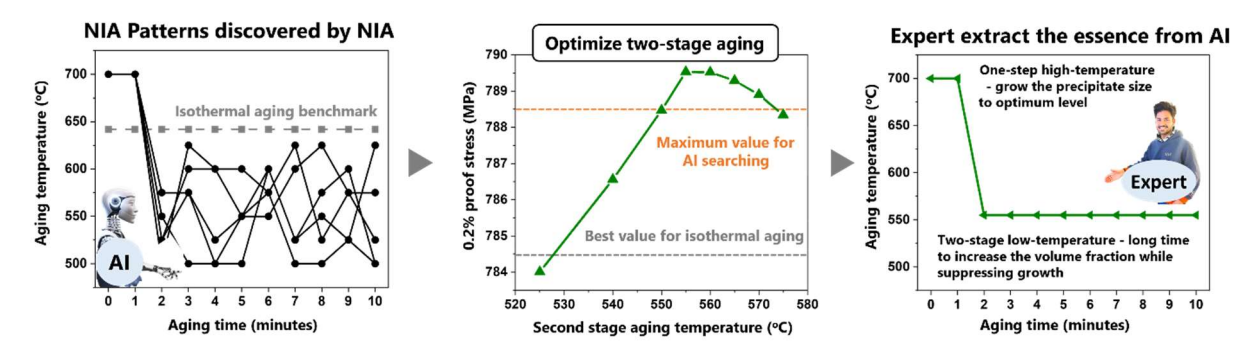


**Figure 1:** The graphs depict the NIA pattern optimized through the collaborative efforts of AI and experts with the aim of improving the 0.2% proof stress in binary Ni-Al alloys.

**Acknowledgments:** This work was partly supported by the Council for Science, Technology and Innovation (CSTI), Cross-Ministerial Strategic Innovation Promotion Program (SIP), "Materials Integration for Revolutionary Design System of Structural Materials" (Funding agency: JST) and by MEXT Program: Data Creation and Utilization Type Material Research and Development Project Grant Number JPMXP1122684766.

**References:** [1] Demura M, Koseki T 2020 Mater Trans 61 2041 [2] Minamoto S, et al. 2020 Mater Trans 61 2067 [3] Osada T, et al. 2023 Mater Des 226 111631 [4] Nandal V, et al. 2023 Sci Rep 13 [5] Dieb S, et al. 2017 STAM 18 1.

### **Energy-Saving Preparation of Chitin/Chitosan Composite Materials**

### Tomohisa Suzuki, Olaf Karthaus

Graduate School of Science and Engineering, Chitose Institute of Science and Technology

**Introduction.** A paste is prepared by mixing chitin, chitosan 100, citric acid, sodium hypophosphite, and distilled water. The mixed material was prepared by hot pressing[fig.1]. It was found that even a low temperature hot-press application produced a difference in strength in the presence or absence of a cross-linking agent.

Results and Discussion. From fig. 2, it was found that there is some relationship between the reaction temperature and tensile strength as a result of changing the reaction temperature by keeping the pressure during hot pressing to 40 MPa and the reaction time to 1h as the specimen preparation conditions. The strength of the material changed even at a comparably low temperature of 90°C depending on the presence or absence of the cross-linker, indicating that the cross-linker can increase the tensile strength of the material even at temperatures lower than the



fig.1 Sample prepared for strength testing

temperature that is usually applied for this type of samples, 220°C. From fig. 3, it can be seen that changing the pressure during hot-pressing has a similar effect on the tensile strength: it increased due to the increased density of the material caused by the high pressure.

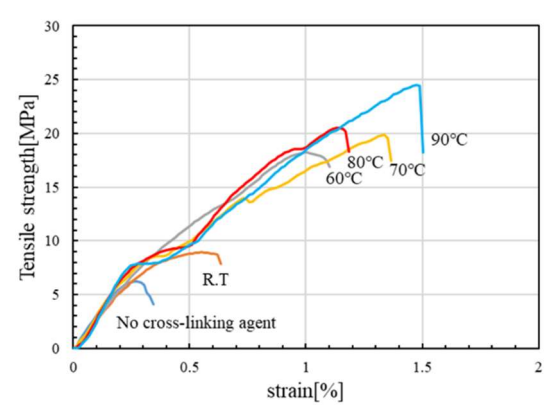


fig.2 Tensile test results with samples prepared at 40 MPa, reaction time 1 hour, and reaction temperatures (sample without cross-linking agent was at different)

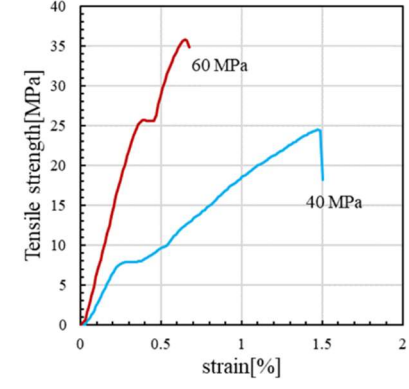


fig.3 Tensile test results of samples prepared at 90% for 1 hour and different pressures.

- M.M.Hassan, N.Tucker, M.J.Le Guen Thermal, mechanical and viscoelastic properties of citric acid-crosslinked starch/cellulose composite foams Carbohydrate Polymers 2020,230
- L. Heux, J. Brugnerotto, J. Desbrie`res, M.-F. Versali, and M. Rinaudo, Solid State NMR for Determination of Degree of Acetylation of Chitin and Chitosan, Biomacromolecules 2000, 1, 746-751

## Universal Design Features and their Accessible Continuity in Shopping Malls of Kolkata, India

Sudeshna Chakraborty, Suguru Mori, Rie Nomura

<sup>1</sup>Department of Architectural and Structural Design, Hokkaido University.; <sup>2</sup>Department of Architectural and Structural Design, Hokkaido University.; <sup>3</sup>Department of Architectural and Structural Design, Hokkaido University.

### Introduction.

Despite a significant increase in the number of elderly and specially-abled, civic administration in Kolkata has not been able to successfully implement the national guidelines on inclusiveness in its shopping malls. The aim of this research is to analyze the Universal Design features in shopping malls of Kolkata, India, and propose their accessible continuity.

### Results and Discussion.

After conducting pilot studies, five shopping malls from the Kolkata Municipal Corporation were considered case areas for the fieldwork. The accessibility audit checklist furnished by the Government of India vis-à-vis the Accessible India Campaign has been used for the year-long fieldwork beginning December 2021.

The first observation was the lack of accessibility in the infrastructure of the shopping malls. The overall accessibility scores of the shopping malls were far from satisfactory: Forum Mall (34.4%), South City Mall (28.8%), Mani Square Mall (44.8%), Quest Mall (24%), and Acropolis Mall (14.4%). Pearson's correlation between the year of establishment and the overall accessibility percentage of each case area was found to be -0.66 indicating the alarming deterioration in universal design considerations with growing years. Furthermore, the correlation between the year of establishment and parameter-wise average accessibility percentage is Main Entrance (-0.79), Ramp (-0.80), Door (-0.85), Corridor (-0.68), Lifts (0.15), Stairs (-0.94), Handrail (-0.76), Toilet (-0.10), Canteen (-0.13), Drinking water (-0.13), and Signage (0.53). Parking and Emergency Exit have been left out due to the absence of these parameters in the case areas. However, assessing shopping malls merely based on their physical infrastructure as practiced in India is insignificant unless they (infrastructure) are evaluated concerning the diverse user groups. Goldsmith's Universal Design Pyramid was used for this section, where user group 1 to 8 has been described. (a) User Group 1 is the fit, agile people; (b) User Group 2 is the able-bodied people; (c) User Group 3 is for able-bodied women; (d) User Group 4 is for elderly people with walking sticks and people with infants in pushchairs; (e) User Group 5 is for ambulant people who have disabilities and are visually impaired; (f) User Group 6 is the independent wheelchair users; (g) User group 7 is the people with assistance in wheelchairs and disabled people who drive electric scooters; and (h) User Group 8 is the wheelchair users who need two people for assistance.

Furthermore, on comparing the accessibility performance with the diverse user groups (as per Goldsmith's Universal Design Pyramid), with a median accessibility value of 41.46%, user group 6 (individual wheelchair users) is likely to face the most difficulty in the case areas. The results of this research thus shall pave the path for accessible continuity as explained hereafter. This section includes mapping the average accessibility percentage of each parameter across each user group. The average percentage of accessibility for the emergency exit parameter is 0% for all user groups from 1 to 8 which explains that the absence of the indicator under the emergency exit parameter does affect all the user groups, so the average percentage of accessibility is 0. For the parking parameter, the average percentage for user groups 1 to 5 is 100% and for users, 6 to 8 is 0%. Figure 3 shows the mapping of the average accessibility percentage of each parameter across each user group.

- 1. Ministry of Housing and Urban Affairs, "Harmonised Guidelines & Standards for Universal Accessibility in India," Government of India, New Delhi, Dec. 2021.
- 2. Central Statistics Office, "Manual on disability statistics," Ministry of Statistics and Programme Implementation, New Delhi, 2012.
- 3. G. Das Mahapatra, S. Mori, and R. Nomura, "Universal Mobility in Old Core Cities of India: People's Perception," Sustainability, vol. 13, no. 8, p. 4391, Jan. 2021, doi: 10.3390/su13084391.
- 4. K. Kumar Joshi and S. Gupta, "Factors Affecting Performance of a Shopping Mall," IOSR Journal of Business and Management (IOSR-JBM), vol. 19, no. 12, pp. 1–14, 2017, doi: 10.9790/487X-1912030114.

### "All-aqueous" Tandem Boc-Deprotection and Alkylation of Benzimidazole Derivatives Under Visible Light with Alkyl Aryl Diazoacetates: Application to Site Selective Insertion of Carbenes into N-H Bond of Purines

Suchismita Rath, Biswajit Mohanty, Subhabrata Sen\*

<sup>1</sup> Department of chemistry, School of Natural Sciences, Shiv Nadar University, Dadri, Chithera, Gautam Budh Nagar, Uttar Pradesh, 201314, India.

**Introduction.** Benzimidazole is an interesting class of heterocycles ubiquitous by its presence in innumerable natural products and drug molecules. Various benzimidazole based pharmaceutical drug candidates have been reported to exhibit antiviral, antibacterial, neuroprotective, anti-inflammatory and antidiabetic properties. Amongst these derivatives N¹-alkylated analogues are important by virtue of their extensive pharmacological and biological applications. Hence numerous strategies have been devised for the N¹-alkylation of benzimidazole derivatives.

**Results and Discussion.** Herein we have reported a blue LED induced tandem Boc-deprotection and NH-alkylation of benzimidazole derivatives with methyl aryl diazoacetates.<sup>4</sup> The reactions occur in water at room temperature. The desired products are obtained in good to excellent yield. The putative mechanism of this reaction is discussed based on control experiments and supported by DFT studies. Additionally, the strategy is used to alkylate various purine derivatives *via* site selective N¹-alkylation to generate acyclic nucleoside analogues.

$$R^1$$
 $R^2$ 
 $R^3$ 
 $R^3$ 

- 1. S. Shaharyar, M. Mazumdar, Arab. J. Chem., 2017, 10, S157-S173.
- 2. R. S. Keri, A. Hiremad, S. Budagumpi, B. M. Nagaraja, Chem. Bio. Drug Des. 2015, 86, 1965.
- 3. P. K. Dubey, P. Reddy, K. Srinivas, Synth. Comm., 2007, 37, 1675-1681.
- 4. S. Rath, B. Mohanty, S. Sen, J. Org. Chem. 2023, 88, 2, 1036–1048.

## **Shallow Landslide Occurrence Relative to Forest Management Including Clearcutting, Forest Thinning**

Sowmya Nagaraj, Fumitoshi Imaizumi

Forest Hydrology and Erosion Control Engineering Laboratory, Faculty of Agriculture, Shizuoka University, Japan

### Introduction

In Shizuoka prefecture, central Japan, an investigation on impact of forest management practices, such as clearcutting and thinning, on shallow landslide triggered by hydro-geomorphic factors. Clearcutting, removing all standing trees, while thinning involves 35-40% tree reduction. Google Earth Pro spanning 17 years (2004-2021) were used to determine landslide frequency in forest age groups (0-5, 6-10, 11-15, 16-20 years). Highest occurrence rates observed in 0-5-year age group, particularly in thinning zones.

### Result and discussion

Our study reveals that both clearcutting and thinning lead to vegetation root depletion, which affects slope stability. However, root regeneration in later stages reduces landslide occurrence. Total rainfall depth peaked from 2010-2013, and 24-hour rainfall peaked from 2018-2020. Forest harvesting, rather than total rainfall and intensity, mainly influenced landslide timing, with the highest landslide area observed in 2013-2014 (190,634m²). Notably, slopes with gradients between 30-50 degrees experienced a higher frequency of landslides, underlining topographic influences.





Fig. 1 Images from field visit on shallow landslides

- 1. F. Imaizumi, and R. C. Sidle, G. Annaler, Physical Geography, 2021.
- 2. H. Saito, D. Nakayama, H. Matsuyama, Geomorphology, 2020, 118 2010, 167-175.
- 3. F. Imaizumi, R. C. Sidle and R. Kamei, Earth Surface Processes and Landforms, 2008 33, 827-840.
- 4. J. R. Evans, F. Imaizumi, O. Ohsaka and S. Ogawa, Earth Surface Processes and Landforms, 2020, 45, 3280-3292.

### **Export and Energy Efficiency: Evidence from Manufacturing Firms in Transition Economies**

### Shohruh KHASANOV

Graduate School of Economics and Business, Hokkaido University

**Introduction**. This study investigates how firm energy efficiency is affected by its foreign trade activities and identifies mechanisms in this relationship for transition economies. These countries deserve special attention as they have experienced rapid decreases in energy intensities partly thanks to market reforms which have addressed issues such as resource misallocation and price distortions (Carvalho, 2018). Moreover, opening the borders to the world following the collapse of the Soviet Union has led to remarkable trade growth which has been higher than even advanced countries (Rahmanov, 2019).

**Data**. For our empirical analysis we use the latest four rounds of World Bank Enterprise Surveys (WBES) data for 29 transition countries. The advantage of using this dataset is that we can create three different firm-level energy intensities: the ratio of energy costs to annual sales, value added and cost of variable inputs. To proxy firm trade activities, we employ firm export decision and intensity (share of exports to total sales).

Significance and contribution. Our contributions to the literature are two-fold. First, we employ data on manufacturing firms in transition economies to explore the association between trade and energy efficiency. This is significant given that, firstly, the manufacturing industry has been found to be the largest energy consuming sector among others (Biscione, 2021) and secondly, transition economies have experienced rapid improvements in their energy efficiencies. Next, we construct three alternative measures of energy efficiency for the analysis, which is, to our knowledge, the first attempt in trade-energy relationship in transition economies. Results and discussion. Preliminary results reveal a significant positive association between firm exporting and energy efficiency measured as the inverse of the cost share, namely the ratio of the annual energy costs to the total annual cost of each firm's variable inputs in last fiscal year. These results may imply that firms increase their innovation and technological ability following internationalization, which can further help to improve their energy use in production. Moreover, international competition may push exporting firms to adopt energy-efficient practices to both reduce costs and meet environmental standards. The empirical evidence reports practical implications for policymakers and environmental scientists to achieve the greener growth, energy efficiency and sustainable development goals of emerging states.

- 1. A. Carvalho, Energy efficiency in transition economies: A stochastic frontier approach. *Econ. Trans.* 2018, 26(3), 553-578.
- 2. R. Rahmanov, Financial Constraints and Export Participation of SMEs in Post-Communist Countries. *Acta Oecon.* 2019, 69(2), 289-319
- 3. A. Biscione, D. Boccanfuso, A. De Felice, Regulations and Corporate Environmental Responsibility: evidence from a panel of firms in Transition economies. *App. Econ.* 2021, 53(54), 6286-6299.

### A Low-Cost Downflow Hanging Sponge (DHS) Reactor for Nitrogen Removal in Urban Wastewater

Shehani Sharadha Maheepala<sup>1</sup>, Masashi Hatamoto<sup>1</sup>, Takahiro Watari<sup>1</sup>, Takashi Yamaguchi<sup>1,2</sup>

<sup>1</sup>Department of Civil and Environmental Engineering, Nagaoka University of Technology.; <sup>2</sup>Department of Science of Technology Innovation, Nagaoka University of Technology, Nagaoka.

**Introduction** The DHS reactor has been developed and implemented to remove organic matter and NH<sub>4</sub><sup>+</sup>-N from wastewater<sup>1</sup>. To enhance its total nitrogen removal without an additional cost, this study developed an anaerobic condition inside the DHS using the siphon technique. The reactor's performance and its microbial community structure were evaluated.

Results and Discussion. A syphon tube was connected to the effluent port of a DHS reactor to accumulate wastewater inside and create an anaerobic zone. The syphon height was set at 30 cm which was 3/5 of the total volume of developed DHS. When water accumulates inside the reactor the environment conditions were changed from aerobic to anaerobic. After reaching the syphon height, the accumulated water flew out from the reactor and became aerobic. The effluent water discharge process was controlled by the syphon technique, and it did not require extra energy for pumping. A conventional DHS was operated under similar conditions as the control. The schematic diagram of the reactors is shown in Figure 1. The sCOD removal is approximately similar in both reactors which were reported as 62±33% and 61±36% in the developed DHS and control reactor, respectively. The NH<sub>4</sub><sup>+</sup>-N removal rates were 64±31% in the developed DHS which was almost the equivalent of the conventional DHSs' performance. The results indicated that the organic matter removal and nitrification of the modified DHS and conventional DHS were almost identical, and the developed anaerobic column did not affect the removal efficiencies. Furthermore, the anaerobic zone of the reactor facilitated the enhancement of the total nitrogen (TN) removal twofold than the control system and was measured as 18±16%. Nitrifiers, denitrifiers and anammox bacteria were present in the sludge samples of the DHS systems as nitrogen-removing bacteria. Comamonadaceae was the most abundant denitrifier in all samples of the developed DHS system. The developed anaerobic conditions in the syphon-DHS enhanced denitrification without using extra energy for operation. As nitrifiers, Nitrosomonadaceae and Nitrospiraceae were observed. 'Candidatus Brocadia' was observed in the reactor as anammox bacteria, and the highest number was recorded in the middle part of the modified DHS. The denitrification and anammox processes removed TN from the system and enhanced the reactor performance. The results indicate that the DHS reactor with the syphon technique is favourable for nitrogen removal of urban wastewater treatment and is a low-cost technique which can be used as a sustainable system in developing countries.

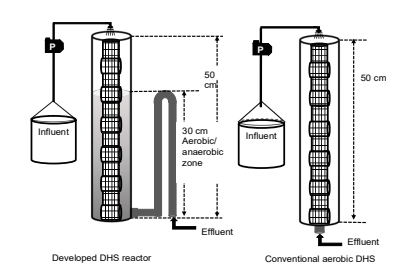


Figure 3 Schematic diagram of the DHS

#### References

 M. Hatamoto, T. Okubo, K. Kubota, T. Yamaguchi, Characterization of downflow hanging sponge reactors with regard to structure, process function, and microbial community compositions. Applied Microbiology and Biotechnology. 2018, 102(24), 10345–10352. <a href="https://doi.org/10.1007/s00253-018-9406-6">https://doi.org/10.1007/s00253-018-9406-6</a>

### Photoresponsive-Auxin Induced Degron (PAID) Technology for Spatiotemporal Control of Intracellular Protein Level

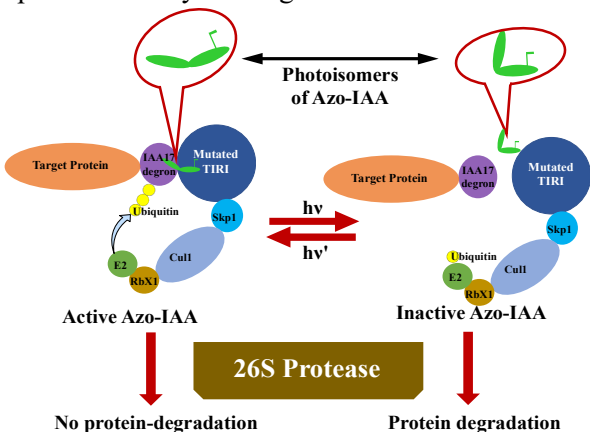
Saugata Sahu<sup>1</sup>, Koya Yoshizawa<sup>2</sup>, Ryota Uehara<sup>2</sup>, Nobuyuki Tamaoki<sup>1</sup>\*

<sup>1</sup>Research Institute for Electronic Science, Hokkaido University.; <sup>2</sup>Graduate School of Life Science, Hokkaido University, Sapporo, Japan

### Introduction.

Controlling the protein activity with light offers to explore various biological processes at spatiotemporal resolution.<sup>1</sup> Photo switchable molecules which effectively toggle between two structurally dissimilar isomers can behave as a molecule glue to control the binding between E3 ligase and protein of interest (POI) for the effective ubiquitination and successive protein degradation.<sup>2,3</sup> Herein, we introduce a photoactive auxin induced degron (PAID) technology where the POI can be degraded with a spatiotemporal resolution with suitable light irradiation.

Results and Discussion. Different Azo-auxin molecules were synthesized to control the auxin induced degradation of target GFP protein in HAP1 cells. The Azo-auxin molecules show well separated absorption spectra for E and Z isomers and efficiently switch between two isomers with suitable light irradiation. Ectopic expression of F74G-OsTIR1 protein and expression of IAA-7 degron tagged GFP in human cell was successfully performed with gene editing technology.<sup>3</sup> The degradation of GFP was monitored using fluorescence microscope, flow cytometer and western blot techniques. We observed that sub-micro to nano molar concentration of E-isomers of Azo-auxins efficiently depleted the POI. Contrary, Z-isomer of Azo-auxins fails to degrade the protein with similar efficiency. The distinct behavior of the isomers attributed to their structural dissimilarity. Theoretical calculation suggests that E-isomer possesses a planar structure which accommodates inside the ligand binding pocket with EC-50 in sub-micromolar concentration. The Z-isomer holds a non-planar structure which leads to an inefficient binding with F74G-OSTIR1 and results less efficient ubiquitination and consequently lower depletion of GFP. We utilized the PAID technology to control the GFP expression with on-off light switching. The expression of GFP in the presence of Azo-auxin was achieved with suitable light irradiation. In summary, we developed a photoactive auxin induced degron (PAID) technology for controlling the intracellular protein activity with light irradiation.



Scheme 1. photoactive auxin induced degron (PAID) technology. Rational design of Azo-Auxin attributes to the protein degradation with a selective photo-isomer.

- N. N. Mafy, K. Matsuo, S. Hiruma, R. Uehara and N. Tamaoki, J. Am. Chem. Soc., 2020, 142, 1763–1767.
- N. Uchida, K. Takahashi, R. Iwasaki, R. Yamada, M. Yoshimura, T. A. Endo, S. Kimura, H. Zhang, M. Nomoto, Y. Tada, T. Kinoshita, K. Itami, S. Hagihara and K. U. Torii, *Nat. Chem. Biol.* 2018, **14**, 299–305.
- A. Yesbolatova, Y. Saito, N. Kitamoto, H. Makino-Itou, R. Ajima, R. Nakano, H. Nakaoka, K. Fukui, K. Gamo, Y. Tominari, H. Takeuchi, Y. Saga, K. ichiro Hayashi and M. T. Kanemaki, *Nat. Commun.* 2020, **11**, 1–13.

## Development of Alternative Materials to Plastics Using Fomes fomentarius

Ryuya Abe, Olaf Karthaus

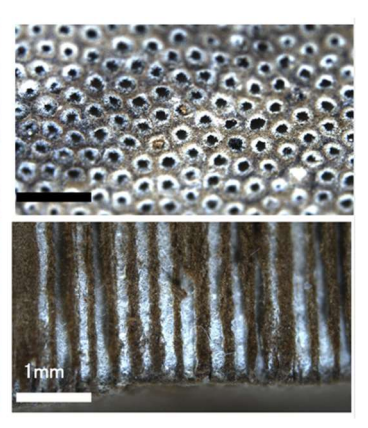
Chitose Institute of Science and Technology, Department of Applied Chemistry and Bioscience

**Introduction.** Today, the problem of plastic waste is becoming more and more serious on a global scale. Although plastic hurts the environment, it is an inseparable part of our daily lives. Therefore, we would like to make it possible to use plants, which can be a sustainable resource, as an alternative material to plastics. Here, we focus on a fungus, fomes fomentarius, that is widespread in Hokkaido.

**Results and Discussion.** Fomes fomentarius is a fungi that infects mainly birch trees. It is known for its hardness and the highly porous structure at the underside. It can be used as a natural Chinese medicine, but has no value as a cellulosic material. Dried fungi specimen were mechanically powdered and used without any further treatment. The powder was mixed with water and a cross-linking agent to make a paste, and the samples were hot-pressed at 60 MPa at 90°C for 60 minutes using a JIS test piece JIS-K7139 type mold tensile tests gave values of around 10 MPa. Details of the sample preparation and characterization will be presented.









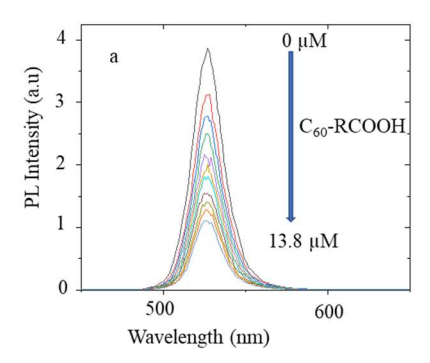
## Photoinduced Electron Transfer from Perovskites Nanocrystals to a C<sub>60</sub>-RCOOH Ligand for Solar Cells Development.

Rumana Akter<sup>1</sup>, Tianci Wang<sup>1</sup>, Palyam Subramanyam<sup>1, 2</sup>, Takuya Okamoto<sup>1, 2</sup>, Yuta Takano<sup>1, 2</sup>, Vasudevanpillai Biju<sup>1, 2</sup>

<sup>1</sup>Graduate School of Environmental Science, Hokkaido University and <sup>2</sup>Research Institute for Electronic Science, Hokkaido University

**Introduction.** Perovskite, a novel photoactive material with high electron transfer efficiency and solution processability, opens the door to low-cost, high-performance optoelectronic devices. The reported power conversion efficiency of 25 % of the halide-based perovskite solar cells makes them promising materials. Recently, electron transfer studies in PNC-based electron donor—acceptor (D–A) systems received great momentum due to their potential applications to solar cell technology. Among acceptor compounds,  $C_{60}$  is remarkable because it can stably accept up to six electrons. In this study, we demonstrate the  $C_{60}$ -based ligand  $C_{60}$ -RCOOH effects on MAPbBr<sub>3</sub> PNCs' properties, such as its – photoluminescence (PL), for revealing photoinduced electron transfer (PET).

**Results and Discussion.** The significant negative Gibbs free energy change ( $\Delta G$ = -0.31 eV) for the C<sub>60</sub>-ligand-MAPbBr<sub>3</sub> donor-acceptor (D-A) system indicates the feasibility of PET. For further investigation of the nature of PET from PNCs, we perform PL studies of PNC solutions in the absence or presence of C<sub>60</sub>-RCOOH. Figure 1a shows the PL spectra of a MAPbBr<sub>3</sub> PNCs solution in the presence of C<sub>60</sub>-RCOOH at different concentrations. The PL intensity of the PNC solution decreases with increases in the C<sub>60</sub>-RCOOH concentration, suggesting efficient PET from MAPbBr<sub>3</sub> PNC to C<sub>60</sub>-RCOOH. The PL lifetimes remained unchanged with increases in the concentration of C<sub>60</sub>-RCOOH (Figure 1b).



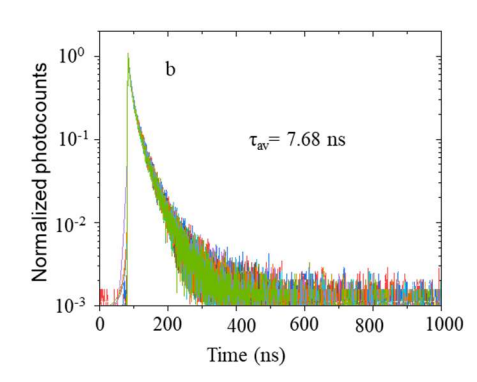


**Fig. 1: a)** PL spectra of a MAPbBr<sub>3</sub> PNC solution supplemented with different concentrations of  $C_{60}$ -RCOOH ( $\lambda_{ex}$ : 365 nm). **b)** The PL decay profiles of a MAPbBr<sub>3</sub> PNC solution without or with different concentrations of  $C_{60}$ -RCOOH ( $\lambda_{ex}$ : 405 nm).

These results suggest the adsorption of the  $C_{60}$ -RCOOH ligand onto the hydrophobic-capped surface of a PNC quenches the photo excited PNC, enabling efficient static interfacial electron transfer. Such an electron acceptor ligand can be a promising electron transport material in perovskite solar cells.

- 1. B. M. Sachith, T.Okamoto, S. Ghimire, T. Umeyama, Y. Takano, H. Imahori, V. Biju, *J. Phys. Chem. Lett.* **2021**, *12*, 8644.
- 2. J. Y. Kim, J. Lee, H. S. Jung, H. Shin, N. G. Park, Chem. Rev. 2020, 120, 7867-7918.

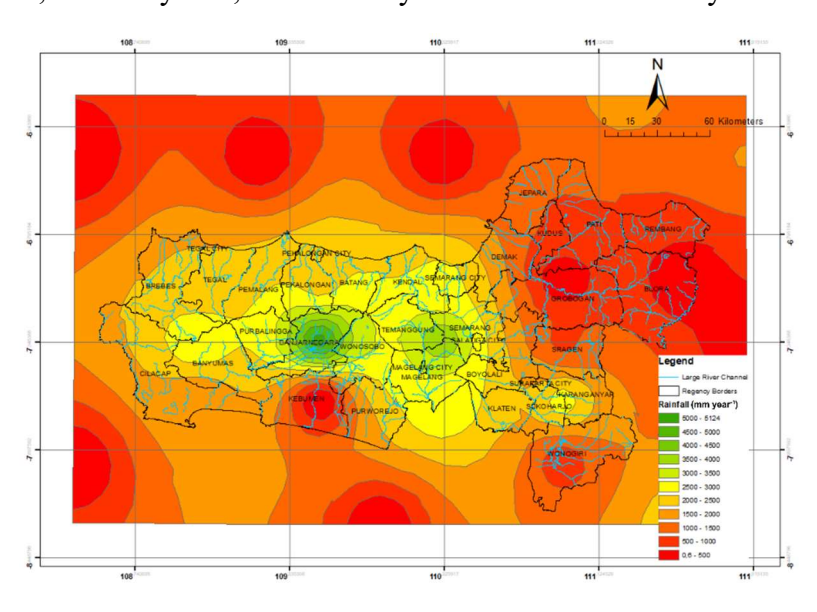
### Near Future Projection of Rainfall Distribution Pattern Assessment Under Climate Change by GIS-Based Adaptive Neuro Fuzzy Interference System in Central Java Province, Indonesia

Reza Kusuma Nurrohman<sup>1,2</sup>, Bayu Dwi Apri Nugroho<sup>3</sup>

<sup>1</sup>Graduate School of Agriculture, Hokkaido University, Japan.; <sup>2</sup>Department of Agricultural Engineering, University of Mataram, Indonesia.; <sup>3</sup>Department of Agricultural Engineering, Universitas Gadjah Mada, Indonesia

Introduction. Climate change occurs globally, both in tropical, subtropical, temperate, and polar regions. According to Mawardi (2016), climate change, a direct result of global warming, already, is and will continue occur on earth. The direct result of climate change is a change in the hydrological cycle which results in the changes on water availability (quantity and quality) of water that can be utilized by plants, animals, and humans. This change in water availability will directly affect the environmental system of plants, including agricultural crops, both in the regional and global regions. The water crisis is likely to threaten several countries, especially islands such as Indonesia as predicted by the FAO (Sekhar, 2018). The study location was chosen in Central Java province because it is the province with the highest rice production in Indonesia. Thus, it is important to analyze the rainfall distribution patterns and land suitability assessments to prepare future cropping patterns to adapt to projected climate change.

**Results and Discussion.** During 2024-2028, projected there is drastic decrease rainfall of 0.6-500 mm year<sup>-1</sup>, and there is a change in the distribution pattern of rainfall, with lower in the west and south, and higher in the center compared to previous years. Areas that had low rainfall or around 0,6-2,000 mm year<sup>-1</sup>, increased by 16.78% from the last 5 years. Areas with medium rainfall or around 2000-4000 mm year<sup>-1</sup>, decreased by 16.14% from the last 5 years. Areas with high rainfall, or around 4,000-5,124 mm year<sup>-1</sup>, decreased by 0.64% from the last 5 years.



Based on the IPCC Report on Impact, Adaption and Vulnerability of Climate Change, states that global climate change causes changes in rainfall and temperature increases. Increases in temperature and changes in rainfall patterns can cause changes in vegetation naturally and in the long-term will affect the hydrological cycle and water quality in the area. Furthermore, Projected increases in temperature and changes in rainfall patterns can increase malnutrition; disease and injury due to heatwaves, floods, storms, fires and droughts; diarrheal illness; and the frequency of cardiorespiratory diseases due to higher concentrations of ground-level ozone (IPCC, 2007).

- 1. Mawardi, M. 2016. Irigasi Asas dan Praktek. Yogyakarta, Indonesia: Bursa Ilmu.
- 2. Sekhar, C. S. C. 2018. Climate Change and Rice Economy in Asia: Implications for Trade Policy. Rome: FAO.
- 3. IPCC. 2007. Climate Change 2007: Impacts, Adaptation and Vulnerability. eds. M. L. Parry, O. F. Canziani, J. P. Palutikof, P. J. van der Linden, and C. E. Hanson, 976. Cambridge, UK: Cambridge University Press.

## Non-Targeted LC-MS Analysis of Lipid Composition in Adzuki and Soybean Cultivars

Rachana M. Gangadhara <sup>1</sup>, Siddabasave Gowda B. Gowda <sup>1,2</sup>, Divyavani Gowda <sup>2</sup>, Ken Inui <sup>3</sup>, and Shu-Ping Hui <sup>2</sup>

**Introduction:** Beans, belonging to the Leguminosae family, play a vital role in providing millions of people with protein, energy, and dietary fiber. Approximately 20 different leguminous plant varieties are extensively utilized as dried grains to provide nourishment to humans. Beans are highly nutritious, containing complex carbohydrates, vitamins, minerals, protein, fiber, resistant starch, and phytochemicals, among other beneficial components. These elements contribute to a low glycemic index and provide numerous health benefits<sup>1,2</sup>.

Results and Discussion: Since the global profiling of lipids in beans is limited in the study. We applied a non-targeted lipidomic approach based on high-performance liquid chromatography coupled with linear ion trap-Orbitrap mass spectrometry (HPLC/LTQ-Orbitrap-MS) to comprehensively profile and compare the lipids in six distinct bean cultivars which are native to Japan, namely, adzuki red beans-adzuki cultivar (ARB-AC), adzuki red beans-Benidainagon cultivar (ARB-BC), adzuki red beans-Erimoshouzu cultivar (ARB-EC), soybean-Fukuyutaka cultivar 2021 (SB-FC21), soybean-Fukuyutaka cultivar 2022 (SB-FC22), and soybean-Oosuzu cultivar (SB-OC) (Fig.1). MS/MS analysis defined 144 molecular species from four main lipid groups. Multivariate principal component analysis indicated unique lipid compositions in the cultivars except for ARB-BC and ARB-EC. Evaluation of the concentrations of polyunsaturated fatty acid to saturated fatty acid ratio among all the cultivars showed that SB-FC21 and SB-FC22 had the highest value, suggesting they are the most beneficial for health. Furthermore, lipids such as acyl sterol glycosides were detected and characterized for the first time in these bean cultivars. Hierarchical cluster correlations revealed the predominance of ceramides in ARB-EC, lysophospholipids in SB-FC21, and glycerophospholipids in SB-OC. This study comprehensively investigated lipids and their compositions in beans, indicating their potential utility in the nutritional evaluation of beans as functional foods.

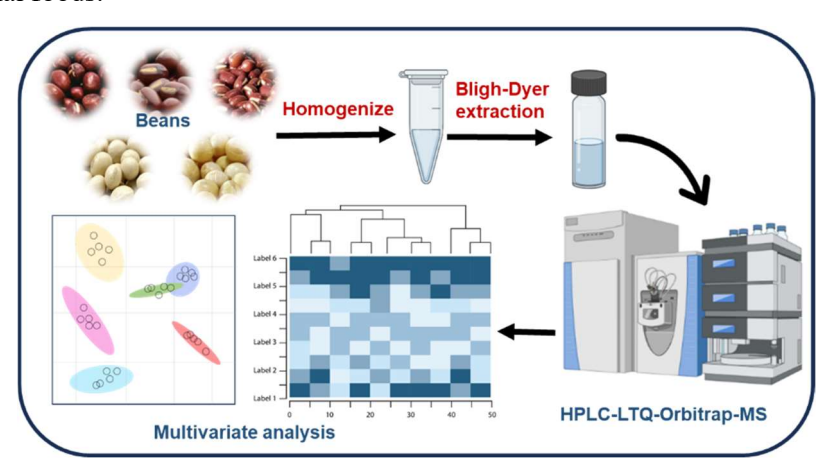


Fig.1 Workflow of the overall study

- F.G.B. Los, A.A.F. Zielinski, J.P. Wojeicchowski, A. Nogueira, I.M. Demiate, Curr. Opin. Food Sci. 2018, 19, 63

  71.
- 2. I. Hayat, A. Ahmad, T. Masud, A. Ahmed, S. Bashir, Crit. Rev. Food Sci. Nutr. 2014, 54, 580-592.

<sup>&</sup>lt;sup>1</sup> Graduate School of Global Food Resources, Hokkaido University.; <sup>2</sup> Faculty of Health Sciences, Hokkaido University.; <sup>3</sup> HIRYU Co., Ltd., Chuo-Cho 2-32, Kashiwa-Shi 277-0021, Japan.

## Caging Bioactive Imidazoles: A Photopharmacological Approach to Achieve Spatiotemporal Regulation on Drug Action

Jiajun Qi, a, b, Ammathnadu S. Amrutha, a, b, and Nobuyuki Tamaoki\* a, b a Research Institute for Electronic Science, Hokkaido University, Kita 20, Nishi 10, Kita-ku, Sapporo, Hokkaido, 001-0020, Japan.;

<sup>b</sup> Graduate School of Life Science, Hokkaido University, Kita 10, Nishi 8, Kita-ku, Sapporo, Hokkaido, 060-0810, Japan.

### Introduction

Imidazoles stand as crucial structural components in a variety of small molecule inhibitors designed to target different kinases in anticancer treatment. However, the effectiveness of such inhibitors is often hampered by non-specific effects and the emergence of resistance. Photopharmacology presents a compelling solution by enabling external control over the drug activity with spatiotemporal precision<sup>1</sup>. We developed a novel strategy for caging imidazole-based drugs.

#### **Results and Discussion**

Both 1 and 2, when irradiated with 405 nm light, regenerated the original SB431542 molecule (Figure 1). We propose that upon exposure to 405 nm light irradiation, the C-N bond connecting the imidazole ring carbon atom of SB431542, and the nitrogen atom of the dimethylamino group undergoes homolytic cleavage, generating imidazolyl and dimethylamine free radicals. The imidazolyl radical likely accepts a hydrogen atom from the aqueous medium used in the experiment, leading to the reformation of the original SB431542 molecule. Based on HPLC analysis about 96% of SB431542 was recovered upon irradiating solution of 1 with 405 nm, indicating high efficency of our photochemical reaction. Introduction of a dialkylamino group at the imidazole ring carbon atom changed the hybridization state of the carbon atom from sp2 to sp3. This change in

hybridization state altered the molecular geometry from planar to tetrahedral and nullified the ability of 1 or 2 to bind to TGF- $\beta$  R1 (transforming growth factor- $\beta$  receptor 1). The spatiotemporal regulation experiment conducted by us demonstrated the applicability of our strategy for achieving external regulation of drug action to minimize adverse effects associated with cancer therapy.

### References

1. Mafy, Noushaba Nusrat; Matsuo, Kazuya; Hiruma, Shota; Uehara, Ryota; Tamaoki, Nobuyuki. "Photoswitchable CENP-E inhibitor enabling the dynamic control of chromosome movement and mitotic progression". J. Am. Chem. Soc. 2020, 142, 1763-1767.

## Development of LC/MS Based Screening Assay for Sphingomyelin Synthase Inhibition

<u>Punith M. Sundaraswamy.</u><sup>1</sup> Jayashankar Jayaprakash<sup>1</sup>, Siddabasave Gowda B. Gowda<sup>1,2</sup>, Divyavani Gowda<sup>2</sup>, Hitoshi Chiba<sup>3</sup>, Shu-Ping Hui<sup>2</sup>

<sup>1</sup>Graduate School of Global Food Resources, Hokkaido University, Kita-9, Nishi-9, Kita-Ku, Sapporo 060-0809, Japan.; <sup>2</sup>Faculty of Health Sciences, Hokkaido University, Kita-12, Nishi-5, Kita-ku, Sapporo 060-0812, Japan.; <sup>3</sup>Department of Nutrition, Sapporo University of Health Sciences, Nakanuma, Nishi-4-3-1-15, Higashi-ku, Sapporo 007-0894, Japan.

**Introduction:** The changes in the sphingolipids biological process are linked to metabolic syndrome including obesity, dyslipidemia, insulin resistance, cardiovascular problems, and type 2 diabetes mellitus [1]. The main driving factor for this metabolic syndrome are imbalance of lipid metabolism. The changes in lipid metabolites are due to altering lipid metabolomic enzyme such as sphingomyelin synthases (SMSs) [2].

Result and Discussion: In this research, we developed a straightforward, highly sensitive, and reproducible liquid chromatography/mass spectrometry (LC/MS) based screening assay method for SMS inhibition. This method involved monitoring C6-Ceramide and C6-Sphingomyelin levels by targeted analysis. The single reaction monitoring channels were established using TSQ Quantum Access Triple Quadrupole Mass Spectrometer in the positive ionization mode. To assess SMS activity, HeLa cells expressing both SMS1 and SMS2 were employed, with C6-Ceramide serving as the substrate. To validate the efficacy of this SMS assay method, we conducted an experiment to assess the inhibitory activity of Ginkgolic acid (GA) on HeLa/SMS1 and HeLa/SMS2 cell lysates. We treated the cell lysates to varying concentrations of GA, a known natural inhibitor and found that GA exhibited remarkable inhibitory effects against both SMS1 and SMS2. Additionally, we conducted *in-silico* investigations of GA binding to SMS1/SMS2, which were further substantiated through molecular docking and molecular dynamics simulations. Our results demonstrate that GA interacts with various amino acids within the binding pocket of the active sites of both SMS1 and SMS2 proteins. An LC/MS based screening assay for SMS inhibition has been developed and *in-silico* insights of GA on SMS were investigated. GA appears to be a promising SMS inhibitor. The establishment of the SMS inhibition screening assay method may help to facilitate the discovery of novel SMS1- or SMS2-specific natural inhibitors.

- 1. Li. Y.L, Qi, X.Y. Jiang, H. Deng, X.D. Dong, Y.P. Ding, T.B. Zhou, L. Men, P. Chu, Y. Wang, R.X. and Jiang. X.C, *Bioorg. Med. Chem.* **2015**, *23(18)*, 6173-6184.
- 2. Zama. K, Mitsutake. S, Watanabe. K, Okazaki. T, and Igarashi. Y, Chem. Phys. Lipids, 2012, 165(7), 760-768.

### Defluorinative Cross Couplings of Trifluoromethyl Arenes by Copper Photoredox Catalysis

Priya Saha<sup>1</sup> and Dennis Chung-Yang Huang<sup>1</sup>

<sup>1</sup> Institute for Chemical Reaction Design and Discovery (WPI-ICReDD), Hokkaido University, Kita 21 Nishi 10, Kita-ku, Sapporo, Hokkaido 001-0021, JAPAN.

**Introduction.** Fluorine-containing organic compounds possess distinctive biological and physiochemical properties. They are extensively studied as they have many valuable applications in material science, pharmaceutical chemistry, and agrochemical development. This protocol involves copper as a photoredox catalyst for selective reductive mono defluorination of trifluoromethyl arenes and also cross-coupling catalyst to construct the carbon-heteroatom bonds.

**Results and Discussion.** In the past decades, the C–F bond functionalization of trifluoromethyl groups has emerged as an effective pathway for the synthesis of various challenging products. Selective defluorination of trifluoromethyl arene is considered difficult because of continuous decrease in the C–F bond strength as defluorination proceeds, which often results in multiple defluorination. According to recent reports, cleavage of one of the C–F bonds in Ar–CF3 substrates has been achieved using metal or electrochemical reductions, photoredox-catalyzed trifluoromethylarene reduction that react with olefin to form C-C bonds. The construction of carbon-heteroatom bond via selective defluorination is still challenging.

The reported approaches to generate C-O bonds require harsh conditions, multistep synthesis, environmentally harmful toxic and expensive reagents.<sup>2</sup> Herein, we report a one pot copper-catalyzed defluorinative coupling of trifluoromethyl arenes to form C-O bonds.<sup>3</sup> Moreover, we could observe dual role of copper. Copper upon forming complex with ligand acts as photocatalyst for selective reduction of trifluoromethyl arene as well as cross coupling catalysis resulting in -CF2O bond formation. The synthesized -CF2O- motifs is expected to act as drug candidates and functional materials due to similarities with biologically active esters.

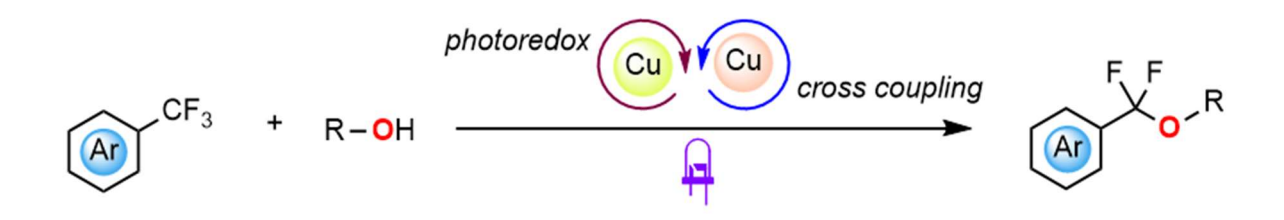


Figure 1: Defluoroetherification of trifluoromethyl arenes

- 1. J. Han, L. Kiss, H. Mei, A. M. Remete, M. Ponikvar-Svet, D. M. Sedgwick, R. Roman, S. Fustero, H. Moriwaki, V. A. Soloshonok, "Chemical Aspects of Human and Environmental Overload with Fluorine" *Chem. Rev.*, **2021**, *121*, 4678–4742.
- 2. Zhou, Q.; Ruffoni, A.; Gianatassio, R.; Fujiwara, Y.; Sella, E.; Shabat, D.; Baran, P. S. Direct Synthesis of Fluorinated Heteroarylether Bioisosteres. *Angew. Chem., Int.* Ed. **2013**, *52*, 3949.
- 3. P. Saha, C.-Y. Huang, manuscript in preparation.

## Photocatalytic Conversion of Glucose into Formate with Comparison of Different Crystal phase of TiO<sub>2</sub>

Pratiksha Babgonda Patil<sup>1</sup>, Sanjay S. Latthe<sup>2</sup>, Shanhu Liu<sup>3</sup>, Sho Usuki<sup>1</sup>, Kazuya Nakata<sup>1,\*</sup>

<sup>1</sup>Research Institute for Electronic Science, Hokkaido University.; <sup>2</sup>Department of Molecular Engineering, Graduate School of Engineering, Kyoto University.

### Introduction

An energy-efficient and environmentally beneficial technique is photocatalysis. Utilizing biomass in combination with photocatalysis is a novel and promising way to increase the sustainability of chemical processes. FA can be produced with high efficiency from biomass-derived compounds abundant in nature. Using different TiO<sub>2</sub> structures, we manifest the efficient formation of FA from glucose. Anatase has the highest FA yield, 76%. For rutile and brookite, FA yield is 69.6% and 63%, respectively. In addition to adjusting the charge of the TiO<sub>2</sub> surface and controlling the adsorption of glucose and the desorption of formic acid, hydroxyl ions are primarily responsible for the rapid formation of active oxidative radicals (O<sub>2</sub>·, ·OH) that lead to the conversion of glucose into formic acid.

### Result and discussion

Effect of reaction time on the formate selectivity and glucose conversion:

Here, the study of the superior performance of anatase compared to rutile and brookite is correlated. With the increase in irradiation time, the FA yield increased from 8.1% to 76% for anatase, and the selectivity of FA yield reached the highest value of 76% at 72 h. Formate selectivity is 69.6% and 63% for rutile and brookite, respectively. Moreover, accompanied by the increase in reaction time, complete conversion of glucose, and higher selectivity in FA production was obtained at 72 h. A further increase in irradiation time gradually decreased the FA yield, which was likely primarily because of the further oxidation decomposition of the FA. [Figure:(A), (B), and (C)].

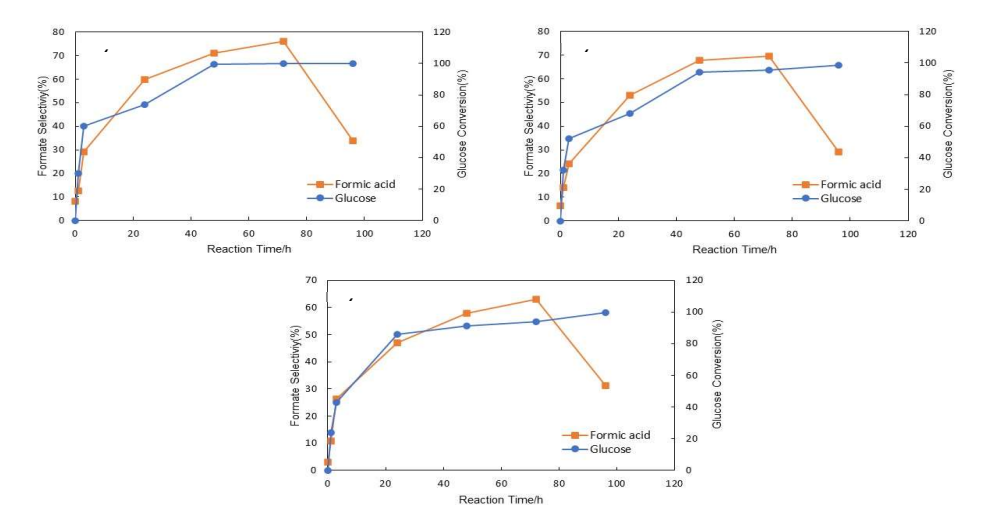


Figure 1. Effect of reaction time on the formate selectivity and glucose conversion.

- 1. Bellardita, M., Loddo, V., & Palmisano, L. (2020). Formation of High Added Value Chemicals by Photocatalytic Treatment of Biomass. *Mini-Reviews in Organic Chemistry*, 17(7), 884–901.
- Chen, X., Liu, Y., & Wu, J. (2020). Sustainable production of formic acid from biomass and carbon dioxide. In Molecular Catalysis (Vol. 483). Elsevier B.V.
- 3. Hou, Y., Niu, M., & Wu, W. (2020). Catalytic Oxidation of Biomass to Formic Acid Using O2 as an Oxidant. In *Industrial and Engineering Chemistry Research* (Vol. 59, Issue 39, pp. 16899–16910). American Chemical Society.

## Development of Visible-Light Active "Heteroaryl Azo" Photoswitches for Photopharmacology Applications

Nusaiba Madappuram Cheruthu<sup>1,2</sup>, P.K. Hashim<sup>1,2</sup>, Hideyuki Mitomo<sup>2</sup>, Kuniharu Ijiro<sup>2</sup>, Nobuyuki Tamaoki<sup>1,2</sup>
<sup>1</sup>Graduate School of Life science, Hokkaido University, <sup>2</sup>Research Institute for Electronic Science, Hokkaido University.

### Introduction.

Pharmacotherapy is often hindered by poor drug selectivity, side effects, and drug resistance. One way to improve drug selectivity is via "photopharmacology" method, where a photoswitchable group is incorporated into a bioactive drug and controls its action by light stimulus. However, most photoswitches require harmful UV light for their structural change. We have recently discovered thiazole based photoswitches that can isomerize by visible light irradiation<sup>1</sup>. Some of the derivatives of thiazole-based photoswitches isomerized by longer wavelength visible light, however their photoisomers are too short-lived for practical applications. In this study we developed photoswitches based on new heteroaryl units (thiadiazole, isoxazole, isothiazole etc) that can isomerize by longer wavelength visible light and show long enough photoisomer stability (Figure. 1)

### Results and Discussion.

We developed a general procedure for the synthesis of type 1 compounds using Mills reaction between nitrosobenzene and corresponding heteroaryl amines. Type 2 photoswitches were synthesized by oxidation of heteroaryl amines. All synthesized photoswitches showed reversible *trans-cis* isomerization by light irradiation,

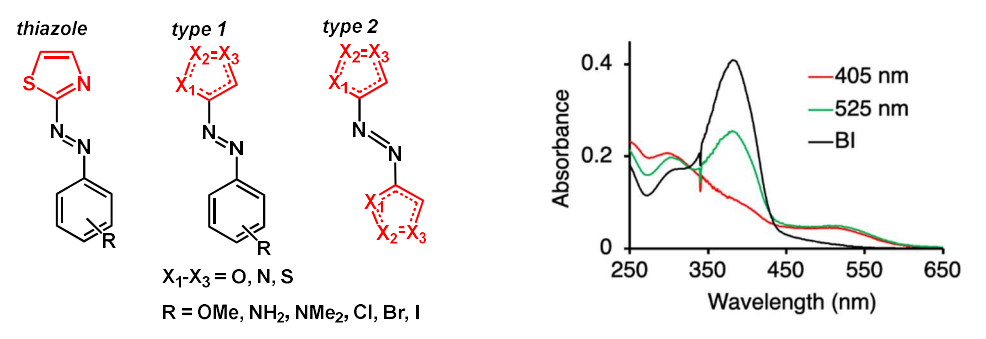


**Figure 1**; Molecular structures of the heteroaryl photoswitches. Absorption spectra of Azo-bis(1,2,3-thiadiazole) photoswitch before irradiation (BI) and after photostationary states obtained by light irradiation at 405 nm and 525 nm.

however their maximum absorption wavelength ( $\lambda_{max}$ ) and the corresponding wavelength required for isomerization varied significantly depending on the type of heteroaryl moieties. For instance, the  $\lambda_{max}$  of photoswitches containing isoxaole showed 302 nm while having thiadiazole moiety was 343 nm. Interestingly, type 2 photoswitches showed longer  $\lambda_{max}$  and longer thermal stability than type 1. The absorption spectra of type 2 compound, of Azo-bis(1,2,3-thiadiazole) is shown in Figure 1. This compound has  $\lambda_{max}$  of 382 nm and exhibited *trans-cis* forward isomerization by irradiation with 405 nm wavelength light. The reverse isomerization occurred either irradiating with longer wavelength light (525 nm) or thermally. We believe that this new category of photoswitches is suitable for photopharmacology applications, and such studies are currently progressing.

### References

1. Lin, R.; Hashim, P. K.; Sahu, S.; Amrutha, A. S.; Cheruthu, N. M.; Thazhathethil, S.; Takahashi, K.; Nakamura, T.; Kikukawa, T.; Tamaoki, N. J. Am. Chem. Soc. 2023, 145, 9072–9

### Oxygen Deficient Co Doped ZrO2 for Selective CO2 Reduction to CO

<u>Nazmul Shaikh</u>, Atsushi Fukuoka, Abhijit Shrotri Institute for Catalysis, Hokkaido University

**Introduction.** The concomitant rise of  $CO_2$  concentration in the atmosphere due to use of fossil fuels is the main reason behind global warming and climate change. Furthermore, fossil fuels are finite resources. As a result, finding substitute carbon source will eventually be needed to maintain a sustainable economy. In this regard, one of the most promising methods is to synthesize CO from  $CO_2$  ( $CO_2 + H_2 \rightarrow CO + H_2O$ ) selectively because CO is a precursor for many industrially important chemicals and fuels. Recently, oxide nanoparticles have emerged as promising catalysts for  $CO_2$  reduction. However, these catalysts are more selective for  $CH_3OH$  or  $CH_4$  formation. In contrast, we show that doping of isolated Co atoms in  $ZrO_2$  creates oxygen deficient sites that are active and selective for CO formation.

**Results and Discussion.** Co doped ZrO<sub>2</sub> catalysts were prepared using co-precipitation method. Ammonia solution was added dropwise to an aqueous solution of Co(NO<sub>3</sub>)<sub>2</sub>.2H<sub>2</sub>O and ZrO(NO<sub>3</sub>)<sub>2</sub>.2H<sub>2</sub>O under vigorous condition. The resulting precipitate was dried and calcined at 500 °C to yield the Co doped ZrO<sub>2</sub>. The catalytic

activity was checked in a high-pressure fixed-bed reactor system equipped with an online GC-TCD.

Undoped  $ZrO_2$  showed negligible  $CO_2$  conversion at 340 °C, 3MPa and 10,000 mL h<sup>-1</sup> g<sub>cat</sub><sup>-1</sup> (Figure 1a). For all Co doped  $ZrO_2$  catalysts,  $CO_2$  conversion was much higher with CO selectivity more than 90%.  $CoZrO_x$  (10) catalyst (Co:Zr=1:9) was most active and did not deactivate even after 400 h on stream. In comparison, a catalyst having Co nanoparticles on  $ZrO_2$  ( $Co/ZrO_2$ ) predominantly produced  $CH_4$ .

The catalysts were characterized to understand the effect of Co doping in ZrO<sub>2</sub>. Co doped ZrO<sub>2</sub> catalysts had tetragonal crystal structure and Co atoms were uniformly distributed throughout the matrix without the formation of Co clusters or particles. Co and Zr were present in +2 and +4 oxidation states, respectively. This charge

a)	Catalysts	X(CO <sub>2</sub> )	S(CO)	S(CH <sub>3</sub> OH)	S(CH <sub>4</sub> )
9	ZrO <sub>2</sub>	1.8	100	0	0
	$CoZrO_x$ (1)	6.9	100	0	0
	$CoZrO_x$ (5)	14	97	3	0
	$CoZrO_x$ (10)	19	97	3	0
	$CoZrO_x$ (15)	17	94	6	0
	Co/ZrO <sub>2</sub>	87	0	0	100

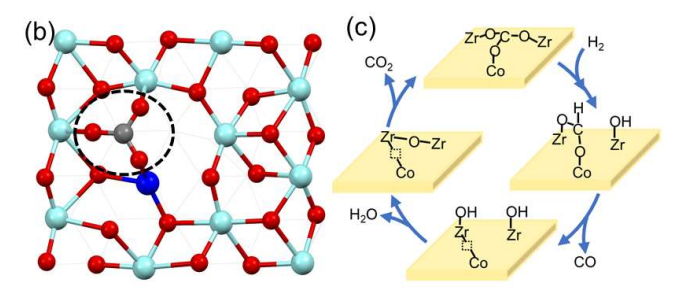


**Figure 1:** (a) Catalytic activity of Co doped ZrO<sub>2</sub> catalysts, (b) DFT structure of CO<sub>2</sub> adsorption as carbonate (blue: Co, cyan: Zr, red: O) and (c) mechanism of CO formation.

imbalance in the crystal generated oxygen vacancy near the interfacial site of Co single atom and neighboring Zr atoms, which promoted the chemisorption of  $CO_2$  in carbonate form (Figure 1b).  $H_2$  dissociation on Co atom and transfer of H to C atom of carbonate formed formate intermediate (Figure 1c). Decomposition of formate species produced CO with high selectivity. The absence of Co particles restricted the formation of methane. Co atoms did not reduce and sinter during reaction due to the strong oxidic interaction between  $Co^{2+}$  and  $ZrO_2$ , which explains the high stability of the catalyst.

- 1. J. Bao, G. Yang, Y. Yoneyama, N. Tsubaki, ACS Catal., 2019, 9, 3026-3053.
- 2. J. Wang, G. Li, Z. Li, C. Tang, Z. Feng, H. An, H. Liu, T. Liu, C. Li, Sci Adv., 2017, 3, e1701290.
- 3. N. H. M. Dostagir, C. Thompson, H. Kobayashi, A. M. Karim, A. Fukuoka, A. Shrotri, *Catal. Sci. Technol.*, **2020**, *10*, 8196-8202.
- 4. N. H. M. Dostagir, R. Rattanawan, M. Gao, J. Ota, J. Hasegawa, K. Asakura, A. Fukuoka, A. Shrotri, *ACS Catal.*, **2021**, *11*, 9450-9461

### Interfacial Defect Passivation of Amphiphilic Ligand-Capped Halide Perovskite Nanocrystals

Most Farida Khatun<sup>1</sup>, Sushant Ghimire<sup>2</sup>, Bhagyashree M. Sachith<sup>1</sup>, Takuya Okamoto<sup>1, 2</sup>, Jeladhara Sobhanan<sup>1</sup>, Ch Subrahmanyam<sup>3</sup>, Vasudevanpillai Biju<sup>1, 2, 3</sup>

<sup>1</sup>Graduate School of Environmental Science, Hokkaido University, Sapporo, Hokkaido 001-0020, Japan; <sup>2</sup>Research Institute for Electronic Science, Hokkaido University, Sapporo, Hokkaido 001-0020, Japan; <sup>3</sup>Department of Chemistry, Indian Institute of Technology Hyderabad, Kandi-502284, Sangareddy, Telangana, India

**Introduction.** Halide perovskites are highly promising materials for next-generation light-emitting and photovoltaic applications.<sup>1</sup> They have excellent optoelectronic properties and low manufacturing cost.<sup>1</sup> However, the journey of perovskites from the laboratory to commercial products faces challenges related to stability, scalability, and toxicity. To address the stability issues, several research groups explore strategies such as halide vacancy filling<sup>2</sup>, polymer coating<sup>3</sup>, and amphiphilic molecule coating<sup>4</sup>. In this work, we demonstrate the synthesis of a new amphiphilic ligand (AL) poly(ethyleneimine)-dodecanoic acid amide (PEDAA) and the halide vacancy passivation in AL-capped CsPbBr<sub>3</sub> perovskite nanocrystals (AL-PNCs) using NaBr.<sup>5</sup> We also report halide exchange in AL-PNCs using NaCl and NaI.

**Results and Discussion.** AL is synthesized by activating dodecanedioic acid (10 mmol) using the coupling reagent DMTMM (5 mmol) in methanol at 60 °C for 12 h. Next, a poly(ethyleneimine) solution (500  $\mu$ L) in

50% water is added to the above mixture under vigorous stirring. The reaction was continued for 4 h at 60 °C. The crude product is separated by precipitating using acetonitrile. The crude AL is purified through repeatedly dissolving in methanol and precipitating with THF. AL-PNCs are prepared by either direct synthesis with AL as one of the ligands in 2-propanol or ligand exchange of oleic acid- and hexadecyl amine-capped CsPbBr<sub>3</sub> PNCs

AL-PNCs disperse well in polar solvents such as 2-propanol, 2-butanol, or 1-pentanol. STEM imaging helps confirm the uniform-size distribution of AL-PNCs (ca. 9.1  $\pm$  1.2 nm). The photoluminescence (PL) quantum yield ( $\Phi$ ) for the PNCs is 57%, suggesting the presence of bromine vacancies. As represented in Fig. 1a–b, NaBr treatment-induced Br vacancy filling accompanies an increase ( $\Phi$  = 0.57 to 0.60) in the PL intensity and average lifetime ( $\tau_{av}$ ) (4.5 and 5.2 ns) for AL-PNCs. Nevertheless,

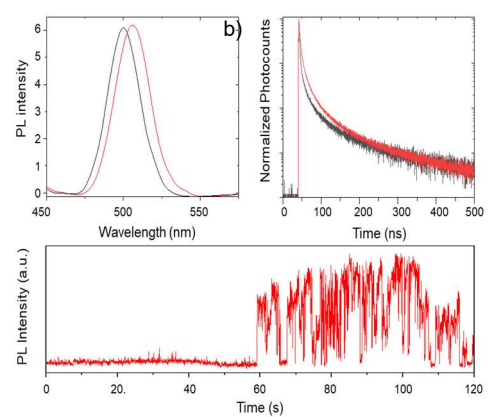


Fig. 1. PL spectra (a) and, decay (b) of AL-capped CsPbBr<sub>3</sub> PNCs, and PL intensity trajectories of (c) single AL-capped CsPbBr<sub>3</sub> PNCs before (black) and after (red) the treatment with the saturated NaBr solution.

the treatment with NaBr induces a slight PL spectral redshift (Fig. 1a). Single particle PL studies show sudden brightening of the particles having low PL intensity initially (Fig. 1c). These results suggest the successful filling of bromine vacancies in AL-PNCs in polar solvent. Details of halide vacancy filling and halide exchange in hydrophobic and hydrophilic solvents for hydrophobic ligands- and AL-capped PNCs will be presented.

- 1. L. Chouhan, S. Ghimire, C. Subrahmanyam, T. Miyasaka, V. Biju, Chem. Soc. Rev. 2020, 49, 4321.
- 2. N. Aristidou, C. Eames, I. Sanchez-Molina, X. Bu, J. Kosco, MS. Islam, SA. Haque, Nat. Commun. 2017, 8, 15218.
- 3. M. R. Kar, S. Kumar, T. K. Acharya, C. Goswami, S. Bhaumik, RSC Adv. 2023, 13, 5946.
- 4. G. Shen, H. Dong, F. Yang, XR. Ng, X. Li, F. Lin, C. Mu, J. Energy Chem. 2023, 78, 454.
- 5. S. Ghimire, M. F. Khatun, B. M. Sachith, T. Okamoto, J. Sobhanan, C. Subrahmanyam, V. Biju, ACS Appl. Mater. Interfaces, 2023, 15, 41081.

### **Evaluation of Biodegradability of Chitin and Chitosan Plastics** in Various Environments

Akihiro Mizuyama , Tomohisa Suzuki, Taiyo Nagai, Olaf Karthaus Chitose Institute of Science and Technology

**Introduction**. In recent years, environmental pollution of plastics has become a problem all over the world. To solve this problem, biodegradable plastics will be important. We observed whether the plastic substitute for chitin and chitosan produced in the laboratory decomposes in compost. Biodegradability in the natural environment was also evaluated.

**Result and Discussion.** Chitin and chitosan plates and foam materials were added to compost under the following conditions and follow-up was observed.

- 1. biodegradable plastic in the finished compost. Fig 1.
- 2. Biodegradable plastic in compost loaded with food waste, and microbial materials. Fig 2.

In the case of condition 1, bioplastic was not decomposed. However, in the case of condition 2, it was confirmed that it decomposed in  $1\sim2$  months.

In addition, biodegradability of chitin and chitosan plastics in various natural environments was evaluated for one month. Especially in environments such as rivers and lakes, no denaturation of the state of the plate material could be confirmed. However, the foam absorbed water and was expanding. But, neither of them was confirmed to be biodegradable in the natural environment.

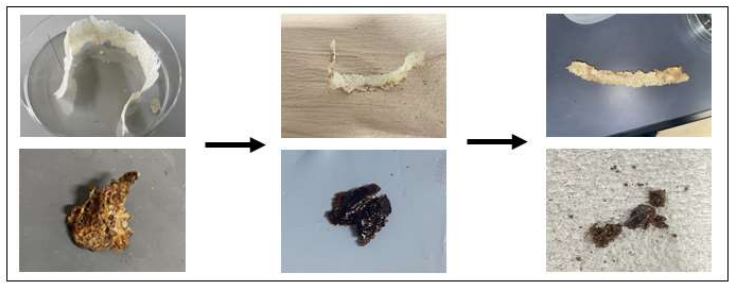


Fig 1 Condition1

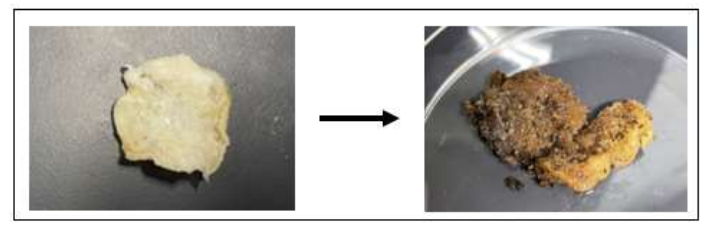


Fig 2 Condition2

### **Dissecting Sorghum Cultivars Lipidome by Untargeted Analysis**

<u>Lipsa Rani Nath</u><sup>1,</sup> Siddabasave Gowda B. Gowda <sup>1,2</sup>, Thomas Roberts<sup>4</sup>, Divyavani Gowda<sup>2</sup>, Hitoshi Chiba<sup>3</sup>, Shu-Ping Hui <sup>2</sup>

<sup>1</sup>Graduate School of Global Food Resources, Hokkaido University, Sapporo, Japan.; <sup>2</sup>Faculty of Health Sciences, Hokkaido University, Kita-ku, Sapporo, Japan.; <sup>3</sup>Department of Nutrition, Sapporo University of Health Sciences, Sapporo, Japan.; <sup>4</sup>School of Life and Environmental Sciences, University of Sydney, Australia.

**Introduction.** Sorghum (Sorghum bicolor (L.) Moench) is ranked as the fifth most significant cereal crop worldwide. The rich array of phenolic compounds discovered in sorghum exhibits a potential contribution to disease prevention[1]. Whole-grain sorghum may combat heart disease, diabetes, and obesity, but more research is needed to confirm its health benefits [2].

Results and Discussion: Utilizing untargeted liquid chromatography mass spectrometry (LC/MS) technique for lipid analysis in sorghum grains can provide valuable insights into the diversity and composition of lipids within the crop. Sorghum grain samples were collected from the field trails in Australia and their lipid extraction was performed using the Bligh-Dyer method. The total lipid extracts were injected into LC/MS and data analysis was performed by MS DIAL. The untargeted LC/MS analysis not only detected a range of lipid sub-classes but also unveiled the presence of novel fatty acid esters of hydroxy fatty acids (FAHFAs) in sorghum grains for the first time. FAHFAs are known for their potential antidiabetic activities. Furthermore, the analysis highlighted substantial variations in lipid composition among different sorghum varieties. This study provides insights into the lipid processing mechanisms within sorghum, offering a pathway to investigate the nutritional advantages associated with specific lipid categories. The untargeted LC/MS lipid analysis method showcased its efficiency in thoroughly profiling the sorghum lipidome, indicating its potential for broader utilization in the field of lipidomics research.

- 1. Smolensky D, Rhodes D, et al, J. Med. Food. 2018, 21, 990-998.
- 2. Stefoska-Needham A, Beck E.J, et al, *Food Rev. Int.*, **2015**, *31*, 401-437.

## Synthesis of Shortwave-Infrared (SWIR) Organic Fluorescent Probes for Specific Biomolecular Imaging

<u>Aravind K. Swamy</u>, <sup>1</sup> Mahadeva Swamy M. M., <sup>1,2</sup> Yuta Murai, <sup>1</sup> Setsuko Tsuboi, <sup>2</sup> Kenji Monde, <sup>1</sup> and Takashi Jin<sup>2</sup>

<sup>1</sup>Faculty of Advanced Life Science, Hokkaido University, Sapporo 001-0021, Japan.; <sup>2</sup>Center for Biosystems Dynamics Research, RIKEN, Osaka 565-0864, Japan.

Introduction. Fluorescence imaging is a safe and cost-effective imaging technology that allows for real-time monitoring, but it has not been widely used in clinical settings due to limited light penetration into tissue and strong background signal from natural chromophores.<sup>1</sup> These challenges can be resolved by employing the shortwave infrared part of the electromagnetic spectrum (SWIR or NIR-II, 1000-1400 nm). Compared to visible (400-700 nm) and near-infrared (700-1000 nm) light, these long-wavelength photons have less scattering, tissue absorption, and autofluorescence. Because of these characteristics, the SWIR region is well-suited for study in small model animals and expanding the depth of optical clinical diagnostics. However, commercially accessible imaging agents for this region are few. Indocyanine green (ICG), an FDA approved NIR fluorophore with a small percentage of emission in the SWIR region, have been using from past 60 years in the clinical applications.<sup>2</sup> The advantages of SWIR imaging for surgical guided techniques in terms of sensitivity and accuracy would be more obvious if bright, SWIR analogs of ICG were accessible.

**Results and Discussion.** Herein, we present the synthesis of  $\pi$ -conjugation extended ICG analogues ICG-C9 and ICG-C11 (**Fig.1a**) and their antibody labeling agents as SWIR-emitting probes. The covalent conjugation reaction was performed between developed organic dyes and monoclonal antibodies to synthesize molecular probes (**Fig.1b**) for specific biomolecular imaging. Using molecular probes, we demonstrate high-contrast *in vivo* optical imaging of brain and breast tumors in living mice (**Fig1c** and **1d**). This study provides a general strategy for SWIR fluorescence molecular imaging using cyanine-dye based biocompatible probes. The presented SWIR-emitting fluorescent probes have a greater potential to apply for possible clinical optical diagnostics.

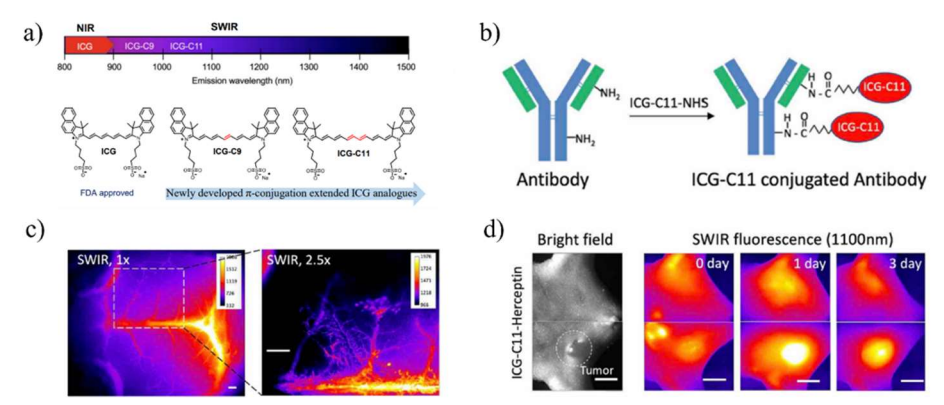


**Fig-1**: a) Fluorescence emission wavelength of ICG, ICG-C9, ICG-C11 and their chemical structures. b) conjugation of ICG-C11-NHS with the antibody. c) Intravital brain imaging through the skull. d) Bright field and SWIR fluorescence (1100 nm) images of nude mice bearing breast tumors.

- 1. C. Li, G. Chen, Y. Zhang, F. Wu, Q. Wang, J. Am. Chem. Soc. 2020, 142, 14789.
- 2. J. A. Carra, D. Frankea, J. R. Carama, C. F. Perkinsona, M. Saifa, V. Askoxylakisb, M. Dattab, D. Fukumurab, R. K. Jainb, M. G. Bawendia, O. T. Bruns, *Proc. Natl. Acad. Sci. U. S. A.* **2018**, 115, 4465.
- 3. M. M. M. Swamy, Y. Murai, K. Monde, S. Tsuboi, T. Jin. Bioconjugate Chem. 2021, 32, 1541.

## Investigating the Impact of Ethanol on Colon Content Lipidome in Mice Models via Nontargeted LC/MS analysis

<u>Jayashankar Jayaprakash</u><sup>1</sup>, Siddabasave Gowda B. Gowda<sup>1,2</sup>, Divyavani Gowda<sup>2</sup>, Hitoshi Chiba<sup>3</sup>, Shu-Ping Hui<sup>2</sup>

<sup>1</sup>Graduate School of Global Food Resources, Hokkaido University, Kita-9, Nishi-9, Kita-Ku, Sapporo 060-0809, Japan.; <sup>2</sup>Faculty of Health Sciences, Hokkaido University, Kita-12, Nishi-5, Kita-ku, Sapporo 060-0812, Japan.; <sup>3</sup>Department of Nutrition, Sapporo University of Health Sciences, Nakanuma, Nishi-4-3-1-15, Higashi-ku, Sapporo 007-0894, Japan.

**Introduction:** Alcohol consumption has widespread effects on the human body [1]. When alcohol is consumed, it is absorbed by the intestines and processed by the liver. However, excessive alcohol use adversely affects the integrity of the gut epithelium, microbiome, and lipid metabolism [2].

Results and Discussion: The present study focused on investigating the impact of ethanol on colon content lipidome in mice models of both sexes using nontargeted liquid chromatography/mass spectrometry (LC/MS). The comprehensive lipidome analysis of colonic flush samples was obtained from ethanol-fed (EF) and pairfed (PF) mice of both sexes. The statistical results of partial least squares discriminant analysis show that ethanol had a greater effect on the colonic lipid composition of male mice compared to female mice. Specifically, male mice in the EF group exhibited a significant increase in free fatty acids, ceramides, and hexosylceramides, along with a decrease in phosphatidylglycerols when compared to the PF group. Both male and female EF groups showed a significant increase in phosphatidylethanolamine (PE) levels compared to the PF group mainly PE (O-15:1/15:0) and PE (O-18:2/15:0) are the common markers in both sexes of EF group. Specifically, the EF group in female mice showed decreased fatty acid esters of hydroxy fatty acids. Significant lipidome variation was observed in EF and PF group mice colon contents. This study provides new insight into the lipids involved in the disruption of the gut microbiota driven by alcohol and its potential impact on health.

- 1. P. Mathurin, R. Bataller, J. Hepatol. 2015, 62(1), 38-46.
- 2. A. Parlesak, C. Schäfer, T. Schütz, J. C. Bode, C. Bode, J. Hepatol. 2000, 32(5), 742–747.

### Low-Dimensional Fluorescent Hybrid Metal Halide Crystals

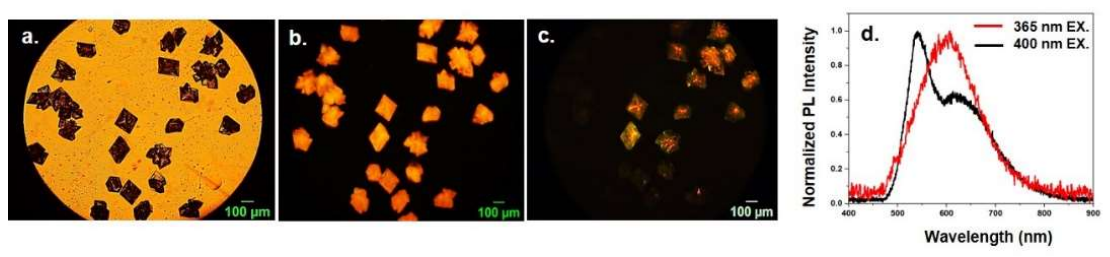
Rahul Ghosh Dastidar, a Takuya Okamoto, a,b Ch. Subrahmanyamc, a,b Vasudevanpillai Biju a,b

<sup>a</sup>Graduate School of Environmental Science, Hokkaido University, Sapporo, Hokkaido, Japan. <sup>b</sup>Research Institute for Electronic Science, Hokkaido University, Sapporo, Hokkaido, Japan, and <sup>c</sup>Department of Chemistry, Indian Institute of Technology Hyderabad, Telangana, India

**Introduction.** Low dimensional hybrid metal halides, comprised of organic ligands and inorganic metal halide units, emerge as a unique class of photoluminescent materials. Besides narrow, room-temperature photoluminescence(PL) of 3D lead halide perovskites, intrinsic broad emission coming from single-phase bulk metal halides are rare and desirable for the next generation solid-state lighting devices. Recently, copper-based hybrid metal halides receive much research interests owing to low toxicity and high abundance of copper. <sup>1</sup> The PL properties of hybrid metal halides are controlled by their dimension, and the dimensionality is related to the connectivity between the inorganic motifs. Among these, zero-dimensional hybrid copper halides find applications such as solid-state lighting<sup>2</sup>, X-ray scintillation<sup>3</sup> and optical sensors<sup>4</sup>. Here in, we introduce a 0D hybrid copper halide, synthesized by a simple wet chemistry method, which exhibits dual emission under blue light excitation.

Results and Discussion: Microcrystals(Fig.1) of 1-butyl-1-methyl piperidinium copper bromide [(Bmpip)<sub>2</sub>Cu<sub>2</sub>Br<sub>4</sub>] are synthesized through simple wet chemistry method. A precursor solution of (Bmpip)<sub>2</sub>Cu<sub>2</sub>Br<sub>4</sub> is prepared by mixing 0.472 g BmpipBr, 0.144 g CuBr, and 30 mL dehydrated ethanol in a 200 mL two-neck flask at 80 °C for 2 h under an Ar atmosphere. After removing the heat, 2mL of the reaction mixture is dropped on a glass cover slip. Single crystals of (Bmpip)<sub>2</sub>Cu<sub>2</sub>Br<sub>4</sub> are formed at room temperature. The photoluminescence (PL) image and spectra of the (Bmpip)<sub>2</sub>Cu<sub>2</sub>Br<sub>4</sub> microcrystals are recorded by exciting with a 365 nm LED or a 404 nm diode laser(fig.1a, c). Time-resolved PL measurements of the (Bmpip)<sub>2</sub>Cu<sub>2</sub>Br<sub>4</sub> microcrystals are carried out using a femtosecond laser Streak camera assembly. These crystals exhibit dual emission under 400 nm excitation(Fig. 1d) and a broad emission under UV excitation. Delayed emissions and low photocounts of the material support the spectral broadening and indirect bandgap nature.

Fig. 1. Optical photographs of (Bmpip)<sub>2</sub>Cu<sub>2</sub>Br<sub>4</sub> under (a) Visible light, (b) 365 nm LED (c) 400 nm laser and (d) PL spectra of a crystal under 400 nm or UV excitation



- 1. Hei, X.; Li, J. Chem. Sci. 12, 3805–3817 (2021).
- 2. Li, Z. et al. Chem. Mater. **31**, 9363–9371 (2019).
- 3. Xu, L. J.; Lin, X.; He, Q.; Worku, M.; Ma, B. Nat. Commun. 11, 1–7 (2020).
- 4. Wang, Y.; Zhang, S.; Zou, B.; Zeng, R.; J. Phys. Chem. C 127, 7380–7388 (2023).

### Phenylazothiazoles pH Indicators

Shifa Ahmad, Nusaiba Madappuram Cheruthu, P. K. Hashim and Nobuyuki Tamaoki Research Institute for Electronic Science, Hokkaido University Kita 20, Nishi 10, Kita Ku, Sapporo, Hokkaido 001-0020

**Introduction**: pH indicators are widely used in many disciplines of material, environmental, biological, and clinical science<sup>1)</sup>. Azobenzene dyes are extensively investigated for the development of colorimetric pH indicators and some of them are commercially available such as methyl yellow, methyl orange, methyl red and alizarin yellow R for practical applications. However, most of the azobenzene dyes show pH detection either in strong acid or alkaline conditions (pK<sub>a</sub> 3.3, 3.5, 5.1 and 11.0). Colorimetric pH indicators that can show distinct color changes in a near neutral pH range are highly advantageous for the detection of pH variation in biological

tissue<sup>2)</sup>. In this study we developed a new class of pH indicator based on phenylazothiazole (PAT) scaffold that detects near neutral pH variation with remarkable color change visible to naked eye.

Results and discussion: We synthesized five novel pH indicators containing PAT and fully characterized by various analytical methods. We found that PAT with a hydroxyl substituent at para position on the phenyl ring, compound 1, showed distinct colors yellow and red in pH 6.2 and 6.9, respectively. Figure 1b shows the UV-Vis titration of 1 for pH ranging from 4.0 to 10.2. The characteristic absorption maxima of 1 at 392 nm gradually decreased with appearance of a new band at 482 nm. Interestingly, electron withdrawing NO<sub>2</sub> substituent on the thiazole ring, compound 2, significantly affected the light absorption properties and color where it exhibited yellow (pH 5.2) and blue (pH 5.6) colors in aqueous solutions. On the other hand, PAT with an electron donating NMe<sub>2</sub> substituent at para position on the phenyl ring, compound 4, also showed pH detection

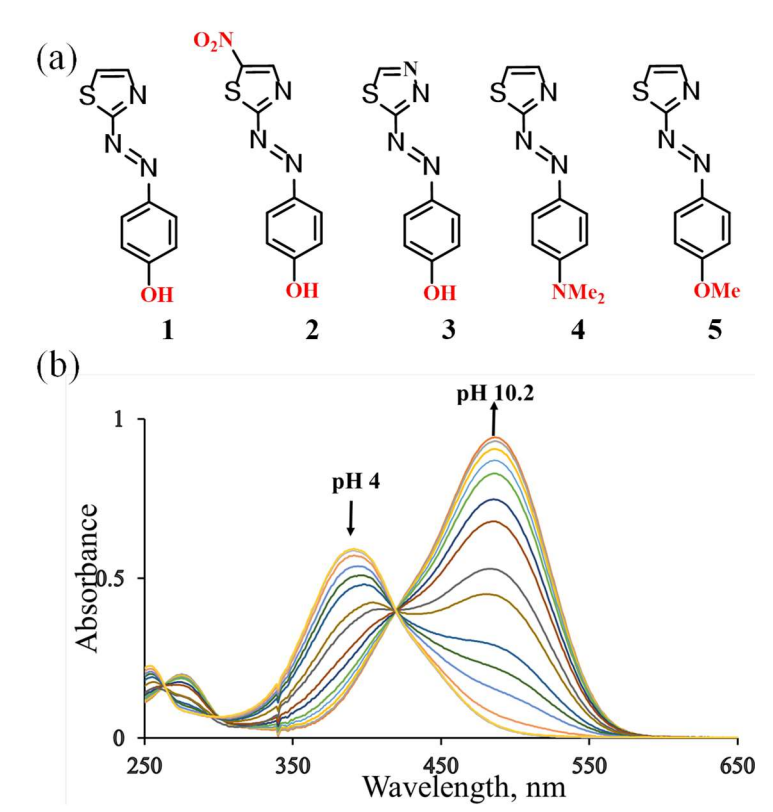


Figure 1: (a) Molecular structures of compounds 1–5 and (b) UV-vis spectra obtained after titrations of 1 for different pH.

ability in highly acidic solutions with blue (pH 1.5) and pink (pH 3) colors. These new pH indicators can potentially detect the pH changes in the cancers due to its acidic characteristics and such experiments are currently undergoing.

- 1) M. A Cardona, & D. C. Magri, (2014). Tetrahedron Letters, 55(33), 4559-4563.
- 2) B. Shan, Y. Deng, B. Tang, Lu R, S. Zhang Chemistry Letters. 2016 Apr 5;45(4):472-4.

### Tunable Chiroptical Activities of Discrete Chiral Gold Nanorods by pH and Electric Potential Dual Modulation

Han Lin<sup>1</sup>, Hideyuki Mitomo<sup>2</sup>, Yusuke Yonamine<sup>2</sup>, Zhiyong Guo<sup>3</sup>, Kuniharu Ijiro<sup>2</sup>

Graduate School of Life Science, Hokkaido University, <sup>2</sup> Research Institute for Electronic Science, Hokkaido University, <sup>3</sup> School of Material Science and Chemical Engineering, Ningbo University

**Introduction.** Chirality as a term describing the geometric structure of an object could not be superimposed on its mirror image. Recent studies have demonstrated an interesting coupling between chiral molecules and metal nanoparticles, with new circular dichroism (CD) responses feeding back near the particle's localized surface plasmon resonance (LSPR) [1]. This is known as plasmon-induced chirality, or CD<sub>LSPR</sub>. Most research on

reconfigurable active chiral plasmons has so far concentrated on dimeric or three-dimensional assemblies [2]. Tunable plasmonic chiroptical activities of discrete metal nanoparticles have rarely reported.

Herein, we demonstrated an active plasmonic chiroptical system based on discrete chiral core-gap-structures@PANI (c-CGS Au NRs@PANI) with tunable CD<sub>LSPR</sub> optical activities controlled by external pH and electric potential (Figure 1) [3].

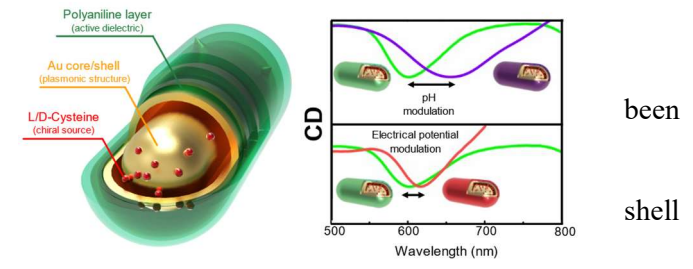


Figure 1: c-CGS Au NRs@PANI-based dual-modulable active plasmonic chiroptical system.

**Results and Discussion.** The c-CGS Au NRs@PANI encapsulating L-cysteine molecules as shown in Figure 2A. The transverse LSPR-induced CD<sub>T-LSPR</sub> was located at 601 nm, when the solution pH was 2. Adjusting the pH increase to 12, PANI had changed from the emeraldine base (ES) to the pernigraniline base (PB) state, and the CD<sub>T-LSPR</sub> peak also completed a red-shift of about 60 nm due to the refractive index difference between the states (Figure 2B).

The electrical potential modulation was performed by applying voltages to the indium tin oxide surface loaded with c-CGS Au NRs@PANI monolayer films (Figure 2C). PANI was in the ES state under a higher voltage (0.4 V), and the CD<sub>T-LSPR</sub> peak was located near 602 nm. As the voltage was reduced to -0.3 V, the ES state gradually transitioned to the leucoemeraldine base (LB) state and the CD<sub>T-LSPR</sub> peak underwent the red shift to 616 nm, due to the increase in refractive index values (Figure 2D).

Satisfyingly, c-CGS Au NRs@PANI exhibited a wide wavelength range of CD<sub>T-LSPR</sub> modulation ( $\approx$  60 nm), stability (more than 100 cycles), accuracy (10 nm/V), and fast switching response (< 1 s), further enhancing their potential in fields such as chiral optical device fabrication.

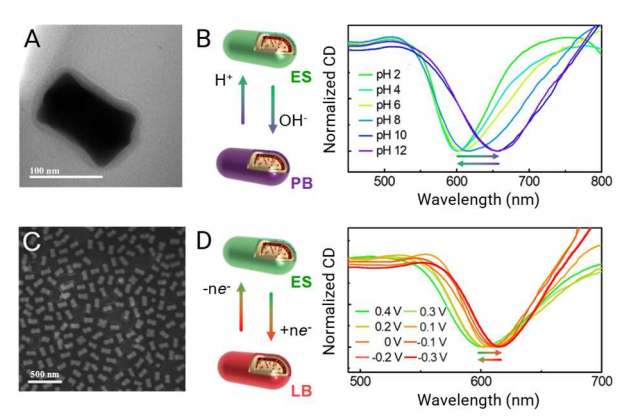


Figure 2: (A) TEM image of c-CGS Au NRs@PANI. (B) Schematic illustration of the dielectric environment switching by proton doping and de-doping, and the CD spectra in response to different pH values. (C) SEM image of c-CGS Au NRs@PANI large-area monolayer films. (D) Schematic illustration of the dielectric environment switching by electrochemical redox, and CD spectra in response to different voltages.

- 1. M. J. Urban, C. Shen, X-T, Kong, C. Zhu, A. O. Govorov, Q. Wang, M. Hentschel and N. Liu, Annual Review of Physical Chemistry, **2019**, 70, 275-299.
- 2. J. Lv, X. Gao, B. Han, Y. Zhu, K. Hou and Z. Tang, Nature Reviews Chemistry, 2022, 6, 125-145.
- 3. H. Lin, H. Mitomo, Y. Yonamine, Z. Guo, and K. Ijiro, Chemistry of Materials, 2022, 34, 4062-4072.

# Investigation of Ni-doped Metal-Organic Framework (MOF-5) for Enhanced Photocatalytic Performance Towards Methylene Blue Dye Degradation

BASKAR MALATHI<sup>a,b\*</sup>, YOHEI MORI<sup>a</sup>, ATSUSHI NAKAMURA<sup>a</sup>, HARISH SANTHANA KRISHANAN<sup>a,b</sup>, JAYARAM ARCHANA<sup>b</sup>, MANI NAVANEETHAN<sup>b,c</sup>

<sup>a</sup> Graduate School of Science and Technology, Shizuoka University, 3-5-1 Johoku, Naka-Ku, Hamamatsu, Shizuoka 432-8011, Japan

<sup>b</sup> Functional Materials and Energy Devices Laboratory, Department of Physics and Nanotechnology, SRM Institute of Science and Technology, Kattankulathur, India, 603203

<sup>c</sup> Nanotechnology Research Center (NRC), Faculty of Engineering and Technology, SRM institute of Science and Technology, Kattankulathur, India, 603203

\*Corresponding author E-mail: baskar.malathi.21@shizuoka.ac.jp

Industrial wastewater discharge has become increasingly an issue for living beings because of the rapid advancement of global industrial development. With wastewater disposal arises the introduction of toxic and dangerous organic contaminants to the ecosystem. Both human health and the biological chain have been severely threatened because of their biological toxicity and inability to degrade. Methylene blue (MB) dyes are commonly used in producing textile factories. It is essential to remain in consideration that MB has a certain level of toxicity and is challenging to remove. Due to its large surface area, tunable pore sizes, and unique chemical characteristics, metal-organic frameworks (MOFs) give a lot of interest in photocatalysis applications. Especially, MOF-5 (Zinc based MOF) have a high surface area, stability and reusability showing a promising material for degradation. While the main challenge is its narrow range of photo-response, rapid recombination of photoinduced carriers and unstable structure. On doping transition metals, they act as an active site for the catalytic oxidation of MB and electron acceptors and donors for facilitating the oxidation of MB to less harmful products. Additionally, the porous nature of MOF-5 allows for high surface area and accessibility of the active sites, leading to enhanced catalytic activity. While using transition metal-doped MOF-5 for the degradation of MBT offers the advantage of improved catalytic activity and mild reaction conditions, making it a promising approach for the remediation of MB-contaminated wastewater. In this work, we synthesized MOF-5 and Nidoped MOF-5 via a solvothermal method. The crystallinity, morphology, surface area, chemical composition and photocatalytic performance are analyzed using XRD, SEM, BET, XPS and photocatalytic studies.

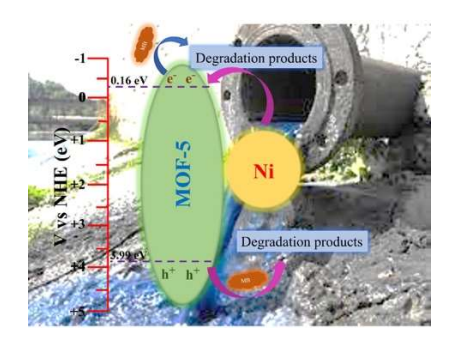


Figure 1. Schematic representation of photocatalytic degradation

- 1. Qin, Xiangtao, Taotao Qiang, Lu Chen, and Shaoting Wang. "Construction of 3D N-CQD/MOF-5 photocatalyst to improve the photocatalytic performance of MOF-5 by changing the electron transfer path." *Microporous and Mesoporous Materials* 315 (2021): 110889.
- 2. Zeng, Yingshan, Qiao Yin, Zhi Liu, and Hao Dong. "Attapulgite-interpenetrated g-C3N4/Bi2WO6 quantum-dots Z-scheme heterojunction for 2-mercaptobenzothiazole degradation with mechanism insight." *Chemical Engineering Journal* 435 (2022): 134918.

## Selective Mono-Hydrodefluorination of Trifluoromethyl Arenes with NHC-Boranes via Organophotoredox Catalysis

Amit K Jaiswal, Dennis Chung-Yang Huang\*
Institute for Chemical Reaction Design and Discovery (WPI-ICReDD), Hokkaido University, Sapporo,
Hokkaido 001-0021, Japan

**Introduction.** Fluorine-containing molecules have found prevalent applications in the pharmaceutical industry and agrochemical sectors because of the thermodynamic and kinetic stability that C-F  $\sigma$ -bonds impart as well as the ability of these substituents to alter the properties of a given biologically active molecule. Hence, demands for novel methods enabling the synthesis of organofluorine molecules have garnered huge attention among chemists, of which tremendous progress have been made in the efficient synthesis Ar-CF<sub>3</sub> molecules as well as manipulation of aryl and alkenyl C-F bonds.

**Results and Discussion.** Although trifluoromethyl units are traditionally incorporated in pharmacophores as prestigious motifs, recent developments have shifted the attention to difluoromethyl motifs (CF<sub>2</sub>H) since they can act as isosteres for ethers and aryl ketones as well as lipophilic hydrogen bond donors (Figure 1).

Here, we report an organophotoredox protocol to selectively replace a single fluorine atom with hydrogen in trifluoromethyl arenes using NHC-boranes as the hydrogen source (Scheme 1). The use of a sufficiently reducing photocatalyst in combination with visible light allows the incorporation of a broad range of trifluoroarene substrates. Under this mild condition, excellent selectivity for mono-hydrodefluorination versus over-reduction can be achieved, and a wide variety of functional groups can be tolerated. Preliminary mechanistic studies suggest a difluoromethyl radical as the key intermediate.

- 1. Kuehnel, M. F.; Lentz, D.; Braun, T. Angew. Chem., Int. Ed. 2013, 52, 3328.
- 2. Müller, K.; Faeh, C.; Diederich, F. Fluorine in Pharmaceuticals: Looking Beyond Intuition. *Science* **2007**, *317*, 1881–1886.

### Development of Quantitative Analysis Method for Oxylipins by LC/MS

Yonghan Li<sup>1</sup>, Siddabasave Gowda B. Gowda<sup>2,3</sup>, Divyavani Gowda<sup>2</sup>, Hitoshi Chiba<sup>4</sup>, Shu-Ping Hui<sup>2</sup>

<sup>1</sup>Graduate School of Health Science, Hokkaido University, Sapporo, Japan 
<sup>2</sup>Faculty of Health Sciences, Hokkaido University, Sapporo, Japan 
<sup>3</sup>Graduate School of Global Food Resources, Hokkaido University, Sapporo, Japan 
<sup>4</sup>Department of Nutrition, Sapporo University of Health Sciences, Sapporo, Japan

**Introduction**. Oxylipins are a kind of lipid that belongs to the fatty acyl family that is found across all mammalian tissues and play pivotal roles in a multitude of biological processes. They are mainly generated by the enzymatic oxidation of polyunsaturated fatty acids via cyclooxygenase (COX), lipoxygenase (LOX), and cytochrome P450 (CYP450) mediated pathways. Oxylipins quantitative determination has always been challenging, due to their low concentrations, complex isomeric structures, and low stability. To overcome these challenges, the aim of this study is to develop a highly sensitive analytical method for targeted quantitative determination of oxylipins in biological samples.

Results and Discussion. Given the inherent challenges in detecting and quantifying oxylipins, we have developed a highly sensitive and selective liquid chromatography/mass spectrometry (LC/MS) method for analysis of COX, LOX, and CYP450 catalyzed oxylipins from linoleic acid, docosahexaenoic acid, arachidonic acid, and eicosapentaenoic acid. Due to isomerism many oxylipins will have the same MS/MS spectra. We have chosen specific single reaction monitoring channels and separated the isomers by modifying different mobile-phase gradients. During method validation, the results showed high linearity of R<sup>2</sup> >0.99. The limits of quantitation were determined to be ranges from 0.5 pg to 100 pg and the limit of detection were ranges from 0.1 pg to 50 pg. The recovery, matrix effect, accuracy, precision, intra and inter day assays were performed. Most of the oxylipins showed excellent recovery of greater than 70%. Upon successful validation of the method, it will be applied to profile the oxylipins in adolescent children plasma samples to reveal their impacts on childhood obesity. Overall, an effort towards the development of efficient and sensitive methods for quantification of oxylipins was made described in this research.

### Effectiveness of Using Visual Deterrents in Lotus Root Cultivation to Control Duck Visitation in Snow-Prone Areas

<sup>1</sup>Uchini Bandaranayake, <sup>2</sup>Maki Yamamoto

<sup>12</sup>Department of Bioengineering, Graduate School of Engineering, Nagaoka University of Technology

The Okuchi area of Nagaoka City, Niigata Prefecture, is famous for its production of lotus roots, but the damage caused by wild ducks in winter is enormous. Unlike other areas, Okuchi cannot use nets to control duck damage because the nets are damaged by heavy snowfall due to their heaviness and the ability of high attachment, so it is necessary to consider duck control measures that do not rely on nets.



Figure 01: Damaged yield observed in Okuchi



Figure 02: Okuchi, Nagaoaka

The purpose of this study was to understand the duck visitation pattern in the Okuchi area and to verify the effectiveness of laser- devices as repellents. First of all, a preliminary survey was conducted to identify the damage situation and the number of ducks flying to the Okuchi area due to information scarcity regarding the problem occurring in this area. The results showed that there was no significant difference in the number of ducks flying to the damaged plots depending on the distance from the rest area. It was also found that the number of ducks flying in was higher during harvest than before or after harvest. The effectiveness of two types of low-power laser devices (Bird Shield Laser Type 1 and OSK 03 Laser) as repellent stimuli was tested by comparing the number of ducks flying to control fields and laser-installed fields.



Figure 03: Bird Shield Laser Type I



Figure 04: OSK 03 laser

As a result, in the effectiveness verification of the Bird Shield Laser Type I, the number of ducks flying by the repellent device tended to decrease, but there was no statistically significant difference, and the number of ducks flying by the device differed depending on the location of the field. On the other hand, for the OSK 03 laser, the effect of the repellent effect was opposite depending on the location of the field, and the repellent effect of the laser was not distinctly demonstrated. Therefore, it is necessary to increase the number of test plots in the future to verify the effectiveness of the device and to improve the waterproof and dustproof performance of the device so that it can withstand use in snow-covered areas.

## Development of a DNA Aptamer Inhibiting Vitamin-D Inactivation Enzyme for Applications in Cancer Therapy

V. Sharma<sup>1</sup>, M. Biyani<sup>2,3</sup>, T. Sakaki<sup>1</sup>, M. Nakajima<sup>2,3</sup>, K. Yasuda<sup>1</sup>

<sup>1</sup>Department of Pharmaceutical Engineering, Toyama Prefectural University, Japan

<sup>2</sup>WPI Nano life science institute (WPI- NanoLSI), Kanazawa University, Japan

<sup>3</sup>Drug and metabolism and Toxicology, Faculty of Pharmaceutical Sciences, Kanazawa University, Japan

Vitamin D3 is metabolized to 25-hydroxyvitamin D3 (25D3) in the liver, and further metabolized in the kidney to 1α,25-dihydroxyvitamin D3 (1,25D3), which exerts various physiological effects such as bone formation, calcium homoeostasis, cell proliferation and differentiation, and so on, by binding vitamin D receptor (VDR). Thus, 1,25D3 and its analogs have been clinically used as therapeutic agents against rickets, psoriasis, and secondary hyperparathyroidism, and they have been also expected as cancer treatments. When 1,25D3 and its analogs bind to VDR, CYP24A1 is also transcriptional activated and the overexpressed CYP24A1 enzyme inactivate them. Thus, resistance to CYP24A1-dependent metabolism could be a key property in prolonging their biological effects.

We recently identified CYP24-inhibiting DNA aptamer (APT-7) as an alternative approach, which enhances vitamin D3 functionally in cancer cells. However, due to low stabilization of the labile nature of DNA aptamers against nucleases and limited distribution to targeted tumor tissues. Then it is redesigned and developed a circular bivalent version of APT-7, called Cb-7. Then we performed systematic studies of Cb-7 to examine stability in nuclease, functional activity, and anti-cancer effects in lung cancer cell (A549 cells).

Figure 1. Metabolic pathway of 1,25D3 by CYP24A1

### Synthesis of 'Dressed' ZnO Nanowires by Overtime Hydrothermal **Growth with Excess Ammonia**

Yuta Kazama<sup>1</sup>, Ryunosuke Matsumura<sup>1</sup>, Narathon Khemasiri<sup>2</sup>, Kazuki Nagashima<sup>2</sup>

<sup>1</sup>Department of Chemistry, Faculty of Science, Hokkaido University <sup>2</sup>Research Institute for Electronic Science, Hokkaido University

#### Introduction.

Metal oxide nanowires grown on substrates are a rational approach to incorporate their unique functionalities into nano-electronic and nano-bioanalytical devices<sup>1,2</sup>. Although the huge surface area is a major advantage of nanowire devices, it is substantially limited by geometric factors such as density, diameter and length. In this study, we demonstrate a way to push the limit of specific surface area discovered in seed-assisted hydrothermal ZnO nanowire synthesis.

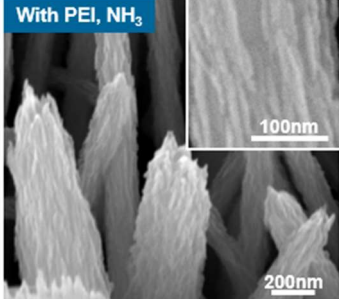
#### Results and Discussion.

Aqueous solution for hydrothermal ZnO nanowire synthesis was prepared by mixing 25 mM hexamethylenetetramine (HMTA), 25 mM zinc nitrate hexahydrate Zn(NO<sub>3</sub>)<sub>2</sub>·6H<sub>2</sub>O, 2.5 mM polyethyleneimine (PEI), and 500 mM ammonia into 100 ml deionized (DI) water at room temperature. A Si/SiO<sub>2</sub> substrate with a sputter-coated ZnO seed layer was immersed upside down in the solution. The hydrothermal synthesis was performed at 95 °C for 5-40 hours. After the growth the samples were removed from the solution, rinsed with DI water, and dried by nitrogen blow. Morphology of the ZnO nanowires were characterized by a field emission scanning electron microscope (FESEM, JEOL JSM-7001F). Ion distribution of the prepared aqueous solution was calculated by Visual MINTEQ ver. 3.1.

When the hydrothermal synthesis with excessive ammonia addition was performed for more than 20 hours, we found that the nano-pleated ZnO nanowire surface was formed. Interestingly, the formation of pleated surface was not seen under no ammonia condition (see Figure). The time-series profile of nanowire length revealed that the nanowires are likely to be pleated after terminating the nanowire growth. By considering the fact that ammonia serves as an etchant for ZnO by forming [Zn(NH<sub>3</sub>)<sub>2</sub>]<sup>2+</sup> complex ion<sup>3,4</sup>, ammonia based chemical etching, triggered by the shortage of Zn source in the growth solution, must play an important role on the formation of such 'dressed' ZnO nanowire surface.

However, it cannot be explained solely ammonia-based etching, because an immersion of well-faceted nanowires into ammonia solution didn't the nano-pleated surface structure. All above results suggest that the dressed nanowires were constructed by a complex competition of ammonia-based chemical etching and crystal growth at the nanoscale. We believe that the proposed technique for constructing high-order nanowire surface structure by etchingincorporated overtime hydrothermal synthesis contributes greatly significantly increase a specific surface of ZnO nanowire and enhances the performance of nanowire-based devices.

Without PEI, NH<sub>3</sub>



by the

form these ZnO

Figure FESEM images of ZnO nanowires grown by overtime hydrothermal synthesis for 40 hours without (left) and with (right) ammonia addition.

#### References

- 1. J. Liu, K. Nagashima et al., ACS Sens. 2022, 7, 534-544
- 2. A. Yokoi, T. Yasui, Y. Inokuma et al., Sci. Adv. 2023, 9, eade6958
- 3. Z. Xixi, K. Nagashima et al., Nano Lett. 2020, 20, 599-605
- 4. J. Zhou, N. Xu, Z. L. Wang, Adv. Mater. 2006, 49, 2432-2435

area

# **Enhancement of Mitochondrial Function with Kaempferol, Contained** as Glycoside in Aojiru

Akiko Sakurai<sup>1</sup>, Toshihiro Sakurai<sup>2</sup>, Hsin-Jung Ho<sup>2</sup>, Hitoshi Chiba<sup>3</sup>, Shu-Ping Hui<sup>2</sup>

<sup>1</sup>Graduate School of Health Sciences, Hokkaido University; <sup>2</sup>Faculty of Health Sciences, Hokkaido University; <sup>3</sup>Department of Nutrition, Sapporo University of Health Sciences

**Introduction.** Fatty liver causes mitochondrial dysfunction<sup>1.</sup> To overcome this, food compounds that activate mitochondria may be promising. Kaempferol belongs to the flavonoid family and is contained as a glycoside in foods. Our laboratory applied for a patent regarding antioxidant function of kaempferol analogues in Aojiru<sup>2</sup>, However, it is unknown how kaempferol affects hepatic mitochondrial function. Here, we aim to elucidate it.

Results and Discussion. To confirm the concentration of kaempferol that causes toxicity, a cell viability test was performed using WST-1 method. As a result, it was confirmed that kaempferol had no cytotoxicity up to  $10~\mu\text{M}$ . Thus, the concentration of kaempferol used to stimulate cells was set at  $10~\mu\text{M}$ . Next, in order to verify whether kaempferol has a protective effect on hepatocytes, we attempted to generate fatty liver model cells. As a preliminary study, we conducted a cytotoxicity test using lactate dehydrogenase (LDH) measurement to confirm the optimal concentration of linoleic acid (LA). As a result, it was confirmed that there was no difference in the amount of LDH produced up to  $1000~\mu\text{M}$  of LA. In addition, lipid droplets were observed using a phase contrast microscope. Compared to the control group, lipid droplets were observed in the  $100~\mu\text{M}$  LA group, and the number of lipid droplets increased as the LA concentration increased, but no difference was observed between the  $800~\mu\text{M}$  and  $1000~\mu\text{M}$  LA groups. Therefore, a fatty liver model was created by adding  $800~\mu\text{M}$  LA in this experiment.

To investigate the cytoprotective effect of kaempferol on fatty liver model cells, we added 10  $\mu$ M kaempferol to fatty liver model cells and measured the amount of LDH produced. Consequently, the amount of LDH was significantly lower in the kaempferol group than in the control, which suggests the cytoprotective effect of kaempferol.

To clarify if kaempferol can improve mitochondrial function, we measured various mitochondrial respiratory function using XFp extracellular flux analyzers. Interestingly, mitochondrial ATP production, basal respiration, and proton leak were significantly higher in the kaempferol group than in the control, which means that kaempferol can enhance mitochondrial function.

To elucidate the mechanism, we measured the expressions at mRNA levels using real-time PCR. Corresponding to the result on mitochondrial respiratory function, the expression level of carnitine palmitoyl transferase  $1\alpha$  (*CPT1A*) showed a significant increase in the kaempferol group. CPT1 $\alpha$  is present in the outer membrane of mitochondria and play a role as a transporter for long-chain fatty acids into mitochondria. CPT1 $\alpha$  is the rate-limiting enzyme for  $\beta$ -oxidation of long-chain fatty acids, and an activation of  $\beta$ -oxidation contributes to the production of ATP<sup>3</sup>. Therefore, the improvement in mitochondrial function by kaempferol may be due to the activation of  $\beta$ -oxidation by the increased expression level of *CPT1A*.

In conclusion, kaempferol enhanced mitochondrial respiratory function including ATP production in C3A cells. In the future, it would be important to prove that an energy metabolism improves in the liver when people drink Aojiru a health food, and to further prove the mechanism.

- 1. D. Pessayre and B. Fromenty, *J. Hepatol.* **2005**, 42,928-40.
- 2. S.-P. Hui, Y.-S. Ma, Z. Chen, H. Fuda, H. Sato, ATP production promoter. Japan Patent P2019-73476A. 2019-05-16.
- 3. S. Eaton, Prog. Lipid Res. 2002, 41, 197–239.

### Development of Sensitive LC/MS Method for trans Fatty Acid Analysis

Rinako Ueda<sup>1</sup>, Siddabasave Gowda B. Gowda<sup>2</sup>, Hitoshi Chiba<sup>3</sup>, Divyavani Gowda<sup>2</sup>, Shu-Ping Hui<sup>2</sup>

- 1. Graduate School of Health Sciences, Hokkaido University
- 2. Faculty of Health Sciences, Hokkaido University
- 3. Department of Nutrition, Sapporo University of Health Sciences

**Introduction.** Lipids such as unsaturated fatty acids are present in all organisms mostly as *cis* isomers. Whereas *trans* isomers are present in several processed foods and detected in human plasma as minor components. *Trans* fatty acids are reported to have a higher risk of coronary heart disease; hence, their measurement in food and biological samples had great significance. However, the currently available techniques for *cis* and *trans* fatty acid analysis utilize gas chromatography/mass spectrometry (GC/MS), but it is less sensitive, time-consuming, and requires large sample amounts. In other words, liquid chromatography/mass spectrometry (LC/MS) based analysis would be more sensitive and require the least sample amount. Hence, in this study, we aimed to develop a highly sensitive analytical method for *trans* fatty acids determination using targeted tandem mass spectrometry coupled with high-pressure liquid chromatography.

Results and Discussion. The authentic standards including both *cis* and *trans* isomers of palmitoleic acid (C16:1 9E/Z), oleic acid (C18:1, 11E/Z), and linolenic acid (C18:2, 9,12EE/ZZ) were prepared in acetonitrile and injected directly to triple quadrupole mass spectrometer. The results showed a weak ionization and less sensitivity. To improve the detection sensitivity of *cis* and *trans* fatty acids a 2-(2-pyridyl) ethylamine (PEA) derivatization technique was applied. The derivatization of *cis* and *trans* fatty acids carboxyl moiety with PEA was optimized in the presence of Triethylamine (TEA) and 2-chloro-1-methyl pyridinium iodide (CMPI). The derivatized fatty acids were injected to a triple quadrupole mass spectrometer and the results showed 1000 folds increased detection sensitivity (Fig. 1). Then, the chromatographic separation of *cis* and *trans* isomers was optimized using various columns and found best separation in Hypersil GOLD<sup>TM</sup> C18 column (2.1 × 50 mm, 1.5  $\mu$ m) and a total run time of 20 min. The linearity of the standards was evaluated, and method validation is in progress. Upon successful development of the method, it will be applied to profile the cis and *trans* fatty acids in processed foods and adolescent children plasma samples. This method will have potential application in detecting *trans* fatty acids sensitively and selectively with potential benefit to the food and health industry.

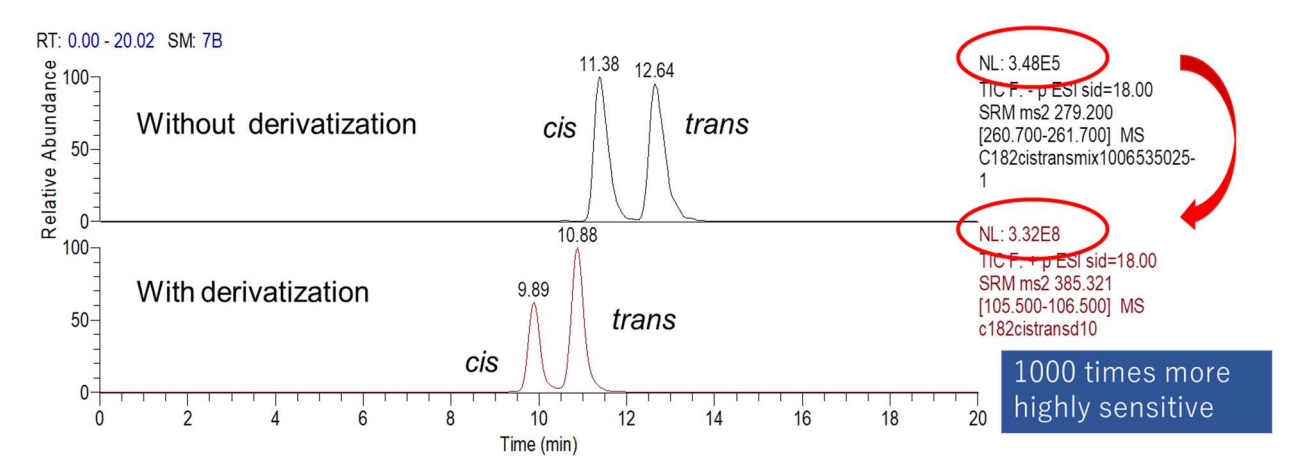


Fig. 1. Isomers with improved sensitivity for linoleic acid.

### Analysis of Lipid Nutrients in Edible Rose Samples by LC/MS

Malek Md Abdul<sup>1</sup>, Siddabasave Gowda B. Gowda<sup>1,2</sup>, Divyavani Gowda<sup>2</sup>, Shu-Ping Hui<sup>2</sup>

<sup>1</sup>Graduate School of Global Food Resources, Hokkaido University, Kita-9, Nishi-9, Kita-Ku, Sapporo 060-0809, Japan.

<sup>2</sup>Faculty of Health Sciences, Hokkaido University, Kita-12, Nishi-5, Kita-Ku, Sapporo 060-0812, Japan.

**Introduction:** Rose phytochemicals have been discovered for having potential anti-inflammatory, anticancer, and antioxidant properties<sup>1</sup>. A study demonstrated the positive heath impact of Sahime rose water on elderly population with dementia<sup>2</sup>. Despite the significant health benefits of roses, there is a lack of information in literature regarding lipid metabolites. To investigate the lipid compositions between two edible roses named, Sahime and Apple rose that are harvested in Shimane prefecture, Japan, an untargeted LC/MS technique was implemented.

Results and Discussion. The homogenized rose samples were used for the total lipid extraction by the monophase extraction method and analyzed by LTQ-orbitrap MS. In this analysis, about 166 distinct lipid molecular species were identified by MS/MS analysis in both positive and negative ionization modes. The results of a multivariate statistical analysis of each lipid molecular species revealed distinct variations between the two rose samples. In both cases saturated fatty acids are predominant compared to monounsaturated and polyunsaturated fatty acids (Fig.1). The phospholipids including phosphatidylcholine, phosphatidylglycerol and cardiolipins are significantly higher whereas lysophosphatidylinositols are lower in Sahime compared to Apple rose. Sahime rose contains more sphingolipids and sterol lipids than Apple rose. For the first time, among various lipid metabolites, sterylglycosides and acylsterylglycosides have been identified in this analysis. Edible roses are expected to be tremendously beneficial in accelerating the development of essential foods and cosmetic products.

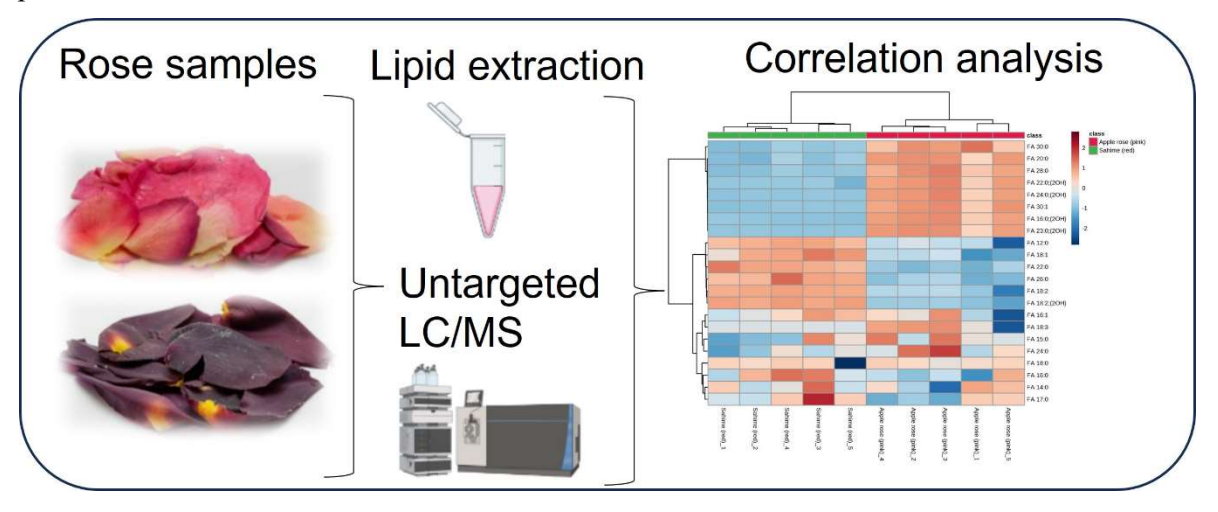


Figure 1: Schematic graphical representation of lipid analysis between two rose samples.

- 1. Samtiya, M. et al., "Potential Health Benefits of Plant Food-Derived Bioactive Components: An Overview." *Foods (Basel, Switzerland)* **2021**,10, 839.
- Takeda Y. et al., Usefulness of aromatherapy ("Sahime" Rose water) on bathing process for the elderly people
  with dementia living in a geriatric health service facility. Bulletin of Shimane University School of Medicine, 2012,
  35, 22-31.

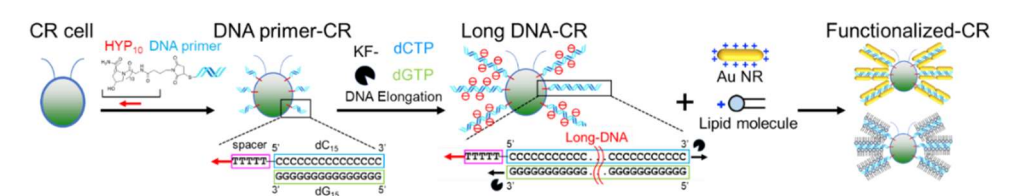
# Confocal Laser Microscopy Examination of Surface Coating of an Algal Cell with Elongated DNA strands via a DNA Polymerase for Functionalization with Cationic Materials

Yingqi Mu<sup>1</sup>, Yusuke Yonamine<sup>2</sup>, Hideyuki Mitomo<sup>2</sup>, Kuniharu Ijiro<sup>2</sup>

<sup>1</sup>Graduate School of Life Science, Hokkaido University.; <sup>2</sup>Research Institute for Electronic Science, Hokkaido University

**Introduction.** Microorganisms have been utilized as excellent conversion systems to produce valuable products for human beings. Artificial materials that show various bioactive characters have been exploited by biomimetic chemistry. By modifying natural cells with artificial materials, "functionalized cells" can be generated. In this project, a unicellular biflagellated alga, Chlamydomonas reinhardtii (CR), is modified with a DNA primer and conjugated with a polypeptide of 4-hydroxyproline (HYP<sub>10</sub>) that binds tightly to the CR cell wall<sup>1</sup>. The immobilized DNA primers were then elongated with DNA polymerases to cover the CR cells with long DNA chains. Highly negatively charged DNA layer can act as a scaffold for functionalization with cationic materials. This methodology opens a new avenue to transform the cellular functions readily and strikingly for various applications.

**Results and Discussion.** Firstly, a DNA primer was conjugated with HYP<sub>10</sub> to prepare HYP<sub>10</sub>-DNA for DNA immobilization. After purification, the product was mixed with CR cell to acquire the DNA primer-immobilized CR cells. By adding DNA polymerase Klenow fragment exo (-) (KF-)<sup>2</sup>, long double-stranded DNA chains with repeating sequence were elongated by slippage amplification<sup>3</sup> from CR cell surface. To demonstrate the feasibility of further modification using the elongated DNA layer as scaffold, the long DNA-coated CR cells are complexed with Au NRs modified with a cationic ligand (11-MTAB) and cationic lipid molecules to form DNA-lipid complexes, respectively (**Scheme 1**).



Scheme 4. Schematic diagram the modification of CR cell surface with long DNA chains for functionalization with cationic materials.

Through the electrostatic interaction, cationic materials were successfully coated onto CR cell surface and the feasibility of cellular functionalization was demonstrated.

- 1. D. B Weibel. et al. (2005). PNAS, 102, 11963-11967.
- 2. H. Klenow. et al. (1970). Proceedings of the National Academy of Sciences of the United States of America, 65, 168-175.
- 3. H. Mitomo. et al. (2015). Chem. Asian J, 10, 455-460.

# What Determines Milk Consumption in Indian Households? - Insights from the NSSO Consumer Expenditure Survey (2011-12) Using Multilevel Analysis

Sakshi Pandey, Tetsuya Araki

<sup>1</sup>Department of Global Agricultural Sciences, Graduate School of Agricultural & Life Sciences, The University of Tokyo

**Introduction:** Milk plays an essential role in the diet, and South Asia has a long tradition of milk production. India is the largest milk producer worldwide; however, evidence suggests that milk consumption and production are not uniform across the country.

Methodology: This study examined milk production and consumption patterns in India. Specifically, sociodemographic and economic lenses were incorporated into the framework of milk accessibility, affordability, and availability using data from a nationally representative consumption survey. Household milk intake data for a 30-day recall period were collected using the Indian Household Consumer Expenditure Survey (2011-2012) by the National Sample Survey Office (NSSO). State-level milk production data was collected from the Ministry of Fisheries, Animal Husbandry & Dairying annual report. Milk consumption data were collected from the. This study compared milk production and consumption variability across Indian states. Negative binomial regressions in a multilevel model were used to identify state- and household-level parameters affecting milk consumption. The coefficients were reported with 95% confidence intervals (CIs). It further utilized a multilevel model approach that enables the modeling of the relationships between predictor variables and the outcome variable while accounting for the hierarchical structure of the data (i.e., households nested within states). The model was used to analyze household milk consumption with state- and household-level characteristics as a function of availability, affordability, and accessibility. The predictor variables included household-level (level 1) and state-level covariates. The model specification is given as  $\log (Yij) = \beta 0 + \beta 1X1ij$  $+\beta 2X2j + \zeta j$ . For each household in state j, variables X1ij are the household-level covariates, whereas variables X2j are state-level covariates.  $\zeta_j \sim N(0, \psi)$  represents the state-specific random intercept accounting for variation between states in the response variable. A regression coefficient with a 95% confidence interval (CI) and a Wald chi-squared value were reported.

Results: Although being the largest producer, the consumer expenditure survey report (2011–2012) indicates that while per capita consumption has been increasing since 2004–2005 in both rural (from 128.87 gm to 144.43 gm) and urban India (170.23 gm to 180.73 gm), the per capita national average consumption was approximately 55% of the recommended intake of 300 g/day. However, the median per-capita consumption was significantly higher in high-availability states than low-availability states. Overall, it was observed that except for four states (Punjab, Haryana, Himachal Pradesh, and Rajasthan), all regions in India had reasonably low per capita consumption, specifically the northeastern states and West Bengal, Odisha, Jharkhand, and Chhattisgarh. From the multilevel analysis, it was observed that state-level milk availability (0.0846 [0.049, 0.121]) and accessibility in rural and urban areas (0.083 [0.024,0.141]) were linked to household milk consumption. However, affordability (household expenditure quintile and absolute milk price) was most strongly associated with consumption that increased with an increase in expenditure quintile and decreased with rising prices. Conclusion: This study highlights three main aspects of milk consumption patterns. First, milk production and consumption patterns vary significantly across states, with evident clusters showing extremely low to high per capita consumption. Second, although availability and accessibility were significant factors in determining household milk consumption, affordability was the predominant factor. Finally, social inequalities, including education and caste, were critical determinants of milk consumption in across Indian households. Policies targeting on improving food and nutrition security among the population, should consider these nuances to improve consumption in a geographically and culturally diverse country like India.

- 1. Swaminathan S, Vaz M, Kurpad A V. Protein intakes in India. Br J Nutr 2012;108:50–8. https://doi.org/10.1017/S0007114512002413.
- 2. John AT, Makkar S, Swaminathan S, Minocha S, Webb P, Kurpad A V., et al. Factors influencing household pulse consumption in India: A multilevel model analysis. Glob Food Sec 2021;29:100534. <a href="https://doi.org/10.1016/j.gfs.2021.100534">https://doi.org/10.1016/j.gfs.2021.100534</a>.
- 3. Kapaj A, Deci E. World milk production and socioeconomic factors effecting its consumption. Elsevier Inc.; 2017. https://doi.org/10.1016/B978-0-12-809868-4.00007-8.

# Prevention of Byproduct Synthesis in Ionic Layer Epitaxy of Monolayered Zinc Oxide Nanosheets

Ryunosuke Matsumura<sup>1</sup>, Yuta Kazama<sup>1</sup>, Narathon Khemasiri<sup>2</sup>, Kazuki Nagashima<sup>2</sup>

<sup>1</sup>Department of Chemistry, Faculty of Science, Hokkaido University

<sup>2</sup>Research Institute for Electronic Science, Hokkaido University

#### Introduction

Monolayerd zinc oxide nanosheets (ZnO NSs), a two-dimensional nanomaterial, have attracted increasing attentions in nano-electronics and photonics due to their fascinating properties such as large band gap of 3.37 eV [1] and high carrier mobility of 60 cm<sup>2</sup>/Vs at room temperature [2]. Although the monolayered ZnO NSs have been synthesized by ionic layer epitaxy using ionic surfactant [3], they are based on a rule of thumb and thus rational design of ZnO NSs has yet been achieved. In this study, we found that the conventional synthetic route of ZnO NSs yields inevitable byproduct nanostructures and explored the way to prevent such byproduct.

#### **Results and Discussion**

For the monolayered ZnO NSs synthesis, an aqueous solution nitrate was prepared by mixing zinc hexahydrate (ZnO(NO<sub>3</sub>)<sub>2</sub>·6H<sub>2</sub>O) and hexamethylenetetramine (HMTA) by the molar ratio of 2:1 in 17 ml deionized (DI) water at room temperature. The concentration of ZnO(NO<sub>3</sub>)<sub>2</sub>·6H<sub>2</sub>O was varied in the range of 0.1-35 mM. Then 0.1 v/v% sodium dodecyl sulfate (SDS) solution was prepared by mixing with DI water at 60 °C. The 10 µl of SDS solution was dropped onto the growth solution and waited for 3 min. The ZnO NSs synthesis was carried out in a forced convection oven for 2 h by varying the temperature in the range of 60-90 °C as a controlling parameter. The ZnO NSs formed at the surface of growth solution was transferred to a Si/SiO<sub>2</sub> substrate by dip-coating method and dried. The morphology of ZnO NSs was characterized by scanning electron

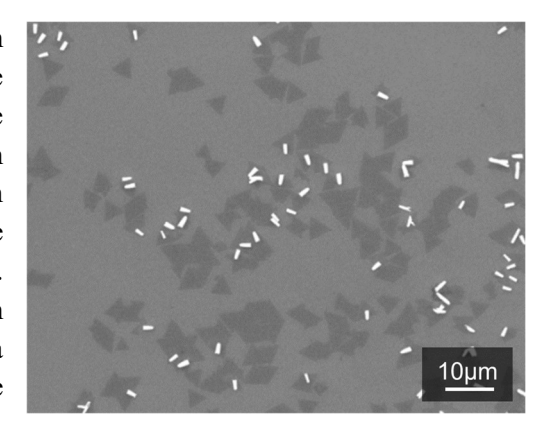


Figure 1. SEM images of the sample synthesized with Zn 5 mM at 80 °C. Both ZnO NSs and ZnO NRs byproduct were seen.

microscope (SEM, JEOL JSM-7001F). When performing a synthesis with the previously reported condition (Zn 35 mM, 60 °C) [1,3], only large aggregation byproduct was formed and none of monolayered ZnO NSs were seen. The byproduct was not removed by applying oxygen plasma but readily disappeared by dropping hydrochloric acid. These results indicate that the byproduct is an insufficiently reacted zinc hydroxide/oxide. The byproduct was further identified by which the byproduct was changed to the nanorods (NRs) shape with increasing the synthesis temperature up to 80 °C (see Figure). In this condition, monolayered ZnO NSs with triangle shape were formed together with the ZnO NRs byproduct. In order to explore the phase selective growth condition based on a difference of critical nucleation concentration at each crystal plane [4], the Zn precursor concentration was systematically varied. When decreasing the Zn precursor concentration down to 0.1 mM, the formation of ZnO NRs byproduct was drastically suppressed with maintaining the ZnO NSs. Further decreasing the Zn concentration to 0.01 mM led to the disappearance of both ZnO NSs and NRs. These results indicate that the critical nucleation concentration for ZnO NSs is lower than that of ZnO NRs. Considering that a (0001) plane is exposed in the triangle shaped ZnO NSs, a nucleation on  $(10\overline{1}0)$  plane becomes dominant at the surfactant-liquid interface against the energetical disadvantage of surface energy. Thuse these interesting findings allow us to selectively synthesize ZnO NSs by preventing the byproduct formation and will lead to a rational design of ZnO NSs by further controlling the nucleation phenomena.

- [1] Y. Huihui et al., Small 2020, 16, 2005520, [2] A. S. Dahiya et al., Appl. Phys. Lett. 2015, 107, 033105,
- [3] F. Wang et al., Nat. Commun. 2016, 7, 10444, [4] Z. Xixi, K. Nagashima et al., Nano Lett. 2020, 20, 599

### **Energy-Saving Preparation of Chitin/Chitosan Composite Materials**

Tomohisa Suzuki, Olaf Karthaus

Graduate School of Science and Engineering, Chitose Institute of Science and Technology

Introduction. A paste is prepared by mixing chitin, chitosan 100, citric acid, sodium hypophosphite, and distilled water. The mixed material was prepared by hot pressing[fig.1]. It was found that even a low temperature hot-press application produced a difference in strength in the presence or absence of a cross-linking agent.

Results and Discussion. From fig. 2, it was found that there is some relationship between the reaction temperature and tensile strength as a result of changing the reaction temperature by keeping the pressure during hot pressing to 40 MPa and the reaction time to 1h as the specimen preparation conditions. The strength of the material changed even at a comparably low temperature of 90°C depending on the presence or absence fig.1 Sample prepared for strength testing. of the cross-linker, indicating that the cross-linker can increase the tensile



strength of the material even at temperatures lower than the temperature that is usually applied for this type of samples, 220°C. From fig. 3, it can be seen that changing the pressure during hot-pressing has a similar effect on the tensile strength: it increased due to the increased density of the material caused by the high pressure.

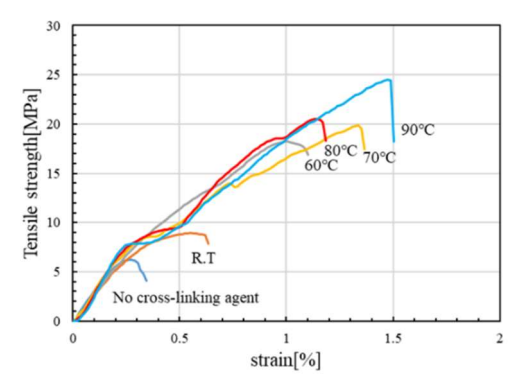


fig.2 Tensile test results with samples prepared at 40 MPa, reaction time 1 hour, and reaction temperatures (sample without cross-linking agent was at different)

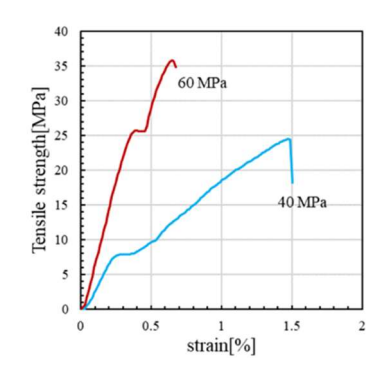


fig.3 Tensile test results of samples prepared at 90°C for 1 hour and different pressures.

- M.M.Hassan, N.Tucker, M.J.Le Guen .Thermal, mechanical and viscoelastic properties of citric acid-crosslinked starch/cellulose composite foams Carbohydrate Polymers 2020,230
- 2. L. Heux, J. Brugnerotto, J. Desbrie'res, M.-F. Versali, and M. Rinaudo, Solid State NMR for Determination of Degree of Acetylation of Chitin and Chitosan, Biomacromolecules 2000, 1, 746-751

### Phenylazothiazoles as Visible-Light Photoswitches

Runze Lin, P.K. Hashim and Nobuyuki Tamaoki

Research Institute of Electronic Science, Hokkaido University, Sapporo, Hokkaido, Japan

**Introduction.** Photoswitching molecules have been widely used in the field of material science, biology, and photopharmacology. However, most photoswitches require UV light irradiation for isomerization, which is harmful and penetrate poorly into the biological tissue. Photoswitches having a five-membered heteroaryl motif have distinct photophysical properties, steric profiles, and molecular geometries. Many drug molecules contain five-membered heteroaryl motif and hence their photoswitchable analogues can be used in the field of photopharmacology. Here, we report a new category of photoswitches, phenylazothiazoles (PATs), which can isomerize by visible regions and showing interesting properties.<sup>2</sup>

**Results and Discussion.** We synthesized PAT photoswitches via cyclization followed by oxidation or via a direct azo-coupling approach from the aminothiazole. All compounds exhibited visible-light triggered switching properties, red-shifted  $(\pi-\pi^*)$  transition bands. Introduction of electron withdrawing groups elongated the lifetime of *cis* isomers, while electron donating groups reduced their lifetime. Generally, all compounds show

fatigue resistance repetitive 405 nm and 525 nm light irradiations. Good E / Z ratios on photostationary states (PSS) of both switching directions were also observed for most of the PAT photoswitches. Furthermore, we succeeded separating and crystalizing trans and cis isomers (Figure 1). The X-ray singlecrystal structures showed a coplanar structure in E isomers and T-shaped conformation with the thiazole ring perpendicular to the phenyl ring in the Zisomers. ab initio calculations also showed the similar conformations. For biological applications, the photoswitch should be stable in reductive environment such as cell cytoplasm. The absorbance originating from the azo chromophore remain unchanged even after incubation of PATs in DTT and glutathione reductants indicating the

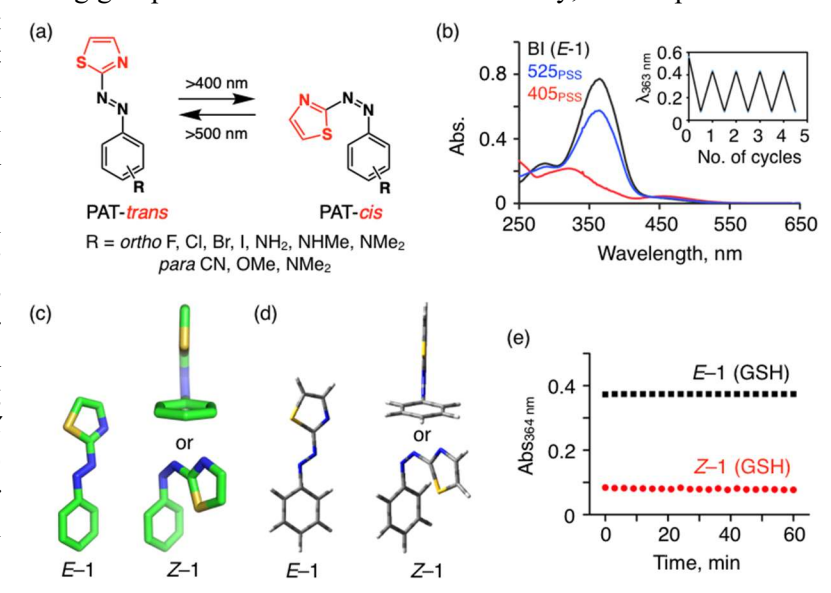
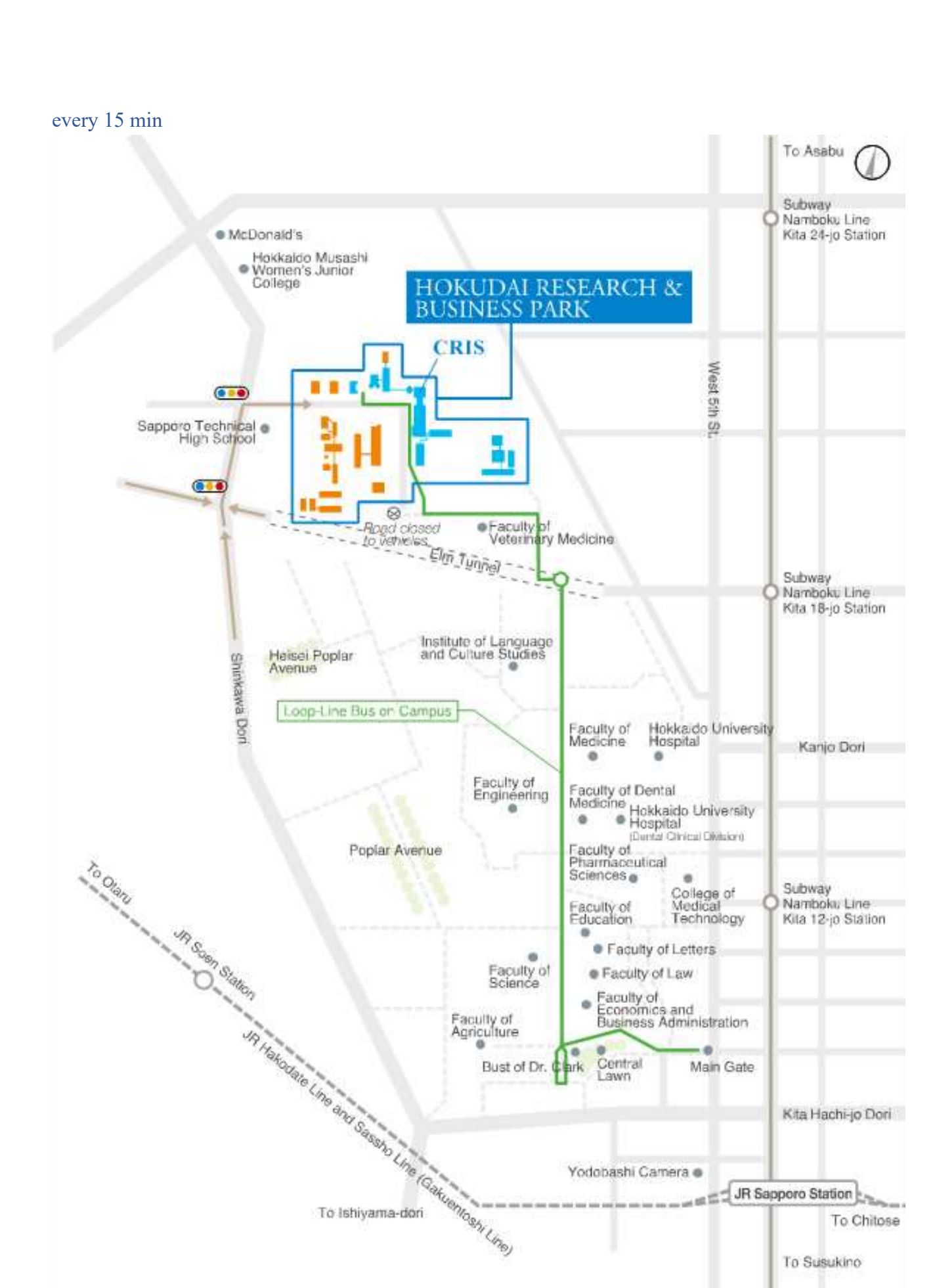


Figure 1: Scheme and absorption spectra showing the trans to cis isomerization of PAT by visible light (a, b). Single crystal X-ray and energy optimized structures of both E and Z isomers of PAT (c, d). Absorbance change over time after PAT incubation in

excellent stability of PATs in their *E* and Z isomers.

In summary, we have developed a novel class of five-membered heteroaryl azo photoswitches that isomerize by visible light reversibly. The PAT photoswitch showed very different spectral characteristics compared to conventional azobenzene as well as other heteroaryl azo compounds.

- 1. Velema, W. A.; Szymanski, W.; Feringa, B. L. J. Am. Chem. Soc. 2014, 136, 2178–21916.
- 2. R. Lin, P. K. Hashim, S. Sahu, A. S. Amrutha, M.C. Nusaiba, T. Shakkeeb, K. Takahashi, T. Nakamura, T. Kikukawa, and N. Tamaoki *J. Am. Chem. Soc.* **2023**, 145, 16, 9072.



To Susukino

# Sponsor:



# Major Sponsor:



## Major Donor:

